SOLUBLE CARBONACEOUS FUEL-AIR FUEL CELL

Report No. 2

Contract No. DA 36-039 SC-89156

ARPA Order No. 247-62

Task No. OST 760200471

FINAL Report, 1 Jan. 1962 - 31 Dec. 1962

U. S. Army Electronics Research and Development Laboratory

Fort Monmouth, New Jersey

ESSO RESEARCH AND ENGINEERING COMPANY
PRODUCTS RESEARCH DIVISION
LINDEN NEW JERSEY

RL 60M 62

SOLUBLE CARBONACEOUS FUEL-AIR FUEL CELL

REPORT NO. 2

CONTRACT NO. DA 36-039 SC-89156
ARPA ORDER NO. 247-62
TASK NO. OST 760200471

FINAL REPORT, 1 JAN. 1962-31 DEC. 1962

OBJECT: CONDUCT RESEARCH AIMED TOWARD DEVELOPING A SOLUBLE CARBONACEOUS FUEL-AIR FUEL CELL

Authored by:

Barry L. Tarmy
Eugene L. Holt
Duane G. Levine
Andreas W. Moerikofer
Joseph A. Shropshire
Charles H. Worsham

Approved by:

Carl E. Heath

This Research Is Part Of The Energy Conversion Project Sponsored By The Advanced Research Projects Agency, Department of Defense

Esso Research and Engineering Company
Linden, New Jersey

CONTENTS

ILLUSTRATIONS

TABLES

APPENDIX ILLUSTRATIONS

APPENDIX TABLES

SECTION 1

PURPOSE

The purpose of these investigations is to perform research on the basic components of an electrolyte-soluble carbonaceous fuel - air fuel cell. The major emphasis of the program is on the simultaneous development of all components in order to optimize the performance of the entire cell and to take into account interactions between components.

This work is aimed toward the development of a practical fuel cell using a partially oxidized hydrocarbon as the fuel and air as the oxidant. The fuel must be capable of reacting completely to CO_2, be reasonably available, and pose no unusual corrosion, toxicity, or handling problems. In addition the cell must use a CO_2 rejecting electrolyte and operate at temperatures and pressures below 152°C and 5 atm. Other objectives include high electrical output per unit weight and volume, high efficiency, long life, high reliability, reasonable cost, and ruggedness.

The program is divided into three parts. These are referred to as Tasks A, B, and C in this report. Tasks A and B are, respectively, the development of improved fuel electrodes, and the development of practical air electrodes. Task C includes work carried out on establishing the basic cell design, especially with regard to the operation of all components in a single cell.

SECTION 2

ABSTRACT

Research on the soluble carbonaceous fuel - air fuel cell has continued to concentrate on improving the performance of individual cell components and on translating these results into compatible electrode-electrolyte systems. These efforts encompass work carried out in three areas, namely the development of the fuel electrode, the development of the air electrode, and their combination into a total cell.

2.1 Task A, Fuel Electrode

A number of catalysts were prepared by the simultaneous reduction of noble and base metals with $NaBH_4$. The Tafel slopes and exchange currents of Pt containing catalysts varied widely but their activities at practical current densities usually fell within a narrow range due to a compensating effect of the kinetic parameters. However, this compensating effect was not general since co-catalysts based on other noble metals did not always behave in a similar fashion. These changes in catalyst performance are due to alloy formation and the $NaBH_4$ reduction represents a convenient process for the preparation of a wide variety of alloys.

A new P-type catalyst was tested with CH_3OH and found to lower the polarization at practical current densities about 150 mv from that obtained with Pt. This represents the most active catalyst yet prepared. Studies were also continued on the Pt-Mo catalyst, previously shown to exhibit significantly lower polarizations at about 1 ma/cm^2 with CH_3OH. Large increases in current density at low polarizations could not be obtained with this system. However, using Mo in solution resulted in current densities in excess of 200 ma/cm^2 at low polarization when HCHO was employed, showing that this system could possibly have some practical significance. Mechanism studies indicated that the reaction involved a surface redox couple.

2.2 Task B, Air Electrode

The electrochemical performance of the HNO_3 redox couple has proven satisfactory. Therefore, research efforts have concentrated on improving the chemical regeneration of HNO_3 and applying the results in a practical cell configuration.

Regeneration efficiencies of 14 coulombs/coulomb equivalent to HNO_3 consumed have been achieved in laboratory studies with air through the use of foaming surfactants. This efficiency was extended to 25 regenerations through the addition of a small amount of high surface area silica powder to the foam. Of the surfactants tested, sodium nonyl oxidibenzene disulfonate has exhibited the best chemical stability, 90 hours under load.

Engineering studies have been initiated in a compact cell with an external regeneration chamber. Limitations of hold up and hydrolysis in this chamber were overcome by increasing HNO_3 recycle to the cell and use of saturated packings.

The regeneration efficiency with air was further increased to the values obtainable in the laboratory by using dense foam and cooling of the external chamber. Furthermore, regeneration efficiency in the dense foam was not sensitive to air flow rate at velocities equivalent to 1-2 times the stoichiometric requirement.

2.3 Task C, The Total Cell

A new compact cell was built designed to permit the convenient testing of both individual components and total cell operation, and to avoid contaminants introduced by materials of construction. Preliminary tests in the cell of a platinized Pt fuel electrode showed the importance of careful control of the fuel feed rate, firm packaging of the electrodes, and proper current collection.

Suitable modifications were made in this test cell to improve these factors and a long term fuel electrode performance test begun. The cell was run at a current density of 50 ma/cm^2 in 30 wt% H_2SO_4 and 1 vol % CH_3OH. The same H_2SO_4 was recycled through the cell with continuous addition of CH_3OH and H_2O. After more than 800 hours of operation, the polarization was only slightly increased. However, periodic open circuiting for several seconds was required. Material balances during this run confirmed the complete conversion of CH_3OH to CO_2. The loss of CH_3OH in the CO_2 exhaust amounted to 3% of the amount reacted electrochemically. Furthermore, the diffusion of CH_3OH beyond the 80 mesh electrode was found to be negligible during cell operation with the 1 vol % fuel concentration.

Preliminary tests of total cell operation were made using the CH_3OH fuel electrode and an HNO_3 redox air electrode. Current densities as high as 95 ma/cm^2 and power densities of up to 15 mw/cm^2 were obtained at the terminals. The power output was somewhat lower than predicted due to higher than desired membrane resistance and lower than normal fuel electrode activity. However, these tests show that the cell components can be combined in a compact total cell without severe losses due to interaction effects.

Additional evaluation of the effect of H_2SO_4 concentration on total cell voltage showed that the optimum is at about 30 wt %. Furthermore, a broad plateau exists in which cell voltage does not vary by more than 20 mv. Therefore, 30 wt % H_2SO_4 will continue to be the standard electrolyte concentration.

December 13, 1962 - Esso Research Center, Linden, New Jersey

Organizations Represented: Esso Research and Engineering Company
United States Army Electronics Research and Development Laboratory

The purpose of the meeting was to brief Dr. H. Hunger, project engineer for the U.S. Army Electronics Research and Development Agency, on our progress in all aspects of the program.

3.3 Reports

This report is written in conformance with the detailed reporting requirements as presented in the Signal Corps Technical Requirement on Technical Reports (SCL-2101N, 14 July 1961) under the terms of our contract; these requirements differ from the usual requirements for reports issued within Esso Research and Engineering Company.

SECTION 4

FACTUAL DATA

4.1 Task A, Fuel Electrode

Since a soluble carbonaceous fuel requires an acid electrolyte to permit rejection of CO_2, the catalyst must be stable in this medium. Although several noble metals meet this requirement, they do not have sufficient catalytic activity. Therefore, studies of the fuel electrode have concentrated on developing catalysts containing noble metals to impart acid stability, and second components to enhance their activity. Work has centered on the preparation and testing of these catalysts, studying their mechanism, and determining their physical and chemical properties.

Phase 1 - Catalyst Performance Studies and New Preparative Techniques

Earlier work has shown that the addition of various metals to Pt often produces catalysts whose kinetic parameters differ widely from pure Pt but whose activities remain approximately constant (1). To improve upon this relatively constant activity and to better understand its cause, a variety of catalysts were prepared containing Pt or another noble metal as one component with one or more noble or base metals added. These catalysts were made primarily by the $NaBH_4$ reduction technique (1), although other methods and reducing agents were also tested.

Part a - Performance of Binary Pt $NaBH_4$ Reduced Catalysts

A number of binary Pt catalyst systems were prepared by the $NaBH_4$ reduction of mixed salt solutions. Various base metals such as Cu, Ni, Co, Pb, V, W or Mn added to Pt were tested, generally at only a single composition. All performance tests were run in 3.7 M H_2SO_4 and 1 M CH_3OH at 60°C using pressed electrodes described in Appendix A-1. Experimental measurements were made using equipment previously detailed (1).

As in previous work with electrodeposited catalysts, it was found that the addition of most metals to Pt increased its Tafel slope and exchange current. As before however, these two effects compensate in such a way that catalyst activity, as measured by polarization* at a given practical current density, remains essentially the same.

Thus, although Pt-Fe has an exchange current of 3×10^{-6} ma/cm^2 compared to 3×10^{-11} ma/cm^2 for Pt, its Tafel slope is increased from 0.049 for Pt to 0.087. The net result is that at a current density of 10 ma/cm^2, Pt-Fe and Pt are both polarized 0.56 volts from the theoretical CH_3OH open circuit potential. All other Pt-cometal catalysts exhibited similar behavior, as shown in Table A-1.

---

* Polarization, unless otherwise noted, is defined here and elsewhere as the difference between observed voltage and the voltage of a reversible electrode operating with the same reactant, temperature, pressure, and electrolyte. It is not the difference between observed and open circuit or standard reference electrode voltages.

Table A-1

Performance Of $NaBH_4$ Reduced Pt-Base Metal Catalysts

Catalyst	Polarization at Indicated ma/cm^2			Kinetic Parameters	
	1	10	50	-Log I_o	b
Pt	0.52	0.56	0.60	10.6	0.049
Pt-Fe	0.48	0.56	0.63	5.5	0.087
Pt-W	0.49	0.55	0.60	8.0	0.062
Pt-V	0.51	0.57	0.61	8.2	0.062
Pt-Ni	0.50	0.56	0.61	8.0	0.062
Pt-Cu	0.52	0.59	0.64	6.8	0.076
Pt-Co	0.47	0.55	0.61	6.2	0.076
Pt-Pb	0.50	0.57	0.64	7.6	0.066
Pt-Mn	0.46	0.52	0.57	6.4	0.071

Although the electrodeposited catalysts studied earlier agree qualitatively with these findings, an experimentally significant difference was observed between the magnitudes of the kinetic parameters of catalysts prepared by electrodeposition or by $NaBH_4$ reduction. Thus, electrodeposited Pt had an exchange current and Tafel slope of 5×10^{-8} ma/cm^2 and 0.066 respectively while $NaBH_4$ reduced Pt showed values of 3×10^{-11} ma/cm^2 and 0.049. The other $NaBH_4$ reduced catalysts had correspondingly smaller exchange currents and Tafel slopes than their electrodeposited counterparts. Again, because of the compensation of the kinetic parameters, activities remained about the same. It was also noted that a different order for the kinetic parameter values of various cometals was obtained. However, these effects with the binary catalysts may be due to differences in composition from the corresponding electrodeposited catalysts. Although no work has been conducted in this area, the differences between the two types of Pt may arise from changes in their surface areas or types of crystal face exposed.

Part b - Effect of Au or Ir Content on Pt Activity

Catalysts composed of varying amounts of Au or Ir in Pt were studied over a range of 20.5 to 76.4 atom % Au and 8.5 to 61.3 atom % Ir. The original solutions were made up to contain 20 to 80% Au and 20 to 80% Ir but because of the lower reactivity of Ir salts with $NaBH_4$, the actual content of this metal was somewhat less.

A variation of kinetic parameters with composition was found for both series of catalysts. The Pt-Ir samples reached a maximum exchange current of 1.6×10^{-7} ma/cm^2 at about 20 atom % Ir and then decreased to about 4×10^{-10} ma/cm^2 at 35%, remaining constant after this out to pure Ir. With Pt-Au, no sharp maximum was observed, rather a gradual increase to an average value of 2×10^{-7} ma/cm^2 at about 40% Au. This remained constant out to the highest concentration studied. Since pure Au has essentially no activity, a sharp decrease in exchange current can be expected between 80 and 100% Au. These results are shown in Figure A-1.

Figure A-1

Effect Of Au Or Ir Addition On Exchange Current

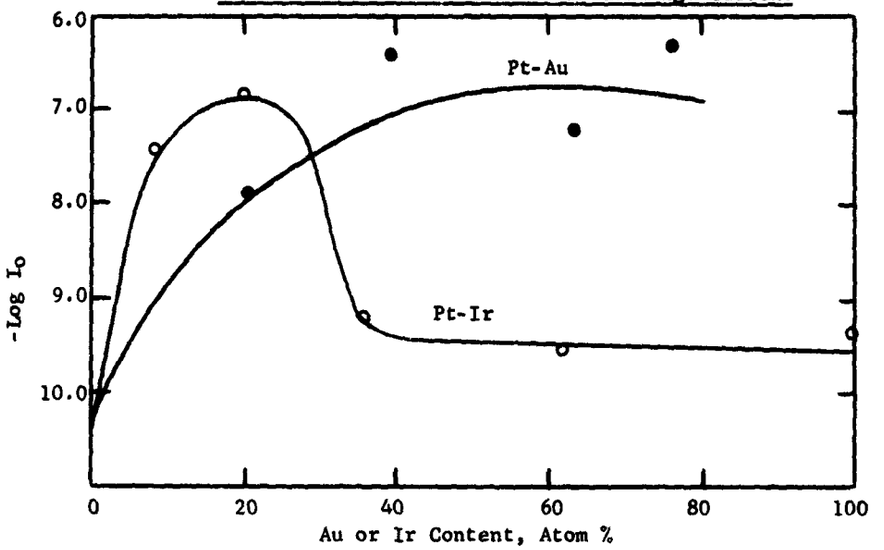

With these two catalysts the compensating effect is again operative so that no sharp changes in activity are noted. Thus, as shown in Table A-2, the polarizations at 10 ma/cm^2 for all concentrations fall within 60 to 70 mv of each other.

Table A-2

Effect Of Au Or Ir Addition On Polarization

Concentration of Cometal, Atom %	Polarization at Indicated ma/cm^2		
	1	10	50
Au			
20.5	0.48	0.54	0.58
39.0	0.50	0.56	0.62
63.0	0.48	0.54	0.59
76.4	0.55	0.60	0.66
Ir			
8.5	0.52	0.58	0.63
19.6	0.48	0.55	0.60
35.5	0.55	0.61	0.65
61.3	0.52	0.57	0.60

Part c - Other Binary and
Ternary Catalysts

The testing of other combinations of metals showed varied results. The addition of Fe and Cu to Rh caused it to lose all its activity while the addition of Au and Re produced catalysts which could not support current densities much beyond 10 ma/cm^2. Only Ir did not poison Rh. An Ir-Fe catalyst showed about the same activity as pure Ir while Ir-Re was slightly less polarized, especially at low current densities. Ternary combinations of Pt-Pd with Fe, Ir or Au showed the same characteristics as a given pair of components. Thus Pt-Pd-Fe behaved like Pt-Fe, Pt-Pd-Ir like Pt-Pd and Pt-Pd-Au as Pt-Au. These results as well as those of all the catalyst results presented in this section are given in Appendix A-2 , along with details of preparation and composition, where available.

Part d - New Catalyst Systems (P-Type)

New proprietary catalyst systems were prepared and tested in 3.7 M H_2SO_4 and 1 M CH_3OH. It was found that polarization could be reduced from that observed with Pt by about 150 mv at 60°C, the most active proprietary catalyst being polarized only 0.45 volts at 50 ma/cm^2. Even at 25°C these catalysts retained as much or more activity as Pt at 60°C, being polarized 0.53 volts at 10 ma/cm^2 compared to 0.56 for Pt. When tested with HCHO instead of CH_3OH they showed a large decrease in polarization, even greater than the 100 mv difference in theoretical potentials of these two fuels. For example, at 50 ma/cm^2 at 60°C, 1 M HCHO showed a polarization of only 0.28 volts from the theoretical CH_3OH potential. By contrast, on Pt, both CH_3OH and HCHO exhibit the same activity. Ethylene glycol was as active as CH_3OH on the new P-type catalysts while CH_3CH_2OH gave considerably more polarization. In both cases electrolyte discoloration indicated the build-up of nonreactive intermediate products.

The addition of other metals to the basic proprietary catalysts in most cases caused a performance loss. Only one metal caused no change while the worst metal produced a 130 mv performance loss. These results are detailed in Appendix A-3 and summarized in Tables A-3 and A-4 .

Table A-3

Activity Of P-Type Catalysts

3.7 M H_2SO_4 - 1 M CH_3OH - 60°C

Catalyst	Polarization@ Indicated ma/cm^2		
	1	10	50
Pt	0.52	0.56	0.60
P -Type	0.28	0.37	0.45
Modified P-Type, A	0.24	0.37	0.46
Modified P-Type, B	0.43	0.51	0.58

Table A-4

Activity Of New P-Type Catalyst With Various Fuels

3.7 M H_2SO_4 - 1 M Fuel - 60°C

Fuel	Polarization@ Indicated ma/cm^2		
	1	10	50
CH_3OH	0.28	0.37	0.45
HCHO	0.14	0.22	0.28
CH_3CH_2OH	0.61	0.71	0.81
$CH_2(OH)CH_2OH$	0.28	0.39	0.48

Part e - Reduction by $NaBH_4$ in Nonaqueous Solvents

As part of the study of reducing agents other than $NaBH_4$, many of which require H_2O free media, several reductions were performed in nonaqueous solutions. The first reducing agent used was $NaBH_4$ itself to permit a direct comparison between catalysts prepared by aqueous and nonaqueous reductions.

Three catalysts, Pt, Pt-Au and Pt-Fe were reduced in a CH_3OH solution of $NaBH_4$, using metal proportions of Pt-50 atom % Au and Pt-10 atom % Fe. All three systems reacted vigorously and the resulting finely divided catalysts were pressed into the sandwich electrodes described in Appendix A-1. They were then tested in 3.7 M H_2SO_4 and 1 M CH_3OH at 60°C. It was found that their activities and kinetic parameters agreed with the values of similar catalysts prepared in aqueous solution. For example, Pt was polarized 0.55 volts from the theoretical CH_3OH potential at 10 ma/cm^2 compared to 0.56 volts for Pt made from an aqueous solution. The corresponding Tafel slopes were 0.050 and 0.049 and the exchange currents 3×10^{-10} and 3×10^{-11} ma/cm^2. These results are shown in Table A-5.

Table A-5

Activity Of Catalysts Prepared In CH_3OH

60°C - 3.7 M H_2SO_4 - 1 M CH_3OH

Catalyst	Polarization, Volts at Indicated ma/cm^2			Kinetic Parameters	
	1	10	50	b	-Log I_o
Pt	0.49	0.55	0.59	0.050	9.6
Pt-Au 50%	0.48	0.54	0.58	0.058	8.4
Pt-Fe 10%	0.41	0.51	0.58	0.100	4.4

Part f - Other Reducing Agents

Reducing agents other than $NaBH_4$ also have been tested. Aqueous solutions of 0.5 M hypophosphorous acid and ammoniacal 0.4 M hydrazine were reacted with salt solutions of Pt, Fe, Au, Cu and Mo. In these tests, N_2H_4 reduced only Au,

Pt and Cu, in that order of reactivity, while Fe and Mo formed oxides. Hypophosphorous acid was poorer, reducing Au to the metal and Mo to molybdenum blue. No reaction was noted with the other salts. Although N_2H_4 reduced several of the metals, its reaction rate was considerably less than that obtained with $NaBH_4$.

Part g - Electrodeposited Catalysts

In addition to the work done with catalysts made by $NaBH_4$ reduction, some electrodeposited Pt and Pt-W electrodes were prepared for further comparison of the two preparative techniques. Attempts were also made to electrodeposit W and Mo from aqueous solution following procedures outlined in the literature (2). The Pt electrodes were similar to earlier ones made under the same conditions while a Pt-W electrode was somewhat poorer than Pt, being polarized 0.76 volts from the theoretical CH_3OH potential at 50 ma/cm^2 compared to 0.64 volts for Pt. These results are shown in detail in Appendix A-4. It was not possible to electrodeposit W alone from a solution of Na_2WO_4 and Na_2CO_3 even with dextrose or $FeCl_3$ added. It was also found that Mo did not deposit from a solution of ammonium paramolybdate in 10 wt % HAc saturated with KAc and NH_4Ac.

Part h - Catalysts of Difficultly Reducible Metals

In addition to the metals successfully reduced by $NaBH_4$, such as the noble metals and some base metals, a number of others showed no reduction or only a partial reduction stopping short of the metallic state when tested in the absence of a more reactive material such as Pt. Thus Zn or Mn solutions yielded only hydroxides upon reduction while W and Cr reacted only very slowly or not at all, depending upon the temperature. In the cases of Mo and V, dark brown precipitates, probably mixtures of oxides were obtained.

That the reduction of these less reactive metals may be catalyzed by the coreduction of an active metal such as Pt is suggested by the electrochemical behavior of catalysts prepared from, for example, a mixed Pt and W solution. It is found that Pt-W has an average Tafel slope of 0.062 and exchange current of 1×10^{-8} ma/cm^2 compared to the values for Pt of 0.049 and 3×10^{-11} ma/cm^2, even though not enough W has been added to offer a clear-cut lattice spacing difference. Table A-6 also shows similar effects with Mn, V and Mo.

Table A- 6

Evidence For Incorporation Of Difficultly Reducible Metals Into Pt Catalyst

Catalyst	Kinetic Parameters		Lattice Spacing, Å
	b	-Log I_o	
Pt	0.049	10.5	3.916
Pt-W	0.062	8.0	3.901
Pt-Mn	0.071	6.4	--
Pt-V	0.062	8.2	--
Pt-Mo	0.077	6.2	--

Part i - Other Catalysts

Catalysts other than those already mentioned were made by a variety of techniques. H_2WO_4 was precipitated by acidification of Na_2WO_4 solution and tested for catalytic activity in 3.7 M H_2SO_4 and 1 M CH_3OH at 60°C both by itself and physically mixed with Pt black. Essentially no activity was observed in either case. In addition, a bright Pt wire and a Pt-5% Ir wire, tested under the same conditions, also failed to exhibit activity.

Phase 2 - Alloy Formation

As part of the program for finding more active fuel electrode catalysts many of the materials prepared for the screening program were analyzed for alloy formation. The purpose was to better understand the nature of the coreduced metal catalysts.

Part a - Formation of Alloys

Many of the catalysts prepared for fuel electrode testing by $NaBH_4$ reduction of mixed salt solutions were also examined for alloy formation by means of X-ray diffraction. It was found that in almost all cases alloys were formed during the low temperature reduction of mixed salt solutions. Alloys of Pt-Au and Pt-Ir, which were most carefully studied, agreed with literature values of their lattice constants. Only with a Pt-20.5 atom % Au and a Pt-61.3 atom % Ir composition were there large discrepancies. These might be explained by a lack of complete alloying at these particular concentrations or perhaps by an error in the X-ray determination. Figure A-2 shows these relations, with the solid lines representing the literature values.

Figure A-2

Effect Of Alloy Composition On Lattice Spacing

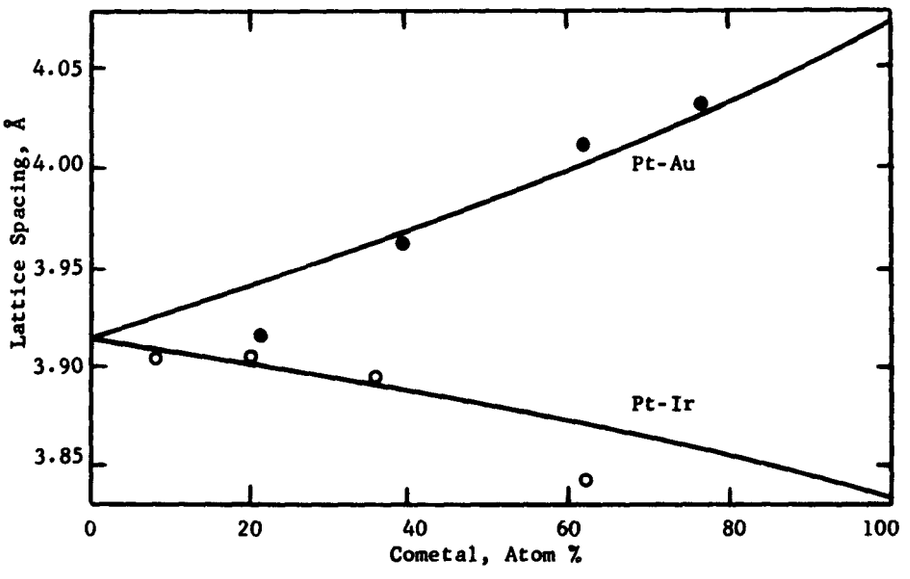

Additional evidence of alloy formation was the appearance of double sets of X-ray spectra when physical mixtures of Pt and Au or Pt and a Pt-Au alloy, for example, were analyzed. These spectra were typical of pure Pt and pure Au or pure Pt and the corresponding Pt-Au alloy respectively. Electrochemical results also confirmed the alloying of Pt and Au. A physical mixture of Pt and Au had the same catalytic behavior as pure Pt, since Au is inactive, while a Pt-Au alloy demonstrated the kinetic parameters described in Phase 1, Part b.

The other catalysts have not been analyzed for metal contents as yet, but their observed lattice constants fall within the limits of the values of the individual components. Thus a Pt-Cu alloy showed a face centered cubic structure with the unit cube length of 3.791 A while Pt and Cu, both of which are also face centered cubic, have unit cube lengths of 3.916 and 3.607 Å respectively. All other alloys also showed face centered cubic structures except for Pt-Pb. This alloy had the most complex structure, showing hexagonal, tetragonal, face centered cubic and body centered cubic phases. The first two correspond in structure and lattice constants with the PbPt and Pb_4Pt intermetallic compounds and the face centered phase is probably a Pb rich solid solution. The fourth phase cannot yet be accounted for. All of the alloys studied are presented in more detail in Appendix A-5.

Phase 3 - Performance of Heterogeneous Mo-Containing Catalysts

It has been reported that a Pt-Mo catalyst can oxidize CH_3OH to CO_2 at polarizations as low as 0.2 volts from the theoretical CH_3OH potential. However, at higher current densities an irreversible loss in performance to the level of pure Pt was experienced. To extend this low polarization activity, additional Pt-Mo catalysts have been prepared and tested. Also, metals other than Pt have been tried as cocatalysts for Mo. Finally, other fuels have been run with Pt-Mo electrodes to see if more active fuels can be found for this system.

Part a - Performance of Pt-Mo Catalysts

A Pt-Mo catalyst was run, in 3.7 M H_2SO_4 and 1 M CH_3OH at 60°C, for 136 hours at a polarization of from 0.21 to 0.27 volts at 1 ma/cm^2. The gas collected during this time was found to be CO_2. Thus the average polarization required for complete CH_3OH oxidation has been lowered to 0.24 volts for a Pt-Mo catalyst. However, at higher current densities a rapid irreversible polarization to the performance of Pt alone was again observed.

To regain the low polarization performance, Pt-Mo electrodes which had been irreversibly polarized were anodized and/or cathodized in both their electrolytes and in fresh acid to remove surface poisons or restore desorbed Mo. In no case was any reversal of the performance loss achieved. Another electrode was stripped of its catalyst. The catalyst was then redistributed on it in order to expose a fresh surface. This treatment also failed to restore the initial activity.

A number of other Pt-Mo electrodes, prepared from catalysts receiving various numbers of acid and/or H_2O washes, were also tested but no significant performance improvements were achieved. Complete results for all Pt-Mo catalysts are given in Appendix A-6 .

Part b - Pt-Mo Performance
With Various Fuels

A series of experiments were performed with Pt-Mo electrodes using HCOOH, HCHO, CH_3CH_2OH and ethylene glycols as fuels. All runs were made in 3.7 M H_2SO_4 and 1 M fuel at 60 or 80°C. Formaldehyde was the most active fuel in these systems, allowing currents of greater than 16 and 32 ma/cm^2 to be attained with low polarizations at 60 and 80°C respectively. By comparison, CH_3OH yielded only 1 and 4 ma/cm^2 at these two temperatures before a rapid polarization increase. Formaldehyde was polarized only 0.30 volts from the theoretical CH_3OH potential at 16 ma/cm^2 at 60°C and 0.25 volts at 32 ma/cm^2 at 82°C. Formic acid was intermediate, giving 8 ma/cm^2 at 60°C with 0.29 volts polarization, while CH_3CH_2OH and glycol were less active than CH_3OH. These results are summarized in Table A-7 and shown more completely in Appendix A-6.

Table A-7

Effect Of Fuel On Pt-Mo Activity

Fuel	Maximum Stable Current Density, ma/cm^2	
	60°C.	80°C
CH_3OH	1	4
HCHO	16	32
HCOOH	8	--
CH_3CH_2OH	--	2

Part c - Activity of Mo With
Other Cocatalysts

In addition to Pt, other metals were tested as cocatalysts for the Mo redox system. These included Au, Pd, Ir and Rh as well as Pt-Ir, Pt-Co and Pt-Fe alloys and various combinations of alloyed or physically mixed Pt and Au. A catalyst consisting of Pt-Mo adsorbed on activated charcoal was also tested. All experiments were performed using 3.7 M H_2SO_4 and 1 M CH_3OH at 60°C.

The only catalyst combination to perform better than Pt-Mo itself was a Pt-Mo-Co preparation which supported a maximum low polarization current of about 1.8 ma/cm^2 compared to 1 ma/cm^2 for Pt-Mo. The performance loss at current densities beyond 1.8 ma/cm^2 remained irreversible however. A Pt-Mo-Fe catalyst gave approximately the same activity as Pt-Mo while all the other combinations were inferior. Some redox activity was observed with several, but Au-Mo, Ir-Mo and Pd-Mo were completely inactive. These results are summarized in Appendix A-6.

Phase 4 - Mechanism of
Pt-Mo Catalysts

The earlier studies also reported that not only is an improvement in low current density performance noted with Mo added to a heterogeneous catalyst, but that a similar effect occurs when a soluble Mo compound is added directly to the electrolyte. Work carried out to improve the solid catalysts has been described in Phase 3. Studies of the mechanism of the CH_3OH-Mo system when Mo is added to the solution will now be presented.

Part a - Experimental Technique

Since it was suspected early in the study that the improvement in electrode performance was due to a redox cycle - chemical reduction of molybdate by fuel and electrochemical reoxidation - the work was carried out along lines designed to investigate both the chemical and electrochemical steps. The chemical step was followed by observing the products and rate of chemical reaction of Mo^{+6} (sodium or ammonium molybdate) with CH_3OH or HCHO in pre-electrolyzed 3.7 M H_2SO_4 at 82°C. The electrochemical studies consisted of obtaining chronopotentiograms on a platinized Pt microelectrode, under various conditions of molybdate - fuel interaction and adsorption, and a coulometric study to ascertain the extent of molybdate reduction. Chronopotentiograms on the platinized Pt were observed oscilloscopically and representative samples recorded photographically. Transient potentials were measured against a reference electrode in the system. Polarizations in this study are referred to the normal hydrogen reference electrode, designated N.H.E.

Part b - Chemical Reaction

The chemical reaction between molybdate (+6) and CH_3OH or HCHO was shown to require the presence of a Pt black catalyst and to result in the production of CO_2 as one product of the reaction. The rate of CO_2 production, as monitored by an infrared analyzer, was shown to be roughly equivalent to 14 ma/cm^2 for 1 M CH_3OH-0.025 M Na_2MoO_4, and about half this rate for 1 M HCHO under comparable conditions, as shown in Figure A-3 . This result is just the reverse of the reactivity order noted with heterogeneous Pt-Mo catalysts. Although continuous data on CO_2 production vs time were recorded for the CH_3OH run, the data did not plot properly for any simple rate expression. Rate data obtained using HCHO fuel and CO_2 pickup in Ascarite, however, did plot equivalent slopes at two different concentrations for a reaction mechanism first order in Mo^{+6}, as shown in Appendix A-7 . Although the reactivity order of CH_3OH and HCHO is reversed from that obtained with the Pt-Mo electrode itself, it should be pointed out that the chemical reactivity as observed by these methods need not correspond to that observed in the redox electrode system since desorption of the product molybdenum is not inherent in the electrochemical scheme while it is required in the chemical measurement.

Figure A-3

CO_2 Production From Chemical Reaction Of Na_2MO_4 - Fuel

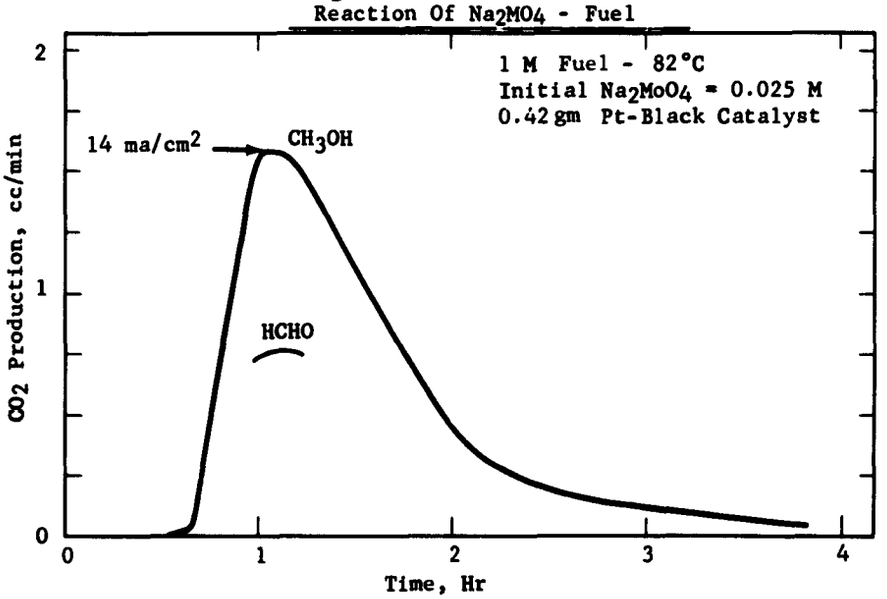

Part c - Coulometry

The molybdenum product of the chemical reaction with fuel in 3.7 M H_2SO_4 forms a red-brown solution. In the absence of a simple method of determining the valence state of molybdenum in this solution, a solution of identical appearance was prepared by electrochemical reduction of molybdate. The quantity of coulombs passed to reach equilibrium at +.25 volts vs N.H.E. was used to determine the valence state of the product solution. It was found that these coulometric results agreed within 1% of the quantity necessary for a one-electron reduction of the molybdenum, i.e. to the pentavalent state. (Table A-8, static system)

In view of the well-known complexing tendencies of molybdenum species, it was considered advisable to verify this result under conditions designed to minimize possible complex formation. Thus, a reaction of the type

$$Mo^{+6} + 3e \longrightarrow Mo^{+3} \quad \text{(electrochemical)}$$

$$Mo^{+3} + 2\ Mo^{+6} \longrightarrow 3\ Mo^{+5} \quad \text{(disproportionation or complex formation)}$$

could possibly be occuring in the system. Such an over-all reaction would also indicate the quantity of coulombs expected for a one-electron reduction.

An apparatus was designed in which Mo^{+6} was reduced at its limiting current density as it flowed through a platinized porous electrode. (Diagram in Appendix A-8). This system permits reduction of Mo^{+6} at the moving boundary in the absence of significant Mo^{+6} concentration downstream. Thus if Mo^{+3} is formed, the coulombs passed should indicate a relatively high recovery of the current from the 3-electron reduction. However, operation of this system confirmed that the reduction of Mo^{+6} was indeed a one-electron process. Based on this electrochemical evidence, shown in Table A-8 , the chemical reaction also is assumed to involve reduction to the pentavalent state.

Table A-8

Potentiostatic Coulometry Of Mo^{+6}

T = 25°C, Potential = +0.25 Volts vs N.H.E.

System	Coulombs Calculated	Coulombs Observed
Static	571	573
Flow	401	390

Part d - Electrochemical Behavior

Anodic chronopotentiograms on Pt in pentavalent molybdenum solutions and on prepared Pt-Mo electrodes in 3.7 M H_2SO_4 indicate the reoxidation of Mo^{+5} starting at potentials near +0.3 volts vs the normal hydrogen electrode (N.H.E.). Half-wave potential for the reaction in both cases was about 0.4 volts more anodic than the N.H.E., as shown in Figure A-4 . Efficient operation in conjunction with a CH_3OH electrode then necessitates that the bulk of the molybdenum be in the +5 state, in order to maintain the least polarization. Thus the chemical reduction reaction must be rapid compared to the desired current load to maintain good potentials.

Figure A-4

Anodic Transients Of Pt And Mo Systems

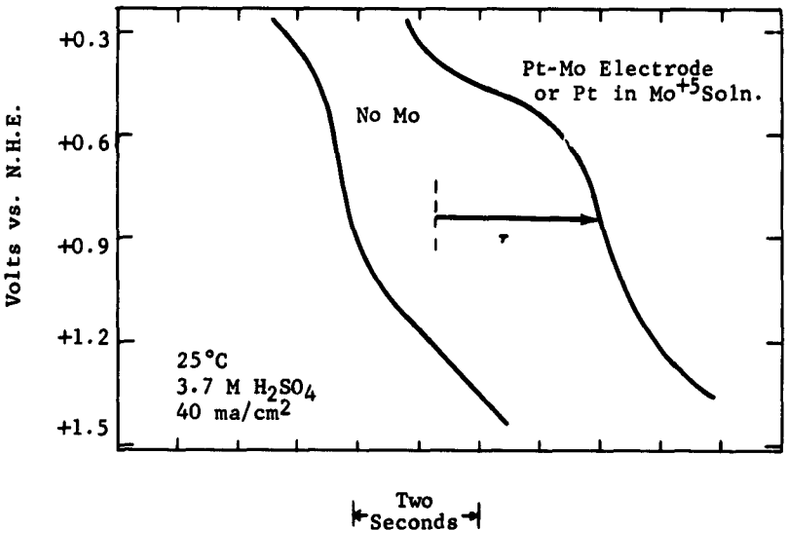

Observations on electrochemically produced solutions of Mo^{+5} indicate that only a very small quantity of Mo^{+5} exists as the free, oxidizable species. Anodic transients immediately following cathodization of the test electrode, however, indicate high quantities of oxidizable Mo^{+5}. Thus it is assumed that Mo^{+5} in solution exists as a relatively inert polymeric species which must dissociate before electrochemical oxidation can take place. Adsorbed Mo^{+5} apparently exists in a form which can be electrochemically oxidized much more easily.

Part e - Adsorption of Molybdenum

Considerable effort was directed toward defining the conditions for maintaining a favorable quantity of reactive molybdenum adsorbed on the Pt electrode surface with and without the presence of fuel. This information was obtained through the analysis of "layers", preadsorbed in various solutions of molybdate and fuel, which were rinsed and anodically stripped in a separate electrochemical cell. This technique, while allowing certain undefined variables, permits the separation and examination of independent factors in molybdate and fuel adsorption. It was found that a single chemisorbed layer of molybdate was sufficient to produce reasonably good performance in a subsequent performance run with HCHO (Appendix A-9). It was also found that molybdate adsorption must occur before contact with fuel (especially HCHO) in order to prevent permanent blocking of adsorption sites by fuel. Furthermore, an adsorbed molybdate layer in the absence of fuel was able to withstand 50 successive complete oxidations and reductions in 3.7 M H_2SO_4 with only a loss of approximately one-half the adsorbed material. A single complete oxidation in the presence of fuel however served to completely eliminate all reactive molybdenum from the electrode (Appendices A-10 and A-11).

Similar experiments designed to test the relative adsorbability of Mo^{+5} and Mo^{+6} indicatedthat adsorption of both species is comparable but that desorption of Mo^{+6} occurs more easily than that of Mo^{+5}. Thus, rinsing of preadsorbed layers of Mo^{+5} and Mo^{+6} removed far more Mo^{+6} from the electrode (Appendix A-12). Additional experiments indicated that a preadsorbed layer of fuel was essentially impervious to replacement by molybdate and thus was a potential cause of failure in the redox system (Appendix A-13).

Part f - The Proposed Mechanism

Based on the observations to date, the Pt-Mo fuel reaction mechanism for both the heterogeneous and homogeneous systems may be summarized as follows:

Chemical Reaction:

$$Mo^{+6}\ (ads) + Fuel \longrightarrow Mo^{+5}\ (ads) + CO_2 + H_2O$$

Electrochemical Reaction:

$$Mo^{+5}\ (ads) \longrightarrow Mo^{+6}\ (ads) + e^-$$

Irreversible Failure:

$$Mo^{+6}\ (ads) \longrightarrow Mo^{+6}\ (soln)$$

$$Fuel \longrightarrow Fuel\ (ads\ strongly)$$

The concept of irreversible failure by strong fuel adsorption is compatible with the fact that monolayer coverage of Pt with fuel occurs at all potentials between zero and $\sim$ +0.4 volts vs N.H.E. although no oxidation reaction occurs in these regions.

Part g - Performance of Pt-Mo Systems

Subsequent to the establishment of the Mo-fuel reaction mechanism, further testing was directed toward improving chemical catalysis of the Mo-fuel reaction, and finding means of avoiding the irreversibility discussed previously.

Platinum catalysts prepared by $NaBH_4$ reduction of Pt salts have been shown to provide superior electrode activity, especially with HCHO fuel. For example, using this catalyst with acid solutions of 1% Na_2MoO_4 at 82°C., HCHO limiting currents have been obtained in excess of 200 ma/cm^2. Activity of this degree provides about 50 ma/cm^2 at +0.26 volts vs N.H.E. (Appendix A-14). This type of electrode shows an activation energy for molybdate electro-oxidation of $\sim$11 kcal/mole (Appendix A-15). Methanol activity on similar electrodes was low, however, the performance being comparable to Pt alone beyond $\sim$ 5 ma/cm^2. A single electrode prepared by this technique showed good reversibility for the HCHO reaction after a long series of tests. It is possible that an aging effect, with loss of fuel adsorbability, was responsible for this improved reversibility. Electrodes in all cases may be reactivated by removal to fresh 3.7 M H_2SO_4 solution and alternate anodization and cathodization. Thus the concept that it is necessary to remove strongly adsorbed fuel from the electrode is reinforced.

A brief screening was carried out to see if other catalysts in addition to Pt might be suitable for the $Mo^{+5} \longrightarrow Mo^{+6}$ electrochemical reaction. Initial

tests were made on Au, W and Ta, using constant current scanning techniques. It was found that of the three tested, both Au and W showed electrochemical activity for Mo^{+5} oxidation. Since neither material shows appreciable affinity for the fuel electrochemical reaction, this finding advances the possibility of a mixed catalyst with electrochemical oxidation and chemical reduction taking place on different sites. A Pt+Au electrode prepared to test this concept, however, exhibited HCHO activity comparable to that of Pt alone. As yet, no more successful system has been prepared. Results with Pt and Pt+Au are detailed in Appendix A-16.

Part h - Other Redox Couples

In addition to the Mo^{+6} - Mo^{+5} couple, a brief survey was made of other couples which might exhibit similar behavior with CH_3OH. Thus, the ferro-ferricyanide, ferrous-ic-tartrate, ferrous-ic-oxalate and cobaltous-ic-oxalate couples were screened in 3.7 M H_2SO_4 at 25°C. The tests consisted of observing the constant current oxidation waves of the reduced forms of the couples on platinized Pt. No significant oxidation was shown by these systems.

Phase 5 - Further Mechanism Studies With Pt

In addition to the mechanism work performed with the Pt-Mo system, further work has been carried out on the reaction of CH_3OH with Pt catalyst in order to better understand the limitations of this system (1).

Part a - Experimental Technique

Information on the CH_3OH reaction limitations on Pt black has been obtained from a voltage scan study. This technique involves the measurement of current at an electrode as its potential is linearly changed between two desired levels. Peak currents during this procedure are related to rate limitations in the system and can be used for kinetic analysis. The scans were obtained by driving a platinized Pt electrode with a potentiostat fed by a motor driven linear potentiometer. Currents were measured from the voltage drop across a precision resistor. A diagram of the apparatus will be found in Appendix A-17. Voltage scans were obtained for the CH_3OH reaction on a Pt black electrode, both as a function of temperature and CH_3OH concentration. A typical scan for 1 M CH_3OH @ 25°C is shown in Figure A-5 . Appearance of distinct separated forward and reverse peaks is characteristic of these oxygenated fuels (3).

Figure A-5

Typical Voltage Scan On Pt In 1M CH_3OH

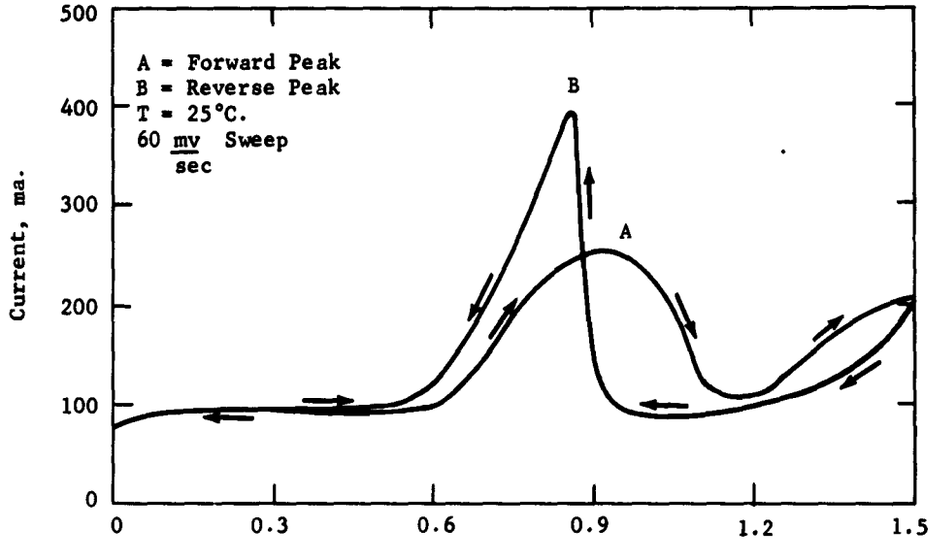

Part b - Temperature Study

The voltage scan technique was applied to a CH_3OH electrode operating at various temperatures in the range 25-75°C. Current-voltage traces were obtained for a potential sweep from 0 - +1.5 volts vs N.H.E. in 1 M CH_3OH - 3.7 M H_2SO_4. Forward and reverse peak currents were measured and plotted vs reciprocal Kelvin temperature.

The data indicate two distinct processes with different activation energies for the forward and reverse scans. Thus forward scanning indicates a process with 9.4 kcal/mole activation, too high for diffusional limitation, while reverse scans indicate the possibility of a diffusion limited reaction with 5.3 kcal/mole activation (Appendix A-18). This evidence indicates activation of the Pt surface following the reduction of surface oxide. Moving the electrode potential into less positive potential regions however appears to deactivate the surface and cause the appearance of a nondiffusional limitation.

Part c - CH_3OH Concentration Study

Voltage scan information was also obtained in systems at 25°C with CH_3OH concentration varying between 0.025-1.0 molar in 3.7 M H_2SO_4. Forward and reverse peak currents were plotted against CH_3OH concentration. It was found that reverse peak currents gave a fairly linear dependence on CH_3OH concentration. Forward peak currents however did not give a linear dependence above CH_3OH concentrations of 0.25 M. (Figure A-6)

Figure A-6

Dependence Of Forward And Reverse
Peak Currents On CH_3OH Concentration

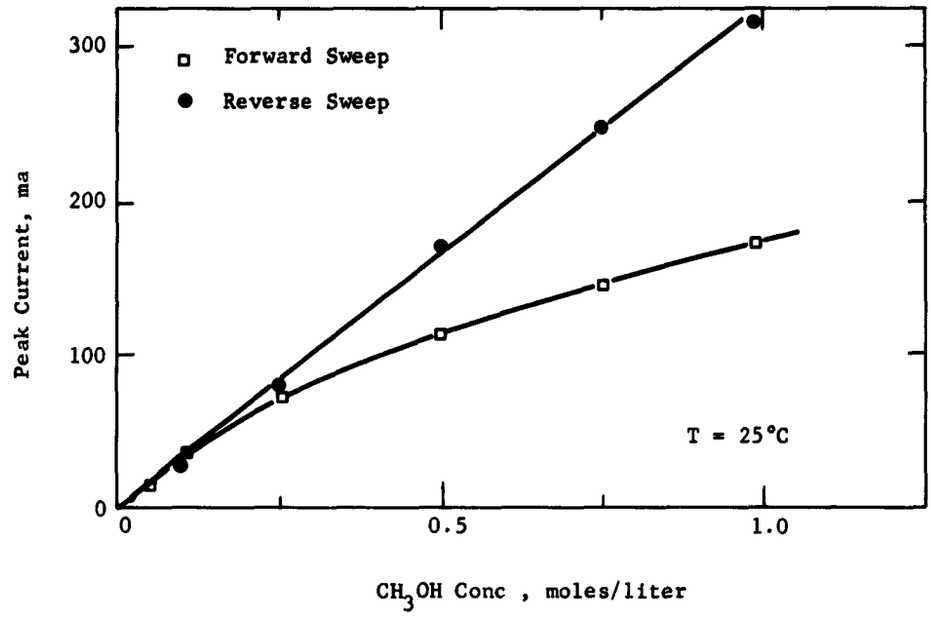

The nonlinear forward peak dependence is compatible with the adsorption control previously postulated from other types of experiments(1). The linearity of reverse peak currents, moreover, is entirely consistent with the low energy of activation observed in the temperature study, if a diffusional limitation is assumed to exist in the reverse scan.

4.2 Task B, Air Electrode

As previously reported (1), a unique redox system is being developed for use at the air electrode in the methanol-air fuel cell. This redox system is based on the electrochemical reduction at the cathode of a small amount of HNO_3 (1 wt %) in the H_2SO_4 electrolyte. Its inherent advantage compared with a conventional air electrode is relatively stable performance with low polarization at practical current densities. However, this system requires efficient chemical regeneration of HNO_3 from the electrochemical reduction products in order to minimize HNO_3 loss and the problems of replacing it. Therefore, laboratory research has concentrated on improving regeneration efficiency. In addition, engineering studies have begun on applying these results to practical cell configurations.

Phase 1 - HNO_3 Regeneration, Laboratory Studies

The regeneration of HNO_3 in H_2SO_4 involves the oxidation of NO formed at the electrode with O_2 from air to NO_2 with subsequent hydrolysis of NO_2 to HNO_3. The first of these steps is slower in the electrolyte solution than the second, and efficient regeneration cannot be achieved by simply passing air through the electrolyte. Therefore, two approaches to improve regeneration were studied. In one approach, increased surface area was provided in and above the solution with a glass wool packing. In the other, a foaming surfactant was added to obtain more effective contacting of NO and O_2 within the resulting small foam bubbles.

Part a - Experimental System

The experiments were conducted under standardized conditions to compare results on a relative basis. All runs were carried out in a concentric glass cell with a driven 5 cm x 7.6 cm platinum basket anode. A platinized platinum electrode with approximately 6 mg/cm^2 of platinum black was employed as the cathode. The equipment was detailed in the previous report (1).

The electrolyte was 3.7 M electrolyzed H_2SO_4 (30 wt %) and 0.2 M HNO_3 (1 wt %). Air or oxygen was injected into the solution at flow rates between 15 and 30 cc/min. These flow rates are several times in excess of the stoichiometric amount. The gas injector was a horizontal glass frit with downward gas flow. The temperature was 82°C and the current density approximately 30 ma/cm^2, with two runs at 72 and 93 ma/cm^2, respectively. Catholyte and anolyte compartments were separated by an alundum thimble wrapped with an ion-exchange membrane. The surfactants were employed in concentrations between 0.05 and 1.0 wt % and the foam layer was held at a fixed level with minimum fluctuations. The polarization of the air electrode increased at lower HNO_3 concentrations and varied between 0.2 and 0.4 volts relative to theoretical O_2. The results of these tests are summarized in Appendix B-1 .

Part b - Test of Surfactants

Previous studies showed that using foaming agents in the regeneration cell improves contacting between NO and O_2 for the gas reaction within the foam bubbles. The foam also furnishes electrolyte in the walls of the bubbles, thus supplying a means for draining HNO_3 back to the bulk electrolyte.

The main difficulty encountered in the previous experiments was that the available surfactants degraded in the highly oxidative cell atmosphere. The best of the tested compounds was sodium dodecyl oxydibenzene disulfonate (Benax 2A1 of Dow Chemical Co.). Thus, several other compounds of the same type were tried. These are listed in Appendix B-1. Of these, only nonyl oxydibenzene disulfonate proved to have improved oxidation stability giving a stable foam during 90 hours under load. Table B- 1 summarizes these results.

Table B-1

Effect Of Structure On Surfactant Stability

Surfactant	Life Under Load in Cell, Hours
Sodium nonyl oxydibenzene disulfonate	90
Sodium dodecyl oxydibenzene disulfonate	30
Sodium dodecyl oxydibenzene disulfonate (higher purity)	30
Mono phosphate ester of tridecyl alcohol-ethylene oxide adduct	20
Tridecyl alcohol-ethylene oxide adduct	10
Oxydibenzene of high molecular weight	Unstable Foam

The use of the longer lived nonyl compound significantly improved the number of regenerations. This effect is shown in Table B-2, where the regeneration results with the two best surfactants are tabulated.

Table B-2

Effect Of Surfactant On HNO_3 Regeneration Using Oxygen

82°C 30 ma/cm^2 3.7 M H_2SO_4 - 0.2 M HNO_3
Platinized Pt Cathode 1 wt % Surfactant,
O_2 Flow 15 cc/min

Surfactant	Regeneration Efficiency Coulombs/Coulomb Equivalent to HNO_3 Consumed
Sodium dodecyl oxydibenzene disulfonate*	24.0
Sodium dodecyl oxydibenzene disulfonate	28.0
Sodium dodecyl oxydibenzene disulfonate (higher purity)	13.3
Sodium nonyl oxydibenzene disulfonate	35.0
Sodium nonyl oxydibenzene disulfonate**	40.4

* Reported earlier (1)
** 0.4 M HNO_3, 1 wt % surfactant added in middle of run

Similar runs using air as oxidant however showed no difference in regeneration efficiency when results with the two more stable compounds were compared. In both cases, the surfactants were not completely decomposed and a stable foam layer was maintained after consumption of the available HNO_3. Thus, using air as oxidant makes the physical stability of the single foam bubbles and the contacting of the gases much more important than the chemical stability of the surfactants.

In the same runs, surfactant concentration was varied from 0.05 to 1 wt % without significant effect. These findings are tabulated in Table B-3.

Table B-3

Effect Of Stable Surfactants On HNO_3 Regeneration Using Air

82°C 30 ma/cm^2 3.7 M H_2SO_4 - 0.2 M HNO_3
Platinized Pt Cathode, Air Flow 10 to 20 cc/min

Surfactant		Regeneration Efficiency Coulombs/Coulomb Equivalent to HNO_3 Consumed
Sodium dodecyl oxydibenzene disulfonate	1 wt %	14.0
Sodium nonyl oxydibenzene disulfonate	1 wt %	11.0
Sodium nonyl oxydibenzene disulfonate	0.2 wt %	14.6
Sodium nonyl oxydibenzene disulfonate	0.05 wt %	12.0

Part c - Effect of Fine Powders on Regeneration

As shown above, regeneration with air was mainly limited by the physical stability of the foam. To increase this stability, extremely fine silica powder was added to the electrolyte. The powder (Cab-O-Sil of Cabot Corp.) had 0.010 to 0.015 micron particle size with 200 m^2/gm surface area. It was soaked in electrolyte solution for 24 hours prior to use. The optimum concentration in the electrolyte was found to be in the range of 1 wt %. When this powder was used alone, a slight increase in the regeneration efficiency due to increased surface area was obtained. When used in combination with surfactant however, a large synergistic effect was observed and the number of regeneration cycles on air more than doubled from 11 to 25. Table B-4 illustrates these results.

Table B-4

Effect Of Fine Silica Powder On Regeneration

82°C 30 ma/cm^2 3.7 M H_2SO_4-0.2 M HNO_3
Platinized Pt Cathode, Air Flow 15 to 20 cc/min

Surfactant	Silica Powder	Regeneration Efficiency Coulombs/Coulomb Equivalent to HNO_3 Consumed
None	None	2.1
None	1.0 wt %	3.5
Sodium nonyl oxydibenzene disulfonate, 1.0 wt %	None	11.0
Sodium nonyl oxydibenzene disulfonate, 0.2 wt %	1.0 wt %	25.0

Part d - Effect of Increased Current Density

Two runs were made using oxygen at 93 and 72 ma/cm^2 with sodium nonyl oxydibenzene disulfonate and compared with corresponding experiments which were performed at 30 ma/cm^2, to find the effect of current density on regeneration efficiency.

Operation at 93 ma/cm^2 proved difficult in this equipment and gave poor results. However, the regeneration efficiency at 72 ma/cm^2 amounted to 225 coulombs/coulomb equivalent to HNO_3 consumed as compared with only 35.2 coulombs/coulomb equivalent to HNO_3 consumed at 30 ma/cm^2. These results are presented in Table B-5. This increased efficiency was probably a result of better foaming patterns and the fact that more coulombs pass through the circuit while the foaming agent is being subjected to the intense oxidizing atmosphere.

Table B-5

Effect Of Current Density On HNO_3 Regeneration

82°C 30 ma/cm^2 3.7 M H_2SO_4 - 0.2 M HNO_3
Platinized Pt Cathode, O_2 Flow 20 to 25 cc/min
1.0 wt % Sodium Nonyl Oxydibenzene Disulfonate

Current Density ma/cm^2	Regeneration Efficiency Coulombs/Coulomb Equivalent to HNO_3 Consumed
30	35.2
72	225.0*
93	10.0

* 0.2 wt % sodium nonyl oxydibenzene disulfonate

Part e - Effects of $NaNO_3$ on Regeneration

Sodium nitrate was tested again as a possible inexpensive and easily storable substitute for HNO_3. When added to H_2SO_4 it forms the HNO_3 required for reduction at the cathode. Previously, it gave slightly lower regeneration efficiencies although the electrode performance was comparable to HNO_3. With the improved technique used in the current tests, it performed similarly to HNO_3 as shown in Table B-6.

Table B-6

Effect Of $NaNO_3$ On HNO_3 Regeneration

82°C 30 ma/cm^2 3.7 M H_2SO_4
Platinized Pt Cathode, Air Flow 12 cc/min

Nitrate Source	Surfactant	Regeneration Efficiency Coulombs/Coulomb Equivalent to HNO_3 Consumed
0.2 M HNO_3	Sodium dodecyl oxydibenzene disulfonate 1.0 wt %	14.0
0.2 M $NaNO_3$	Sodium nonyl oxydibenzene disulfonate 0.2 wt %	14.6

Phase 2 - HNO_3 Regeneration, Engineering Studies

The purpose of the engineering research work in the HNO_3 regeneration study has been to develop a test system which is similar to an ultimate compact fuel cell. This system must fit the anticipated requirements of the ultimate cell, particularly compactness and simple operation, while achieving efficient HNO_3 regeneration.

An external regeneration system wherein the reduction products of HNO_3 are converted to HNO_3 was selected as the most promising. This type of system permits compact cell design since the space required for regeneration is external to the electrolyte compartments. It also minimizes the loss of performance at the nitric acid electrode that has been shown to occur if air flows along the electrode. Finally, it permits a lower temperature in the regeneration chamber which favors more efficient HNO_3 regeneration.

Part a - Experimental System

The compact experimental Teflon cell and external regeneration chamber are shown in Appendix B-2. The Teflon cell has 4 inch square electrodes, a size adopted as a standard for engineering studies. The regeneration chamber is a 1 inch diameter by 6 inch glass tube mounted above the cell and connected by 3 ports. A similar 2 inch diameter tube was used in initial work, but results showed that the larger volume was not used effectively. A schematic of this system is shown in Figure B-1.

Figure B-1

External Regeneration System

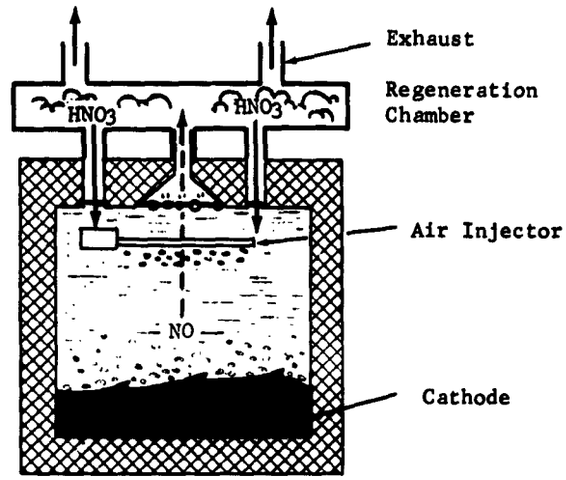

Air is introduced downward through an injector mounted at the top of the cell just below the electrolyte surface. It is mixed with NO gas which is formed at the electrode surface by virtue of the electrochemical reaction of HNO_3. The gases pass through the center exit port into the regeneration chamber which contains a packing material or foam generated in the catholyte by the addition of a small amount of surfactant. Nitric acid formed in the chamber drains back to the cell through the side ports.

Regeneration efficiencies were measured during half cell tests in which the cathode was an 80 mesh or a 150 mesh platinum screen platinized with 8 mg/cm^2 of platinum black. The experimental equipment is shown in detail in Appendix B-3. The tests were made by measuring the amount of HNO_3 consumed from a known initial charge while the cell was operating at 30 ma/cm^2 for a given time interval. The final HNO_3 concentration was determined by measuring the final limiting current in the cell. The relationship between limiting current and HNO_3 concentration is shown in Appendix B-4. In this way the total coulombic output of the half cell was compared with the coulombs equivalent to HNO_3 consumed. The results of all these tests are recorded in Appendix B-5.

Part b - Electrode Performance

The electrode performance was measured on the 4 inch square, 80 mesh electrode at 82°C with 1 wt % HNO_3 in 30 wt % H_2SO_4. The electrode was polarized 0.17 volts from theoretical oxygen at 30 ma/cm^2 and had a limiting current of 160 ma/cm^2. These results agree with values for smaller electrodes used in previous laboratory work. The complete comparison is shown in Figure B-2.

Figure B-2

HNO_3 Electrode Performance

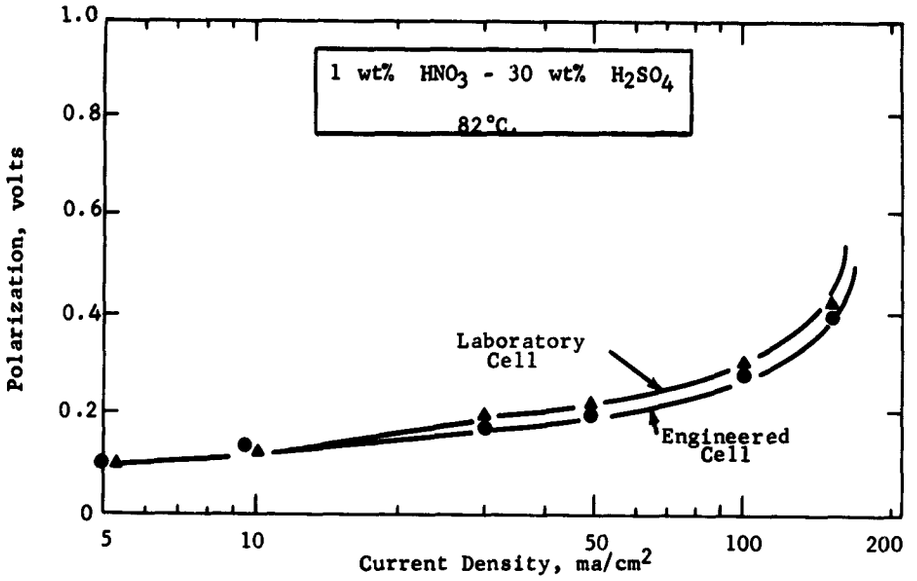

With air injection at the top of the catholyte compartment, there was no loss in the HNO_3 electrode performance due to stirring at air flow rates from 0 to 550 cc/min., a value over ten times the stoichiometric requirement.

Part c - Limitations in
HNO_3 Regeneration

The regeneration of nitric acid from the NO gas produced at the electrode by electrochemical reduction involves the following reactions.

Oxidation: $2\ NO + O_2 \rightarrow 2\ NO_2$

Hydrolysis: $3\ NO_2 + H_2O \rightarrow 2\ HNO_3 + NO$

Either of these reactions can be the rate determining step depending on the type of regeneration system. An added limitation of holdup can occur with an external regeneration system. This results when regenerated HNO_3 is not recycled from the external chamber to the cell catholyte. It was observed in tests where a dry glass wool packing was used in the chamber so that any HNO_3 formed was held in the packing by capillary forces. Holdup was also observed without packing when a foaming agent was used. With gas flow from all exit ports, the liquid recycle to the cell was inhibited. In each case, regeneration with both air and O_2 was limited to approximately 2 coulombs/coulomb equivalent to HNO_3 consumed.

The hydrolysis limitation was observed when a recycling sparse foam was used in the external chamber. This sparse foam consists of large, unstable bubbles. The small surface to volume ratio of the bubbles results in insufficient capacity for the hydrolysis reaction. In such a case both air and O_2 were observed to give approximately 4 regenerations.

To achieve the higher regeneration efficiencies, it is necessary to develop a system in which the rate limiting step is the gas phase oxidation of NO. This was accomplished by using a recycling sparse foam to eliminate holdup, augmented by saturated glass wool to improve hydrolysis. In such a system, regeneration efficiencies of 6 and 15 coulombs/coulomb equivalent to HNO_3 consumed were measured on air and O_2 respectively. The difference in performance for air and O_2 verifies that the oxidation reaction was limiting. These findings are summarized in Table B-7.

Table B-7

Limitations In External HNO_3 Regeneration

Limitations in HNO_3 Regenerator		Regeneration Efficiency, Coulombs/Coulomb Equivalent to HNO_3 Consumed	
Nature	Cause	Air	O_2
Holdup	Unsaturated Packing	1.2	1.5
	Nonrecycling Sparse Foam	2.6	2.2
Hydrolysis	Recycling Sparse Foam	4.4	4.5
Oxidation	Saturated Packing With Surfactant	6.2	15.0

Air Flow Rate = 1.4 - 1.5 Stoichiometric Requirement
O_2 Flow Rate = 7.0 - 7.5 Stoichiometric Requirement
Regeneration Chamber Temperature = 75°C

The equilibrium for the oxidation reaction is shifted in the direction of increased NO_2 production (4) and the specific rate constant is increased (5) by lower temperatures. Therefore more efficient regeneration should be attainable at lower temperatures. Since the rate expression is

$$\text{rate} = k^o P_{O2} P^2_{NO}$$

where

k^o = specific rate constant
P_{O2} = partial pressure of oxygen
P_{NO} = partial pressure of nitric oxide

the reaction rate is also increased by greater O_2 and NO pressures.

Part d - Effect of Foam Density

In the initial studies with the external regeneration system using surfactant as a foaming agent, the air injector was a 3/16 inch diameter by 3 inch Teflon tube with 10 small holes, diameter ~ 300 microns. The resulting foam has been referred to as a "sparse foam" and characterized as having large, unstable bubbles. In order to get more dense foam with a higher surface to volume ratio, the Teflon air injector was replaced with a similar thin wall porous glass tube, pore size = 10-20 microns. The tube wall was 1/16 inch thick which permitted air flow rates up to 150 cc/min at less than 1 psig, approximately 3 times the stoichiometric requirement at 30 ma/cm^2. With the smaller pores in this air injector, very dense small bubble foams were produced in the regeneration chamber using 0.5 wt % sodium nonyl oxydibenzene disulfonate as a foaming agent in the catholyte.

The regeneration efficiency was increased with the dense foam. The hydrolysis limitation which restricted efficiency to 4.5 regenerations with both air and O_2 in the case of the sparse foam was eliminated. The dense foam gave up to 5.4 regenerations on air and 8.6 regenerations on O_2 at a temperature of 75°C in the external chamber. In addition, the rate of NO oxidation in the dense foam was increased by decreasing the foam temperature in the external chamber to 50°C. Regeneration efficiency improved to 14.6 and over 42 coulombs/coulomb equivalent to HNO_3 consumed for air and O_2 respectively. These results are summarized in Table B-8.

Table B-8

Effect Of Foam Density On HNO_3 Regeneration Efficiency

Type of Foam	Temperature in Regeneration Chamber	Regeneration Efficiency, Coulombs/Coulomb Equivalent to HNO_3 Consumed	
		Air	O_2
Sparse	75°C	4.4	4.5
Dense	75°C	5.4	8.6
	50°C	14.6	>42

Air Flow Rate = 1.5 - 2.0 Stoichiometric Requirement
O_2 Flow Rate = 7.5 - 10 Stoichiometric Requirement

In the tests with lense foams, the capacity of the recycle system was not sufficient to give a true value for the regeneration efficiency by the standard procedure. Thus, it was necessary to discontinue the current for 5 or 10 minutes every hour in order to allow the regenerated HNO_3 to drain into the cell. The results of these extended runs showed that the efficiency increased with time until the final steady state value was achieved. At air flow rates greater than stoichiometric and regeneration chamber temperatures of 50°C or less, the efficiency

increased to over 20 coulombs/coulomb equivalent to HNO_3 consumed after about 2 hours. An example at 1.1 stoichiometric air flow is shown in Figure B-3.

Figure B-3

Effect Of Extended Runs On Regeneration Efficiency In Dense Foam

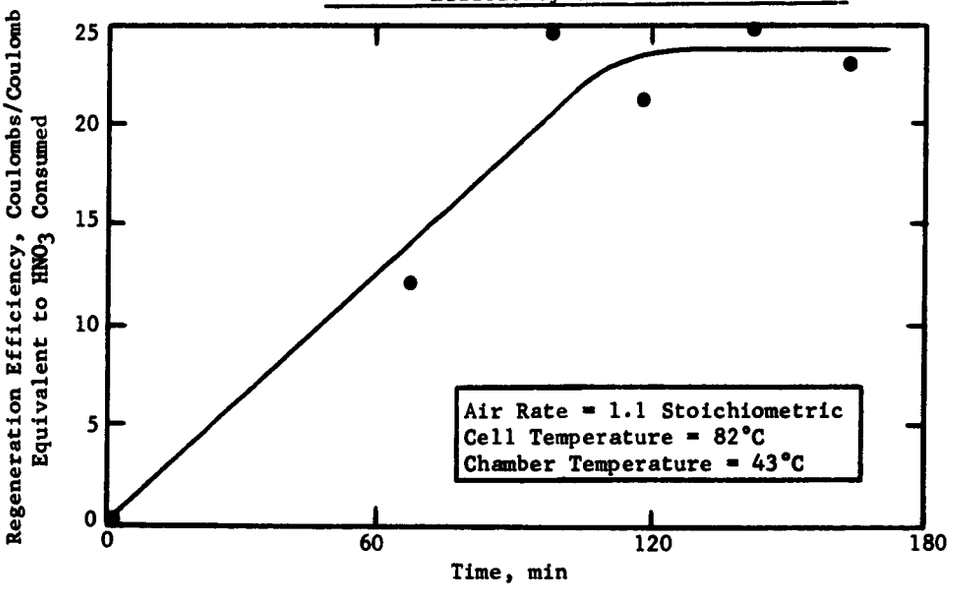

Part e - Effect of Air Flow Rate

An important variable in the operation of the final methanol - air cell will be the air flow rate, since it affects problems of heat and mass transport. Therefore, the effect of air rate on regeneration efficiency was measured in order to determine the sensitivity required for control and possible limitations in total cell operation.

Tests were made in both sparse and dense foams and it was found that the sensitivity of the regeneration efficiency depended on the type of foam. For the sparse foam, under a variety of operating conditions, the efficiency was low and had a sharp maximum of about 6-8 regenerations at an air rate of 1.4 times the stoichiometric requirement. Variation in the air rate of $\pm$10% resulted in little regeneration. The sharpness of this maximum was somewhat influenced by the reflux rate to the cell. However in the case of the dense foam, the efficiency was much greater and remained constant at about 25 regenerations at air flow rates between 1 and 2 times stoichiometric. The results are shown in Figure B-4.

Figure B-4

Effect Of Air Flow Rate On HNO_3 Regeneration Efficiency

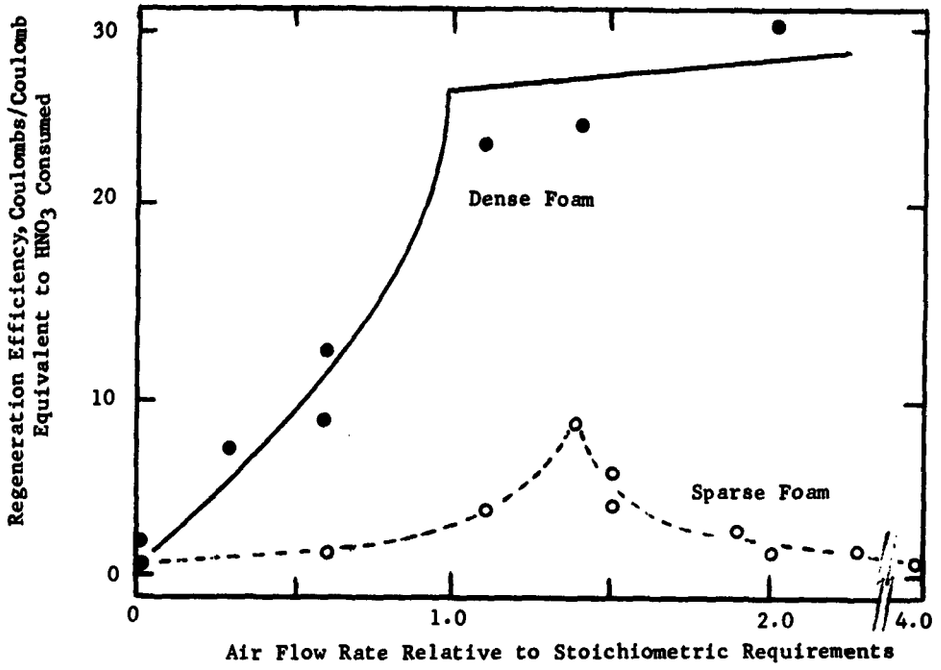

The observed behavior for the sparse foam would be expected from a consideration of the rate equation for NO oxidation, i.e.

$$\text{rate} = k^{o} P_{O_2} P^{2}_{NO}$$

At air flow rates below the stoichiometric requirement, regeneration is low because insufficient O_2 is being supplied to recover all of the NO. At very high flow rates, the increased supply of O_2 is offset by dilution with N_2 which decreases the partial pressure of NO. The large unstable bubbles in the sparse foam favor mixing of NO and air which would account for this general type of behavior. However, the fact that the maximum occurs at 1.4 stoichiometric probably results from the particular design of the cell and regeneration system.

In the case of the dense foam the reaction bubbles are more stable. This results in less thorough mixing and the partial pressure of NO is maintained at a high level. The result is that at air rates greater than stoichiometric the regeneration process is not sensitive to air flow rate.

4.3 Task C, The Total Cell

Several new compact fuel cells were also constructed to study the operation and interactions of these components in a complete unit cell. The major emphasis of the work during the past six months has been aimed at studying the performance of the methanol electrode in the presence of the air-HNO_3 redox system. However, half cell studies were also made in these new units to help determine the nature of the operating problems.

Phase 1 - Construction of Compact Fuel Cell

Briefly, the electrodes in the new cell are square, four inches on the side, permitting the use of more efficient feed addition and product removal ports. The square design facilitates quick modification and assembly. Supports in the electrolyte chambers are used to position the electrodes and membrane. The spacing between the electrodes is easily modified by use of selected Teflon spacers. The new compact Teflon cell is illustrated in Figure C-1 and Appendix B-2.

Figure C-1

New Teflon Fuel Cell

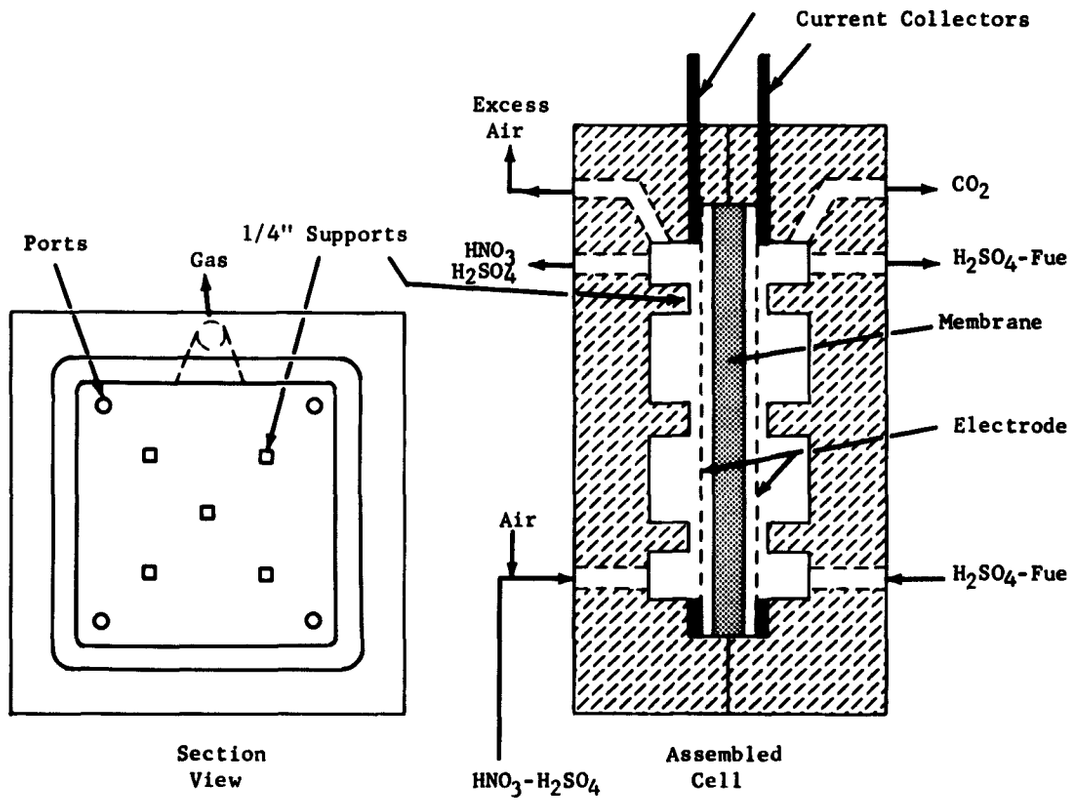

Phase 2 - Methanol Electrode Life Studies

The compact Teflon cell with square 4" x 4" electrodes was set up as a methanol half cell using a direct current source in series to drive the cathode. The purpose of this setup was to evaluate long term electrode performance independently of the other factors that affect total cell operation. This was necessary to distinguish between effects attributable to total cell interactions and those present only at the fuel electrode. In addition, this cell was used to obtain engineering information needed to improve the design of the cell and its components. A total of six long term performance runs were made in addition to a number of short term electrode washing and electrode orientation studies.

Part a - Initial Methanol Electrode Performance Run

All of the methanol electrode performance studies were carried out at about 50 ma/cm^2 and 80°C using 30 wt % H_2SO_4 containing methanol fuel. The H_2SO_4 and methanol were largely commercial grade. In these runs the methanol feed and water were added continuously to an H_2SO_4 electrolyte stream being recycled through the cell in a manner similar to that shown in Figure C-6. Data from these runs are summarized in Appendix C-1.

The first experiment, lasting 140 hours, served to establish the operability of the cell and the auxiliary feed system. It was found that small pressure fluctuations in the exit gas streams or fuel feed resulted in voltage losses as high as 50 mv. Hence, the cell was modified for smoother gas exit and a baffle plate was installed in the fuel chamber for more rapid dispersal of fuel.

With these modifications, the cell was successfully operated for a scheduled 500 hour period using commercial grade methanol. The methanol reacted completely to CO_2 and H_2O, the fuel consumption checking the number of coulombs produced to within 1%. The performance of the electrode gradually decreased with time from its initial polarization of 0.62 volts so that the polarization at 354 hours amounted to 0.77 volts. However, the technique of periodically open circuiting the cell restored a large fraction of the performance. The results of this run are highlighted in Table C-1.

TABLE C- 1

Effect Of Constant Current And Open Circuiting On Polarization

Constant Current		Open Circuiting	
Run Hour	Polarization, Volts	Run Hour	Polarization, Volts
2	0.65	355	0.67
100	0.66	400	0.69
354	0.77	500	0.70

Subsequent analysis of the electrolyte after the run showed that the methanol concentration gradually built up within the cell from 2 vol % to 9 vol %. This excess occurred as a result of a slight error in setting the feed rate. Previous data indicated that increases in concentration of this magnitude would result in an increased polarization. This appears to account for most of the polarization increase that was not corrected by open circuiting the cell.

The initial performance of the platinum black electrode used in the first run was about 50 mv below the value usually obtainable. Hence, it was desired to employ an electrode with normal initial activity. Consequently, other attempts at a long run were made with electrodes having higher initial activity in which closer control of the methanol feed rate was maintained. In these runs operability was poor as evidenced by severe voltage oscillations. These runs were terminated after 120-200 hours because of external failures of the feed pump and heat controller. In view of the operability problems a series of short tests were made, designed to aid in improving performance of the cell.

Part b - Electrode Washing Studies

In the first of these tests an electrode not showing normal activity was washed continuously with fresh electrolyte solution in an attempt to attain normal activity. The electrode consisted of 80 mesh platinum-rhodium screen, freshly coated with 8 mg/cm^2 of platinum black, and separated from the direct driven cathode by an AMFion C313 membrane. The C313 membrane was pretreated in H_2SO_4-HNO_3 solution at 80°C to remove harmful impurities. The electrolyte solution in the tests consisted of 1 vol % methanol in 30 wt % H_2SO_4. The polarization was observed while pumping the electrolyte solution (500 ml/hour) once-through the cell at 82°C and a current density of 50 ma/cm^2.

Normal activity of the electrode was attained after washing it with about 1.5 liters of the electrolyte, as evidenced by a reduction in polarization from 0.60 to 0.54 volts. This washing improvement is shown in Figure C-2. Detailed data are given in Appendix C-2.

Figure C-2

Effect Of Washing On Electrode Polarization

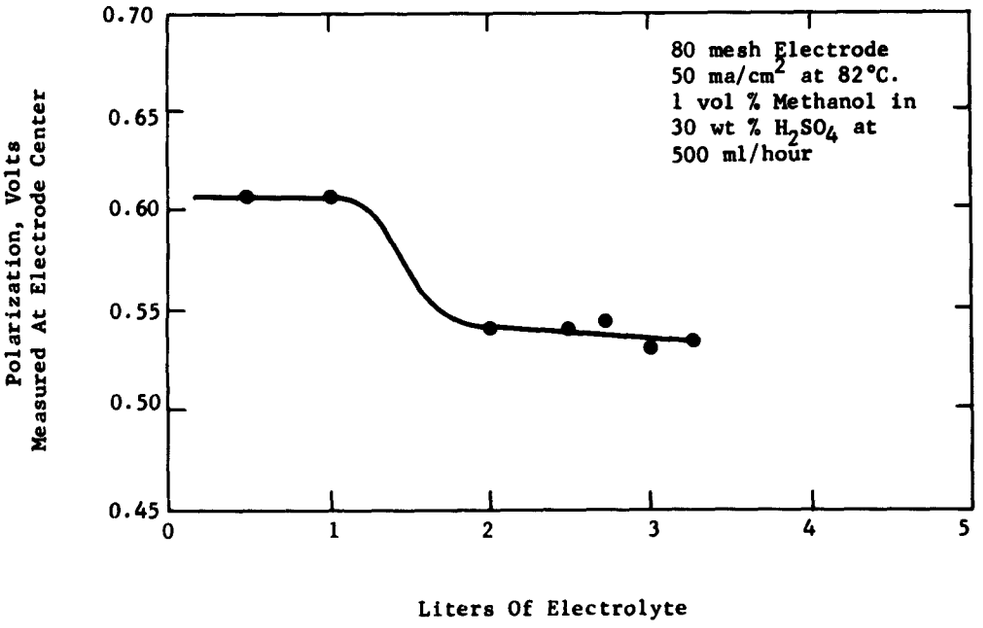

In other similar washing tests, a 150 mesh electrode prepared two months earlier and stored in water had normal activity. A second freshly platinized 80 mesh electrode required washing to attain normal activity. These data suggest that some impurity left from the platinum black electrodeposition step, such as chloride, is removed by washing the electrode.

Part c - Electrode Orientation Studies

A series of tests was made with 52, 80 and 150 mesh size electrodes, which were tilted at various angles to determine the influence on the voltage oscillation. All of the tests were made at 82°C and 50 ma/cm^2 using 1 vol % methanol in 30 wt % H_2SO_4. The 52 mesh electrode showed the smallest oscillations of 5 to 10 millivolts compared with 50 to 60 millivolts using the 80 and 150 mesh screens. The data are summarized in Table C-2 and given in detail in Appendix C-3.

TABLE C-2

Effect Of Electrode Mesh On Voltage Oscillation

Electrode Mesh	52	80	150
Mesh Opening, mils	15.2	9.5	4.7
Millivolts Oscillation At Methanol Electrode In Vertical Position	5-10	60	50-60

1 vol% methanol in 30 wt% H_2SO_4 at 82°C and 50 ma/cm^2.

Tilting the cell by more than nine degrees with the 80 mesh electrodes reduced the oscillations by approximately two thirds. The 150 mesh electrode showed no oscillation at an 18 degree tilt face up and also a two thirds reduction face down. This effect is shown in Table C-3 . Detailed data are given in Appendix C-4 .

TABLE C-3

Effect Of Electrode Orientation On Voltage Oscillation

Orientation	Millivolts Oscillation At Methanol Electrode
80 Mesh Electrode:	
VERTICAL	60
9° tilt face up	62
18° tilt face up	15
26° tilt face up	20
150 Mesh Electrode:	
VERTICAL	50-60
18° tilt face up	None
18° tilt face down	20

1 vol % methanol in 30% H_2SO_4 at 82°C and 50 ma/cm^2.

As a result of these tests it is evident that these observed voltage oscillations were caused by trapping of the escaping CO_2 product from the electrode. The trapping of gas between the electrode and membrane was attributed to warping of the AMFion C313 membrane after installation. Thus, a firm packaging of electrodes against the membrane was found necessary to eliminate the gas-caused voltage oscillations.

Part d - Electrode Current
Collection Studies

Polarization measurements were made on the methanol electrode at various points to determine if current collection was a problem in obtaining the best performance. The measurements were made on an 80 mesh electrode at 50 ma/cm^2 and 82°C with 1 vol % methanol in 30 wt % H_2SO_4. The current collector was a 1 mil by 3/16" wide platinum sheet placed peripherily on the electrode. The polarization from bottom to top of the electrode varied by 0.16 volts as shown in Figure C-3. This voltage difference varied in a linear fashion with current showing the nature of the voltage loss to be ohmic. The gas rejection oscillation region was evident from about one inch from the bottom to the top of the cell.

Figure C-3

Voltage Variation Across Electrode

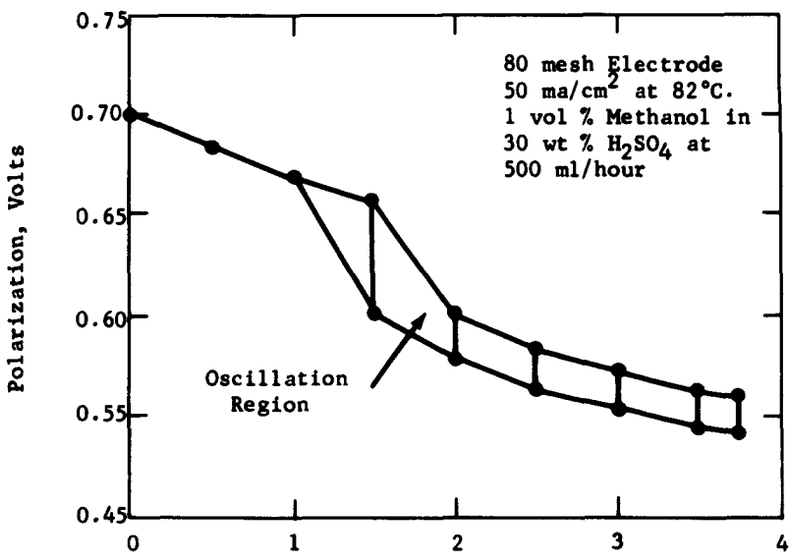

Varying the screen mesh and hence the wire diameter influenced the voltage drop across the electrode. The 52 mesh screen showed 0.10 volts loss compared to 0.16 and 0.12 volts for 80 and 150 mesh screens, respectively. These data summarized in Table C-4 suggested that some voltage loss occurred in the wires of the screen and that this was a factor in current collection.

TABLE C-4

Effect Of Electrode Mesh On Electrode Voltage Drop

Electrode Mesh	52	80	150
Wire Diameter, mils	4	3	2
Electrode*, Volts	0.10	0.16	0.12

* Using 0.001" thick x 3/16" wide platinum sheet around periphery of 4" x 4" square electrode.

The size of the current collector was increased to show the influence of better current collection on voltage loss across the electrode while operating at 50 ma /cm^2 and 82°C. A larger gold sheet reduced the voltage loss about 50% to 82 millivolts. The conventional platinum collector provided with a center cross design for contact at five points on the electrode reduced the voltage loss to about 45 millivolts. These data, summarized in Table C-5, show that proper current collection is important for obtaining best fuel cell performance. Detailed data are given in Appendix C-3.

TABLE C-5

Effect Of Current Collector On Electrode Voltage Drop

Electrode Mesh	80
Volts IR Drop Using A Collector Of:	
0.001" x 3/16" Pt Sheet Around Periphery	0.16
0.002" x 1-1/2" Au Sheet Around Periphery	0.082
0.001" x 3/16" Pt Sheet Around Periphery Plus Five Center Contacts	0.045

Part e - Long Term Methanol Electrode Performance

In view of the tests on electrode washing, voltage oscillation, and current collection, the cell assembly was modified for the test of the behavior of the methanol electrode under long term operation. Modification of the assembly involved using a stable Ionics CR-61 membrane, installation of a good current collector and packaging with the electrodes firmly in place on each side of the membrane. Also a vacuum tube controlled relay shut off was provided in case some failure resulted in excessive electrode polarization.

The long term test was begun using platinum electrodes at 50 ma/cm^2 and 82°C with 1 vol % commercial grade methanol in 30 wt % commercial grade H_2SO_4. A

direct current source was used to drive the cathode. Good control of the methanol was achieved by matching feed rate of the methanol to its utilization and loss. After 813 hours of continuous operation, without any equipment failures, the polarization was 0.65 volts versus 0.58 volts normal activity at the beginning of the run. Furthermore, open circuiting for a few seconds improved the polarization by 30 millivolts to 0.62 volts polarization. Detailed data are given in Appendix C-1. During this run the same H_2SO_4 was recycled through the cell with continuous methanol-water addition. When about 1000 hours running time is attained, the catalyst will be tested for activity with fresh electrolyte-methanol solutions.

Part f - Material Balances on the Long Term Test

During the long term methanol electrode performance runs, material and electrochemical balances were made. These tests confirmed the fact that the methanol is electrochemically oxidized completely to CO_2. The methanol and water in the CO_2 exhaust was determined by condensing the liquid in this gas stream and measuring its composition. This was compared with the methanol content of the electrolyte. The methanol concentration in the exhaust condensate was in agreement with literature equilibrium data (6) at 82°C as shown in Appendix C-4. The amount of methanol condensed from the CO_2 exhaust averaged slightly higher than that calculated for normal saturation at 82°C (Figure C-4). This is probably attributable to entrainment. The total methanol in the CO_2 exhaust amounted to about three pounds per hundred pounds of methanol reacted electrochemically when operating with 1 vol % methanol in the electrolyte.

Figure C-4

Methanol Condensed From CO_2 Exhaust Stream

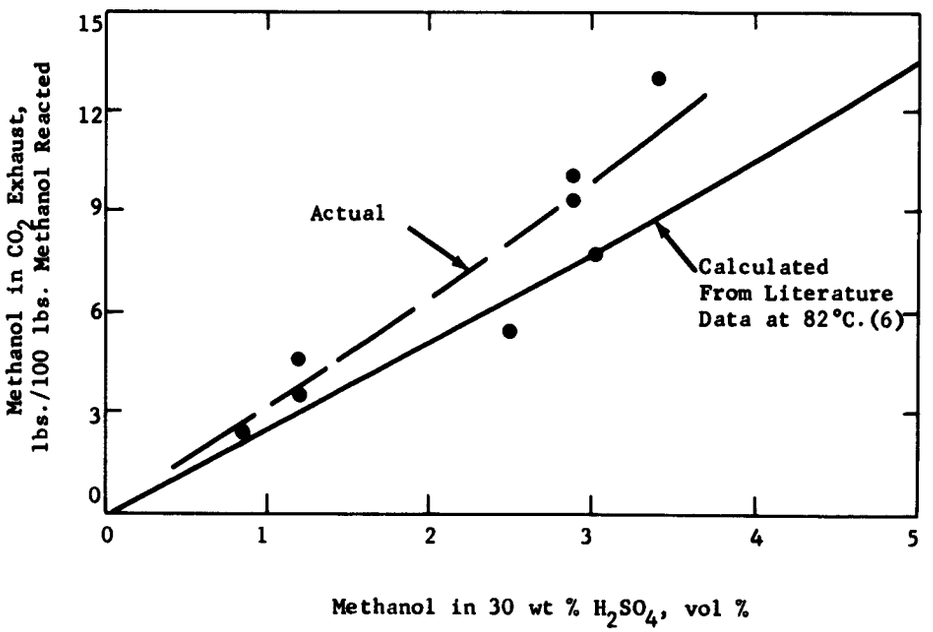

Part g - Performance of the
Electrode As a Methanol Barrier

During the long term methanol half cell run, analyses for methanol content were obtained on both the anolyte and catholyte sides of the cell to determine the influence of electrochemical reaction on the diffusion of methanol to the opposing compartment. This is important in a total cell using the air-HNO_3 redox system since any methanol escaping to the cathode side would be lost by chemical oxidation to CO_2.

The analyses confirmed that the electrochemical reaction at the 80 mesh electrode significantly reduces the methanol content at the air electrode. At 50 ma/cm^2 methanol escape through the electrode is nil when using 1 vol % methanol in H_2SO_4. With 3 vol % methanol in the H_2SO_4, about 1.5 vol % methanol is found in the catholyte after establishment of equilibrium. These results summarized in Figure C-5, are in good agreement with the previous predictions (1). Detailed data are given in Appendix C-1.

Figure C-5

Methanol Concentration Across Electrode

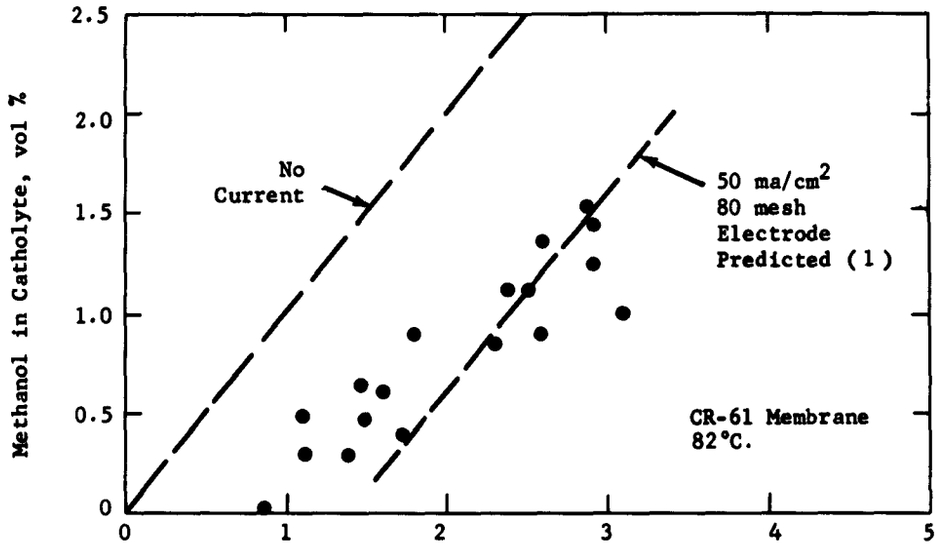

Phase 3 - Total Cell Operation

The new Teflon test cell (Figure C-1) together with feed, monitor, and control systems was assembled for testing the combined methanol and air-HNO_3 redox electrodes. The equipment flow plan is shown schematically in Figure C-6 and further details are given in Appendix C-5.

Figure C-6

Total Fuel Cell Schematic

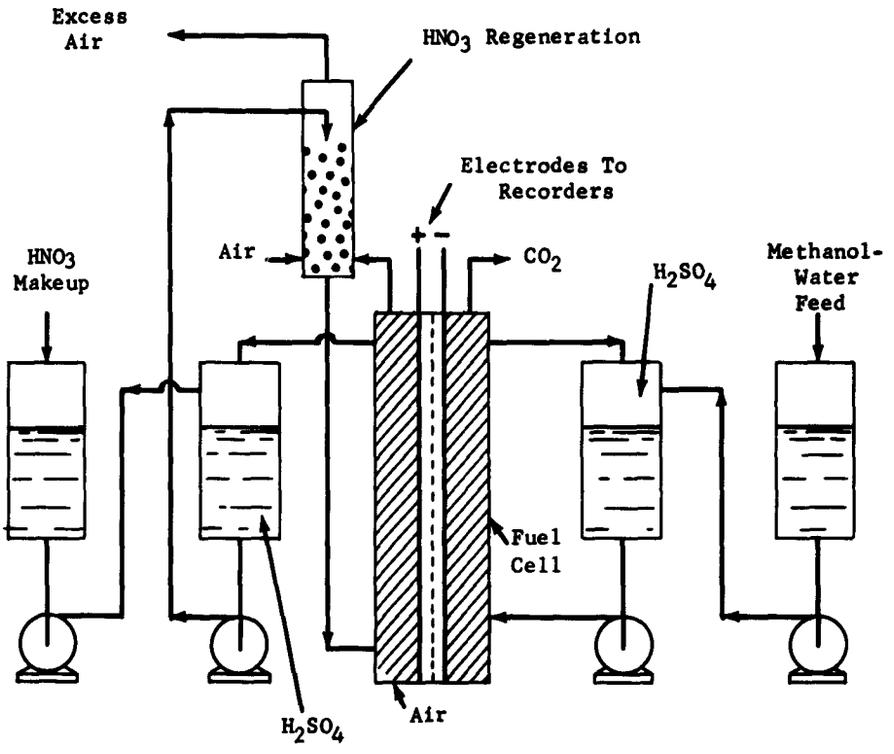

See Appendix C- 5 For Equipment Details

The cell was assembled using the best techniques developed in the previously described structure. Very tight packing of the electrodes and membranes was made in order to eliminate the voltage oscillations due to fluctuations in pressure caused by AMFion electrolyte circulation and gas rejection. The AMFion C313 membrane was found to buckle sufficiently to permit CO_2 interference with ionic conductance and was replaced with an Ionics CR-61 cation sulfonated polystyrene membrane. Finally, current collection was further improved by increasing the thickness of the collectors and the number of contact points with the electrodes. A controller to

regulate the rate of fuel addition to the cell was built and tested. The controller was designed to maintain a desired fuel concentration within the cell by adding fuel at a rate proportional to the current. The circuiting is shown in Appendix C-6.

Part a - Electrical Performance

The new compact Teflon unit was tested as a total cell for the methanol and air-HNO_3 redox systemsto determine electrical performance. The tests were made at 82°C using 1 vol % methanol in 30 wt % H_2SO_4 anolyte and 1 wt % HNO_3 in 30 wt % H_2SO_4 catholyte with air regeneration. Currents up to 95 ma/cm^2 were drawn from the cell. At 50-60 ma/cm^2 about 15 $mwatts/cm^2$ of power was obtained at the cell terminals as shown in Figure C-7. This power production was about 50% greater than obtained in the earlier cell previously reported (1). The power at 50 ma/cm^2 was short of expectations by about 5 $mwatts/cm^2$ due to greater IR losses and below normal anode activity. The detailed data are presented in Appendix C-7.

Figure C-7

Total Cell Power Versus Current Density

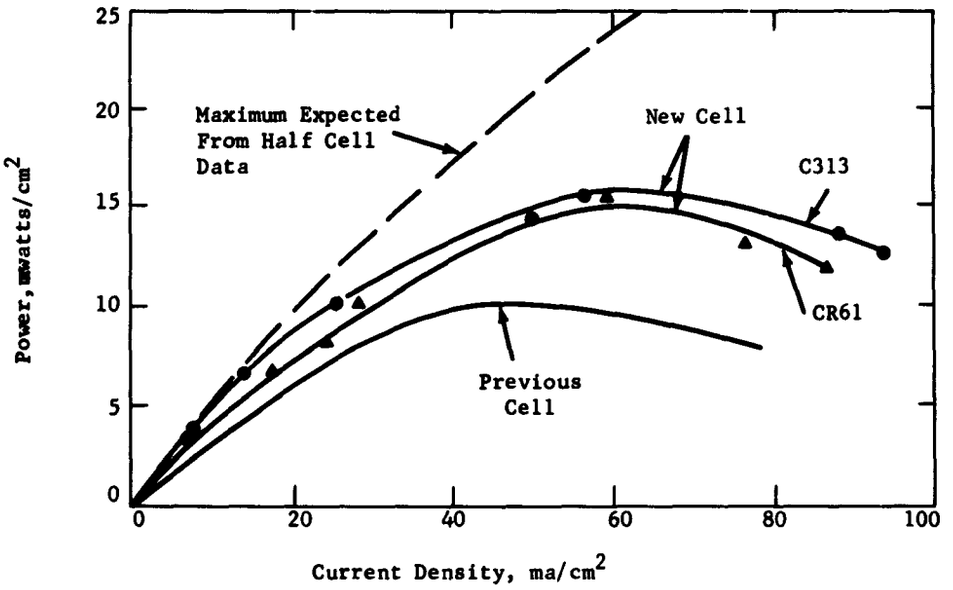

The IR loss in the new compact cell was considerably improved over the previous cell. At 50 ma/cm^2 the IR loss was 0.03 volts when using the 5.6 mil AMFion C313 membrane close packed between the electrodes versus 0.17 volts in the previous cell. The Ionics 21 mil CR-61 stable membrane showed an IR loss of 0.05 volts as shown in Figure C-8.

Figure C-8

IR Loss In Total Fuel Cell

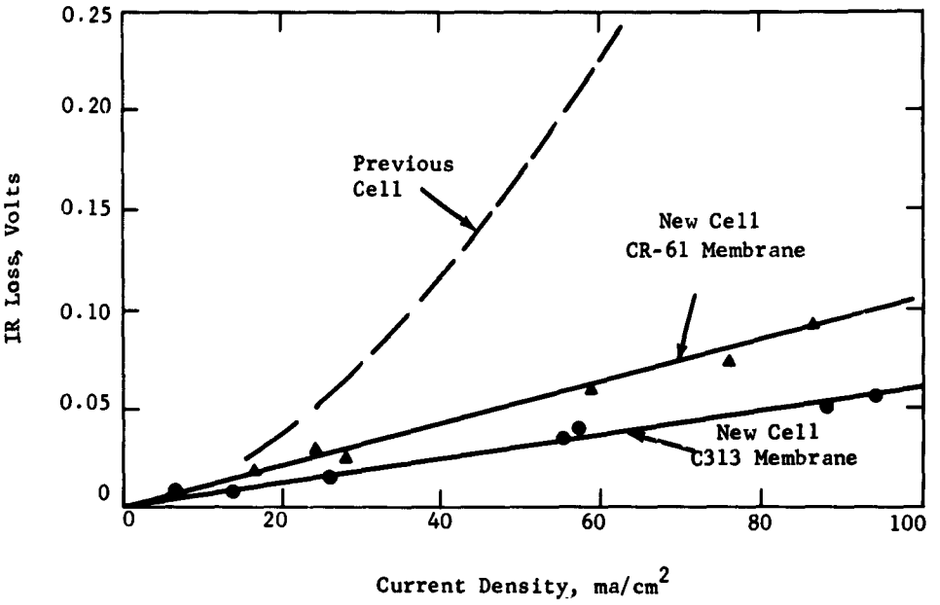

Part b - Optimum Electrolyte Composition

The effect of H_2SO_4 concentration on the performance of the methanol electrode had been studied extensively. However, additional data was needed on its effect on the performance of the HNO_3-air electrode in order to determine the optimum acid concentration for a complete cell. Therefore a platinized Pt electrode was tested with 1 wt% HNO_3 over a range of 20 to 60 wt% H_2SO_4. These data, combined with the data on the performance of the methanol electrode, were used to evaluate the effect of changing acid concentration in the total cell voltage.

Combining these data and using a typical experimentally measured cell resistance of 0.5 ohm-cm^2, it was calculated that the optimum is obtained at 30 to 35 wt% H_2SO_4. Furthermore, there was a wide plateau of acid concentrations in which voltage decreased by less than 20 mv from the maximum. Therefore, 30 wt% H_2SO_4 will continue to be the electrolyte acid concentration. These results are shown in Table C-6 and detailed data are presented in Appendix C-8.

TABLE C-6

Effect Of Acid Concentration On Cell Performance

Current Density ma/cm^2	H_2SO_4 Range For 20 mv Change, wt%	H_2SO_4, wt% For Maximum Cell Voltage
50	29-43	30
100	23-53	35

Part c - Effect Of Cell Materials On Performance

As previously reported (1), harmful impurities can be removed from AMF-ion C313 membranes by pretreatment in H_2SO_4-HNO_3 mixtures. Two total cells were assembled to test the effect of this treatment on the membrane conductivity and to evaluate the total IR loss to be expected between the fuel and air electrodes. Cell performance was measured at 82°C in 30 wt% H_2SO_4 - 1 wt% HNO_3. In one cell with a 60 mil separation between electrodes, IR loss at 30 ma/cm^2 amounted to 0.06 volts. This was in agreement with earlier values obtained using untreated membranes. The second cell with an electrode separation of 35 mils was surprisingly better, giving an IR loss of less than 0.02 volts at 55 ma/cm^2. In any event the removal of impurities from the membrane does not impair their conductivity and therefore the total cell IR loss does not appear to be a serious problem.

Part d - Development Of New Materials

Tests were made of the ability of thin gold coatings to protect base structural materials against electrochemical attack. Gold-coated 250 mesh stainless steel screen and a Cu-Sn electrode consisting of 1 mil diameter tubes of 30 mil length bonded together were tested as fuel electrodes. The electrodeposition of Pt black catalyst on these electrodes resulted in some corrosion, probably resulting from chemical attack of the gold by the evolved Cl_2. Further corrosion occurred during their testing because of anodic dissolution of the underlying base metals. Data on the total cell testing of the gold coated 250 mesh stainless steel screen are given in Appendix C-7.

SECTION 5

CONCLUSIONS

5.1 Task A, Fuel Electrode

Phase 1 - Catalyst Performance Studies And New Preparative Techniques

The use of $NaBH_4$ reduction to incorporate other noble or base metals into Pt has the same effect as was previously found using electrodeposition. Both Tafel slopes and exchange currents increase. However, they generally compensate each other so that over-all activity is not appreciably improved. Furthermore, the kinetic parameters can be varied widely so that it appears that the incorporation of other metals into Pt might produce less expensive catalysts of comparable activity.

This characteristic is not universal, since other metals respond differently when combined with noble or base metals. They can be poisoned completely or not affected by the same metals which cause large changes in the kinetic parameters of Pt. The reasons for these effects have not been completely defined, but are probably electronic in nature, producing changes in the d-band structures, work functions, electrocapillary maxima or other properties of catalysts.

A new catalyst system proved to be significantly more active. It not only represents the most active catalyst yet prepared for the electrochemical oxidation of CH_3OH, it also shows that the compensating effect of increasing Tafel slope accompanied by increasing exchange current does not always prevent improved catalytic activity at practical current densities.

Sodium borohydride failed to reduce a number of metals, hence more active reducing methods were sought. However, better compounds were not found. Sodium borohydride is still the most active reducing agent available to date and gives catalysts of similar performance when used in aqueous or nonaqueous solutions.

Phase 2 - Alloy Formation

The wide variety of catalysts produced is apparently a direct result of the fact that the reduction of mixed metal salt solutions by $NaBH_4$ produces finely divided alloy powders. Alloying, and not merely physical mixing, is necessary to produce most of the catalyst performance changes demonstrated. Its great utility lies in the fact that it is a low temperature process that works with a large number of metals.

Phases 3 and 4 - Performance Of Heterogeneous Mo Containing Catalysts; Mechanism Of The Pt-Mo Catalysts

Limiting, low polarization current densities of up to 4 ma/cm^2 are attainable with CH_3OH on Pt-Mo electrodes while HCHO, the most active fuel, can give from 32 to 64 ma/cm^2. It has not been possible to increase this current or prevent the irreversible performance loss at higher current densities. Unless further improvements can be made the Pt-Mo heterogeneous system will not be of practical utility for CH_3OH.

Solutions of Mo used with Pt or Pt + Au catalysts and HCHO fuel give low polarization current densities of 200 ma/cm^2 or more. Methanol gives only the low current density performance of the heterogeneous catalyst system. Under certain, as yet undefined conditions, the performance with HCHO is reversible, giving a system that under special circumstances might have some practical significance.

The Mo-fuel reaction in both cases appears to be a surface redox mechanism. Adsorbed Mo^{+6} is reduced by the fuel to adsorbed Mo^{+5}, with the production of CO_2. Electrochemical oxidation of the Mo^{+5} then restores the Mo^{+6}. Failure of the system occurs when the Mo^{+6} is desorbed and replaced on the catalyst surface by the more readily adsorbed fuel.

Phase 5 - Further Mechanism Studies With Pt

The oxidation of CH_3OH on ordinary Pt surfaces appears to be adsorption limited. However a freshly reduced surface is instead limited only by the diffusion of fuel to it.

5.2 Task B, Air Electrode

Phase 1 - HNO_3 Regeneration, Laboratory Studies

Practical levels of HNO_3 regeneration with air, namely 20 coulombs/coulomb equivalent to HNO_3 consumed, appear attainable through the use of packings or foaming agents to improve contacting of the HNO_3 reduction products with O_2 and H_2O. The previous limitation caused by degradation of the foaming agent has been partially overcome by the use of more stable surfactants.

The regeneration efficiency can be further increased through the use of high surface area silica particles in combination with the foaming agent to augment contacting. Furthermore, increased current density does not impair and in fact appears to improve the efficiency.

$NaNO_3$ continues to look like a convenient substitute for HNO_3. It is more easily transported and there is no resulting loss in electrode performance or regeneration efficiency.

Phase 2 - HNO_3 Regeneration, Engineering Studies

Engineering studies with the HNO_3 redox system show that both the electrochemical reduction and chemical regeneration reactions can be carried out successfully in a practical cell with an external regeneration chamber. Electrochemical performance agrees with values obtained on smaller laboratory electrodes. In addition, performance loss due to air injection is eliminated by diverting the air flow away from the electrode surface. Holdup and hydrolysis limitations in the external chamber can be avoided by proper design of the system. Furthermore, the regeneration target of 20 coulombs/coulomb equivalent to HNO_3 consumed and a low sensitivity to air flow rate can be achieved in this type of system through the use of dense foams and cooling of the regeneration chamber.

5.3 Task C, The Total Cell

Phases 1 and 2 - Construction of Compact Fuel Cell; CH_3OH Electrode Life Studies

A compact cell, designed for evaluating both cell components and total cell operation, has been tested to a point where it now has the desired degree of reliability, ease of handling, freedom from extraneous impurities and low electronic and electrolytic IR losses.

Long term tests of the platinized platinum fuel electrode showed that its performance could be maintained for extended periods (e.g. over 800 hours) without a significant loss in performance providing very careful control is maintained on the CH_3OH concentration in the anolyte and the cell is periodically open circuited for several seconds. The reaction goes completely to CO_2. The CH_3OH loss in the CO_2 exhaust when used in 1 vol % concentration amounted to about 3 % of the CH_3OH used. However, most of this is probably recoverable by air condensation at ambient conditions. In addition, the fuel electrode, as expected, prevented the transfer of CH_3OH to the cathode.

Phase 3 - Total Cell Operation

The new cell design and the necessary auxiliaries operated satisfactorily. In preliminary tests in the cell, current densities up to 95 ma/cm^2 were drawn and 15 mw/cm^2 were obtained at the terminals. However, this performance can be improved upon because resistance of the membrane separator used was high and the fuel electrode exhibited below normal performance. However, even this performance is high enough to permit study of total cell performance variables.

Further evaluations of the effect of H_2SO_4 concentration shows that 30 wt % H_2SO_4 is optimum, but not critical, since a 10 wt % H_2SO_4 change in either direction results in only a 20 mv loss in performance.

SECTION 6

OVER-ALL CONCLUSIONS

During the contract period work has been carried out on the performance and compatibility of the major components of a soluble carbonaceous fuel - air fuel cell. These studies have resulted in both improved performance and a greater understanding of the processes involved. The following represent the highlights of this work.

Fuel Selection

Methanol was selected as the prime fuel. It proved to have such advantages over other oxygenated hydrocarbons as highest reactivity, lowest polarization under long term operation, and lowest cost. Its two inherent disadvantages, a high vapor pressure and a poisoning effect on the air electrode were circumvented by reducing the concentration at the anode to tolerable limits. Its concentration in the catholyte was further reduced by designing the anode so that most of the fuel is reacted within its structure.

Fuel Electrode Catalysts

The severe polarization occuring at the CH_3OH electrode was the greatest source of voltage loss. Efforts directed toward finding a catalyst more active than platinum and yet stable in H_2SO_4 have uncovered a variety of such catalyst compositions. Included are Pt-Fe, Pt-Mo, and a proprietary catalyst first prepared with corporate funds. These catalysts have activities up to 150 mv better than Pt. In addition, a life study of about 800 hours on a Pt electrode showed that efficiency is essentially unimpaired if the cell is occasionally open circuited for several seconds and the CH_3OH concentration within the cell is closely controlled.

HNO_3 Redox Air Electrode

The air electrode being developed is a redox system based on the electrochemical reduction of a small quantity of HNO_3 dissolved in the electrolyte. Air is used indirectly for chemically regenerating HNO_3. Its advantage lies in the prospects for low polarization and long life. Its major problems were ensuring efficient HNO_3 regeneration and establishing the compatibility of HNO_3 and its reduction products with the fuel electrode. Regeneration efficiencies with air of about 30 coulombs/coulomb equivalent to HNO_3 consumed were achieved in a practical cell configuration. In addition the tolerance levels for HNO_3 and CH_3OH were determined and shown to be usable for efficient cell operation.

The Operation Of A Complete Cell

A variety of complete cells have been built and tested in experiments ranging in duration from 3 to 35 hours. Good agreement was found when the results were compared with half cell studies. Considerable improvements have been made in their performance and reliability. Current densities as high as 95 ma/cm^2 have been achieved. Furthermore, power outputs of 32 mw/cm^2, ex IR losses and 15 mw/cm^2 at the terminals have been obtained with the expectation of higher performance levels in the foreseeable future.

SECTION 7

RECOMMENDATIONS

The work during this contract period has been directed at research and analyses of problems associated with the development of a single fuel cell rather than in developing or building battery systems. The major efforts have concentrated on improving the performance of individual cell components and translating the results into compatible electrode-electrolyte systems in an actual operating cell. It is recommended that such investigations continue. However, work should also begin on the development of multiple cell systems. These should not be finished assemblies, but instead they should be rudimentary packages designed to evaluate the performance.

Therefore the following objectives should be pursued:

Fuel Electrode Research

Although significant progress has been made in developing improved catalysts, this still should be the area where the largest increases in cell efficiency can be made. Higher activities and improved temperature response remain desirable goals. Thus the compositing and testing of new catalyst compositions merit further efforts. It also is expected that problems in maintaining long term activity would arise during the work in the unit and multiple fuel cell packages and will require further basic research.

Air Electrode Research

Assuming the HNO_3 redox electrode development continues to be successful, the major efforts should be concerned with improving catalyst efficiency, especially at high current densities, and with reducing the volume required for HNO_3 regeneration.

Cell Development

Many problems relating to long-term cell operation remain to be solved. These include handling feed introduction and product removal during long term operation, minimizing ohmic losses, and developing methods for startup and shutdown. Such problems should receive attention.

SECTION 8

IDENTIFICATION OF PERSONNEL AND DISTRIBUTION OF HOURS

8.1 Background Of New Personnel

I Ming Feng (Ph.D., Mechanical Engineering, University of Michigan)has 12 years experience, primarily in disciplines relating to the mechanisms and principles of lubrication. In this field he has to his credit well over 40 publications. He joined Esso Research in 1960 after a diversified career at several industrial organizations and M.I.T. He is currently working on the development of the total cell.

8.2 Distribution Of Hours

The following are the technical personnel who have contributed to the work during the reporting period 1 July 1962 - 31 December 1962 and the approximate number of hours of work performed by each:

Carl E. Heath	347
Barry L. Tarmy	779
Eugene L. Holt	892
Duane G. Levine	906
Andreas W. Moerikofer	847
Joseph A. Shropshire	825
James A. Wilson	60
Charles H. Worsham	934
I Ming Feng	150
Total	5740

SECTION 9

REFERENCES

(1) Heath, C. E., Tarmy, B. L., et al, Soluble Carbonaceous Fuel-Air Fuel Cell, Report No. 1, Contract DA 36-039 SC-89156,(1 Jan. 1962 - 30 June 1962)

(2) Yntema, L. F., J.A.C.S., 54, (1932) p. 3775
Fink, C. G. and Jones, F. L., Trans. Electrochem. Soc., (1931) p. 461
Holt, M. L., ibid, (1934) p. 453

(3) Buck, R. P. and Griffith, L. I., J. Electrochem. Soc., 109, (1962) p. 1005
Gilman, S. and Breiter, M. W., ibid., p. 1099

(4) Bodenstein, M., Z. Phys. Chem., 100, (1922) p. 68

(5) Hoftijzer, P. J., Chem. Weekblad, 52, (1956) p. 71

(6) Othmer, D. F. and Benenati, R. F., Ind. Eng. Chem., 37, (1945) p. 299

(7) Duke, F. R. and Smith, G. F., Ind. Eng. Chem., Anal. Ed., 12, (1940) p. 201

(8) Carr, J. C. and Riddick, J. A., Ind. Eng. Chem., 43, (1951) p. 692

APPENDIX A-1

PREPARATION OF PRESSED ELECTRODES

The electrode structure consists of a Pt gauze welded to a piece of Pt foil cut to the same size. A slurry of the finely divided catalyst in H_2O is applied to the electrode with a dropper or spatula, depending upon the consistency of the catalyst. The slurry is partially dried in an oven or by blotting with filter paper. A smooth Pt sheet is then placed over the catalyst and the entire assembly subjected to 2000 psi in a hydraulic laboratory press. The result is a uniform, stable catalyst coat which can be handled in the same manner as an electrodeposited electrode.

APPENDIX A-2

PREPARATION AND TESTING OF $NaBH_4$ REDUCED CATALYSTS

Electrode		Composition, Atom%	Preparative Solution, Moles/Liter Salt	$NaBH_4$	Polarization vs. Theor. CH_3OH at Indicated ma/cm^2 0	1	10	50	100	b	-Log I_o	Remarks*
Pt	80		0.073 H_2PtCl_6	0.53	.45	.53	.57	.61	.63	.047	11.2	Reduction carried out on electrode surface
	180		0.50 "	"	.40	.50	.55	.58	.61	.050	10.0	
Pt-Fe	90		1.0 H_2PtCl_6, 1.0 $FeSO_4$	"	.36	.47	.55	.60	.62	.073	6.5	Reduction carried out on electrode surface
	203		0.25 " , 0.25 $FeCl_3$	1.85	.32	.48	.57	.65	---	.087	5.5	
Pt-Au	177		0.25 " , 0.25 $HAuCl_4$	1.20	---	.50	.57	.62	---	.070	7.1	
	178		0.50 " , 0.025 "	"	.38	.51	.57	.60	---	---	---	
	179		0.50 " , 0.0025 "	"	.45	.55	---	---	---	---	---	
	187	Au-20.5, Pt-77.7	0.40 " , 0.10 "	1.85	.36	.48	.54	.58	---	.060	7.9	
	188	" 39.0, " 58.5	0.30 " , 0.20 "	"	.37	.50	.56	.62	---	.076	6.4	
	189	" 63.0, " 36.5	0.20 " , 0.30 "	"	.34	.48	.54	.59	---	.066	7.2	
	190	" 76.4, " 22.1	0.10 " , 0.40 "	"	.35	.55	.60	.66	---	.083	6.3	
Pt-Ir	182	Ir- 8.6, Pt-90.1	0.40 " , 0.10 H_2IrCl_6	"	.38	.52	.58	.63	---	.069	7.4	
	183	" 19.8, " 78.7	0.30 " , 0.20 "	"	.32	.48	.55	.60	---	.071	6.8	
	184	" 35.8, " 63.1	0.20 " , 0.30 "	"	.42	.55	.61	.65	---	.060	9.2	
	185	" 61.3, " 40.0	0.10 " , 0.40 "	"	.38	.52	.57	.60	---	.054	9.5	
Pt-W	201		0.25 " , 0.25 Na_2WO_4	1.85	.15	.46	---	---	---	---	---	
	202		" " , " "	"	.12	.46	---	---	---	---	---	
	205		" " , " "	"	.19	.50	.57	.62	---	.066	7.7	
	209		" " , " H_2WO_4	"	.35	.47	.53	.57	.59	.062	7.5	
	211		" " , " "	"	---	.64	---	---	---	---	---	
	213		" " , " "	"	---	1.30	---	---	---	---	---	2 Acid Washes, No H_2O Wash
	215		" " , " "	"	.35	.48	.54	.57	.59	.052	9.3	
	217		" " , " "	"	.37	.50	.57	.63	---	.068	7.3	
Pt-V	236		0.25 H_2PtCl_6, 0.25 V_2O_5	1.85	.35	.51	.57	.61	.63	.062	8.2	
	237		" " , " "	"	---	.47	---	---	---	---	---	
	240		" " , " "	"	---	.51	.59	---	---	---	---	1 M HCHO
Pt-Ni	224		0.25 " , 0.25 $NiCl_2$	"	.38	.50	.56	.61	---	.062	8.0	
Pt-Cu	225		" " , 0.25 $CuCl_2$	"	.36	.52	.59	.64	.67	.076	6.8	
Pt-Co	226		" " , 0.25 $CoCl_2$	"	.34	.47	.55	.61	---	.076	6.2	
Pt-Pb	227		" " , 0.25 $Pb(Ac)_2$	"	.37	.50	.57	.64	---	.066	7.6	
Pt-Mn	239		" " , 0.25 $MnCl_2$	"	.33	.46	.52	.57	.60	.071	6.4	
Ir	97		1.0 H_2IrCl_6	0.53	.40	.52	.58	.62	.66	.053	9.9	Paste electrode
	181		0.5 "	1.85	.41	.53	.59	.63	---	.062	8.5	

APPENDIX A-2 (CONT'D)

PREPARATION AND TESTING OF $NaBH_4$ REDUCED CATALYSTS

Electrode	Composition, Atom%	Preparative Solution, Moles/Liter Salt	$NaBH_4$	Polarization vs. Theor. CH_3OH at Indicated ma/cm^2 0	1	10	50	100	b	-Log I_o	Remarks*
Ir-Fe 231		0.25 H_2IrCl_6, 0.25 $FeCl_3$	1.85	.34	.51	.56	.60	.61	.055	9.2	
Ir-Re 252		" " , 0.25 Re_2O_7	"	.29	.39	.48	.55	.58	.096	4.0	
255		0.40 " , 0.10 "	"	.25	.42	.51	.57	.60	.100	4.0	
Rh-Fe 228		0.25 H_3RhCl_6, 0.25 $FeCl_3$	"	.69	1.40	---	---	---	---	---	
Rh-Cu 229		" " , 0.25 $CuCl_2$	"	.69	1.40	---	---	---	---	---	
Rh-Au 230		" " , 0.25 $HAuCl_4$	"	---	---	.71	1.41	---	---	---	
Rh-Ir 232		" " , 0.25 H_2IrCl_6	"	.47	.57	.61	.64	.66	.045	12.6	
Rh-Re 248		" " , 0.25 Re_2O_7	"	.42	.55	.63	1.41	---	---	---	
Au 186		0.5 $HAuCl_4$	"	.74	---	---	---	---	---	---	No Activity
Au-Re 253		0.25 " , 0.25 Re_2O_7	"	.30	.45	.53	.58	.60	.076	6.0	
Au-Pd 210		0.25 " , 0.25 H_2PdCl_6	"	.62	.74	.90	---	---	---	---	
Re 251		0.50 Re_2O_7	"	.42	.52	---	---	---	---	---	No Activity, Re dissolved anodically

*All runs in 3.7 M H_2SO_4-1 M CH_3OH at 60°C. with pressed electrode unless otherwise noted.

APPENDIX A-3

PERFORMANCE OF P-TYPE AND MODIFIED P-TYPE CATALYSTS

P-Type Catalysts	Polarization vs. Theor. CH_3OH at Indicated ma/cm^2 0	1	10	50	100	b	-Log I_o	Remarks*
P1	0.29	.43	.53	---	---	0.098	4.4	25°C
1a	---	.32	.42	.49	.52	.099	3.2	
1b	.17	.24	.36	.44	.47	.116	2.1	80°C
1c	.17	.20	.28	.37	.41	.117	1.7	95°C
1d	.39	.61	.71	.81	.90	.164	3.5	1 M CH_3CH_2OH
P2	.17	.29	.40	.47	.53	.115	2.4	
2a	.17	.21	.33	.41	.45	.118	1.8	80°C
2b	.11	.14	.22	.28	.32	.095	1.3	1 M HCHO
2c	.11	.13	.18	.25	.28	.091	1.4	80°C, 1 M HCHO
P3	.24	.41	.51	.59	---	.112	3.6	
P4	.29	.41	.53	.62	---	.118	3.8	
P5	.20	.32	.40	.47	.50	.097	3.1	
P6	.31	.37	.47	.54	.57	.101	3.7	
P7	.19	.28	.37	.45	.48	.109	2.4	
P-Type Catalysts Modified By Metal Addition								
P8	.23	.35	.45	.53	.56	.117	2.9	
P9	.19	.32	.42	.51	.55	.132	2.2	
P10	.22	.37	.47	.54	.58	.114	3.1	
P11	.17	.31	.39	.49	.52	.130	2.0	
P12	.22	.28	.39	.48	.51	.117	2.3	1 M glycol
P13	.25	.34	.45	.52	.55	.110	3.5	
P14	.32	.43	.51	.58	.61	.096	4.4	
P15	.18	.24	.37	.46	.49	.129	1.8	

* All runs in 3.7 M H_2SO_4-1 M CH_3OH at 60°C. with pressed electrodes unless otherwise noted.

APPENDIX A-4

PREPARATION AND TESTING OF ELECTRODEPOSITED CATALYSTS

Electrode		Preparative Soln, Moles/Liter	Polarization vs Theor CH_3OH at Indicated ma/cm^2 0	1	10	50	100	b	-Log I_o	Remarks
Pt	87	0.073 H_2PtCl_6	--	--	.60	.65	.68	.064	8.3	Electrodeposition followed by $NaBH_4$
"	88	"	--	.53	.60	.65	.68	.066	8.0	"
"	91	"	--	.58	.66	.71	--	.072	8.1	1 M HCHO
"	92	"	.37	.56	.63	.66	--	--	--	1 M HCHO
"	92b	"	.41	.53	.57	.63	.66	.051	10.3	
Pt-W	148	" 0.025 Na_2WO_4	.48	.60	.67	.76	--	.055	10.9	

APPENDIX A-5

ALLOYS PREPARED BY $NaBH_4$ REDUCTION

Catalyst	Lattice Spacing, Å		Structure Type
	Observed	Literature	
Pt	3.910	3.916	f.c.c.
Au	4.071	4.070	"
Pt-20.5%Au	3.918	3.944	"
Pt-39.0%Au	3.967	3.974	"
Pt-63.0%Au	4.013	4.004	"
Pt-76.4%Au	4.033	4.036	"
Ir	3.837	3.831	"
Pt-8.6%Ir	3.907	3.900	"
Pt-19.8%Ir	3.906	3.881	"
Pt-35.8%Ir	3.896	3.865	"
Pt-61.3%Ir	3.848	3.852	"
33%Pt-33%Au-33%Pd*	3.984	---	"
33%Pt-33%Ir-33%Pd*	3.896	---	"
33%Pt-33%Fe-33%Pd*	3.884	---	"
Pd	---	3.883	"
Au-50%Pd*	4.013	3.976	"
W	---	3.159	b.c.c.
Pt-50%W*	3.910	---	f.c.c.
Pt-80%W*	3.901	---	"
Ni	---	3.517	"
Pt-50%Ni*	3.877	3.877(15%Ni)**	"
Cu	---	3.607	"
Pt-50%Cu*	3.791	3.791(44%Cu)**	"
Co	---	3.537	"
Pt-50%Co*	3.862	3.862(19%Co)**	"
Pb	---	4.940	"
Pt-50%Pb*	a=6.67 c= -	a=6.65 c=5.97	Tetr., Pb_4Pt
	a=4.31 c= -	a=4.25 c=5.46	Hex., $PbPt$
	5.98	---	b.c.c.
	4.81	---	f.c.c.
Rh	---	3.797	"
Rh-50%Au *	4.054	---	"

* Compositions are of preparative solutions.

** Refers to composition given in literature corresponding to observed lattice spacing.

All compositions in atom %

APPENDIX A-4

PREPARATION AND TESTING OF RaNiMo SUPPORTED REDOX CATALYSTS

Electrode		Composition, wt %	Preparative Solution, Moles/Liter Salt					NaBH$_4$	Polarization vs Theor CH_3OH at Indicated ma/cm^2 0	1	10	50	100	Remarks*
Pt-Mo	93		0.67 H_2PtCl_6,		0.33 $(NH_4)_6Mo_7O_{24}$			0.53	.43	.53	.60	.66	.70	Reduction carried out on electrode surface
	94		"	"	"	"		"	.32	.48	.54	.58	.61	"
	95		"	"	"	"		"	.20	.47	.53	.57	.60	"
	96		"	"	"	"		"	.15	.37	.52	.56	.59	"
	106		0.33	"	0.17	"		"	.15	.50	--	--	--	
	120		"	"	"	"		"	.17	--	--	--	--	no activity
	122		"	"	"	"		"	.15	--	--	--	--	catalyst dropped off
	123		"	"	"	"		"	.13	--	--	--	--	catalyst dropped off
	99		0.25	"	0.25	"		"	--	.28	--	--	--	
	100		"	"	"	"			.12	.23	--	--	--	
	101		"	"	"	"		"	.16	.49	--	--	--	
	102		"	"	"	"		"	.13	.46	--	--	--	
	103		"	"	"	"		"	.12	.27	--	--	--	
	104		"	"	"	"		"	.15	--	--	--	--	
	107		"	"	"	"		"	--	.25	--	--	--	
	108		"	"	"	"		"	--	.27	--	--	--	
	109		"	"	"	"		"	.17	--	--	--	--	
	110		"	"	"	"		"	.13	.28	--	--	--	
	111		"	"	"	"		"	.15	--	--	--	--	
	112		"	"	"	"		"	.15	.34	--	--	--	
	113		"	"	"	"		"	.13	.28	--	--	--	
	115		"	"	"	"		"	.13	--	--	--	--	
	116		"	"	"	"		"	--	--	--	--	--	catalyst dropped off
	117		"	"	"	"		"	.15	--	--	--	--	
	118		"	"	"	"		"	.12	.24	--	--	--	
	119		"	"	"	"		"	.13	.30	--	--	--	
	125		"	"	"	"		"	.19	--	--	--	--	
	126		"	"	"	"		"	--	--	--	--	--	
	132		"	"	"	"		"	.16	--	--	--	--	
	133		"	"	"	"		"	--	--	--	--	--	catalyst dropped off
	135		"	"	"	"		"	.16	.25	.56	--	--	catalyst dropped off
	136		"	"	"	"		"	.11	.22	--	--	--	catalyst dropped off
	139		"	"	"	"		"	.16	--	--	--	--	
	140		"	"	"	"		"	.12	.25	--	--	--	
	149		"	"	"	"		"	.13	.25	--	--	--	
	150		"	"	"	"		"	.10	.21	--	--	--	
	153		"	"	"	"		"	.13	.19	--	--	--	1 N HCOOH
	154		"	"	"	"		"	.12	.14	.23	--	--	1 N HCOOH
	155	Pt-97.6, Mo-0.58	"	"	"	"		"	.13	.16	--	--	--	80°C
	156	Pt-99.2, Mo-0.65	"	"	"	"		"	.15	.16	.25	--	--	1 N HCHO
	157		"	"	"	"		"	.17	--	--	--	--	1 N HCHO
	158		"	"	"	"		"	.15	.15	.18	.30	--	1 N HCHO, 80°C
	171	Pt-92.1, Mo-1.0	"	"	"	"		"	.16	.40	--	--	--	
	172		"	"	"	"		"	.22	.31	--	--	--	1 N glycol
	195		"	"	"	"		1.85	.16	--	--	--	--	1 N glycol
	196		"	"	"	"		"	.16	.23	--	--	--	
	197		"	"	"	"		"	.12	.20	--	--	--	
	198		"	"	"	"		"	.17	--	--	--	--	
	199		"	"	"	"		"	.16	.21	.27**	.34***	--	
	204		"	"	"	"		"	.29	.47	.55	.62	--	b = 0.077; - Log I_o = 6.1
	105		"	"	0.50	"		0.53	--	.46	--	--	--	
	121		"	"	"	"		"	.13	--	--	--	--	
	127		"	"	"	"		"	.15	.25	--	--	--	
	130		"	"	"	"		"	.17	--	--	--	--	
	128		"	"	"	"		"	.13	.20	--	--	--	
	131		"	"	"	"		"	.12	.19	--	--	--	
	141		"	"	"	"		"	.16	--	--	--	--	catalyst dropped off
	142		"	"	"	"		"	.17	--	--	--	--	catalyst dropped off
	143		"	"	"	"		"	.17	--	--	--	--	
	144		"	"	"	"		"	.12	--	--	--	--	
Au-Mo	129		"	$HAuCl_4$	0.25	"		"	--	--	--	--	--	no activity
	220		"	"	"	"		"	.59	.81	--	--	--	
Pt-Mo-Fe	168	Pt-96.4, Mo-1.0, Fe-1.8	0.33	H_2PtCl_6,	0.33	"	0.33 $FeCl_3$	1.85	.12	.47	.54	.59	.61	b = .069; -Log I_o = 6.8
	169	Pt-97.6, Mo-0.64, Fe-0.59	"	"	"	"	0.50 "	"	.16	.50	.57	.62	.65	b = .073; -Log I_o = 6.8
Pt-Mo-Ir	170	Pt-82.6, Mo-3.1, Ir-11.3	0.125	"	0.25	"	0.125 H_2IrCl_6	"	.13	.39	--	--	--	
Pt-Mo-Co	233		0.25	"	"	"	0.25 $CoCl_2$	"	.25	.45	.52	.58	.60	b = 0.077; -Log I_o = 6.4
	234		"	"	"	"	" "	"	--	.30	--	--	--	
	235		"	"	"	"	" "	"	--	.13	.14	--	--	95°C
Rh-Mo	165	Rh-57.8, Mo-1.8, O_2-10.8			"	"	" H_3RhCl_6							
Pt-Mo+Au	218		"	"	"	"		"	.30	.49	.55	.60	--	b = .058; -Log I_o = 8.4
	222		"	"	"	"		"	--	.40	--	--	--	
Pt-Mo-Au	219		"	"	"	"	" $HAuCl_4$	"	.35	.51	.58	.63	--	b = .078; -Log I_o = 6.4
Pt+Au-Mo	221				"	"	" "	"	.18	--	--	--	--	no activity
Pt+H_2MO_4	146								.36	--	--	--	--	
	147								--	--	--	--	--	no activity
	152								.46	--	--	--	--	no activity

* All runs in 3.7 N H_2SO_4 - 1 N CH_3OH at 60°C unless otherwise noted

** 2 ma/cm^2

*** 4 ma/cm^2

APPENDIX A-7

FIRST ORDER RATE PLOT FOR HCHO-Mo^{+6} CHEMICAL REACTION

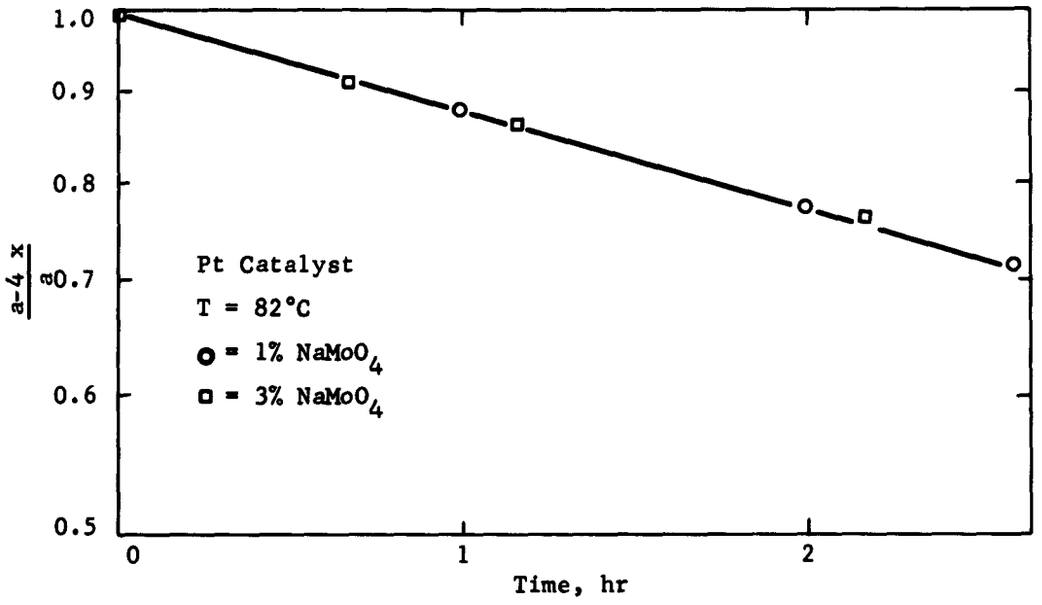

$$HCHO + H_2O + 4\ Mo^{+6} \longrightarrow CO_2 + 4\ Mo^{+5} + 4\ H^+$$

b = moles HCHO, a = initial moles Mo^{+6} x = moles CO_2

$$\frac{dx}{dt} = k\ (a-4x)^n\ b^m \qquad \ln \frac{a-4x}{a} = k't$$

Rate plot assumes n = 1 and concentration of HCHO (b) in excess and constant.

APPENDIX A-8

DIAGRAM OF EQUIPMENT FOR FLOW COULOMETRY

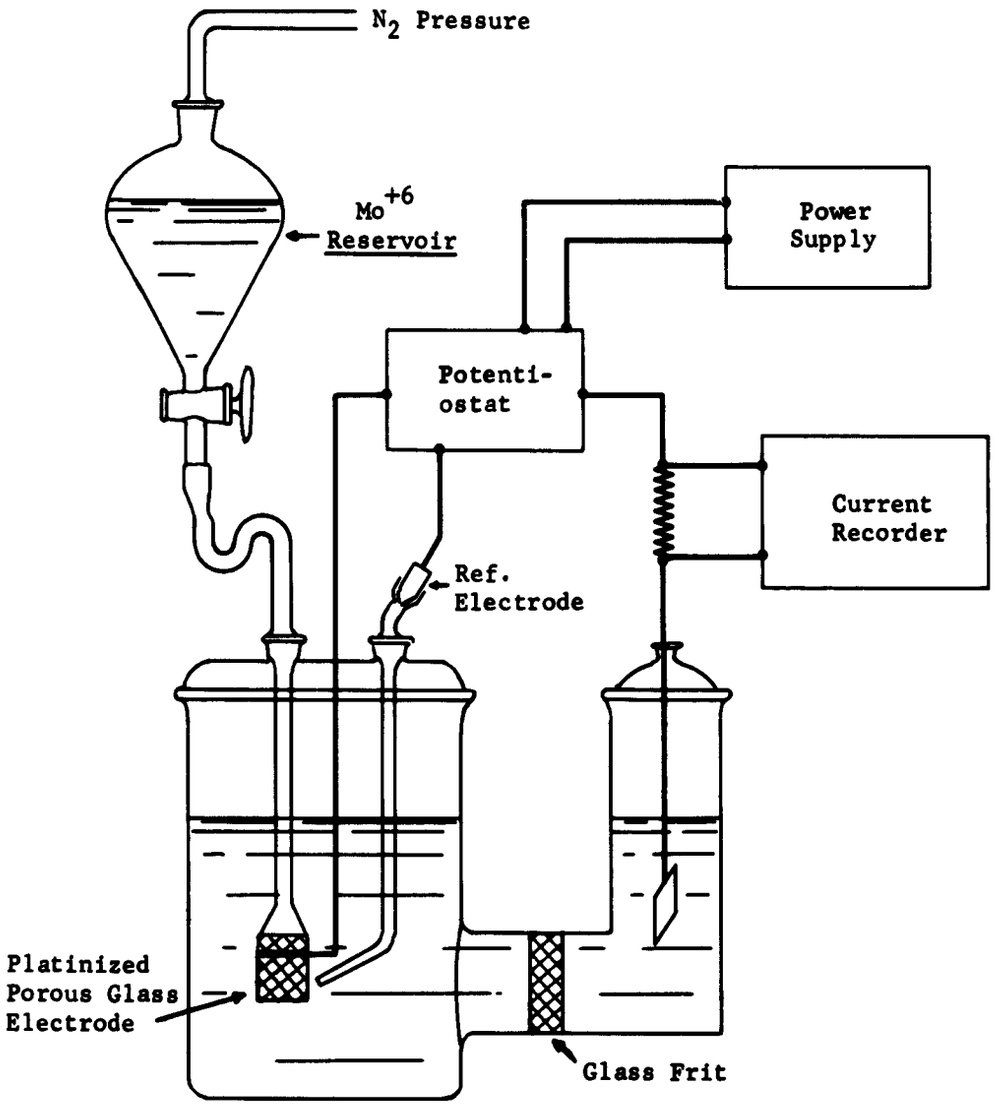

APPENDIX A-9

PERFORMANCE OF HCHO - Pt ELECTRODE WITH SINGLE ADSORBED Mo^{+6} LAYER

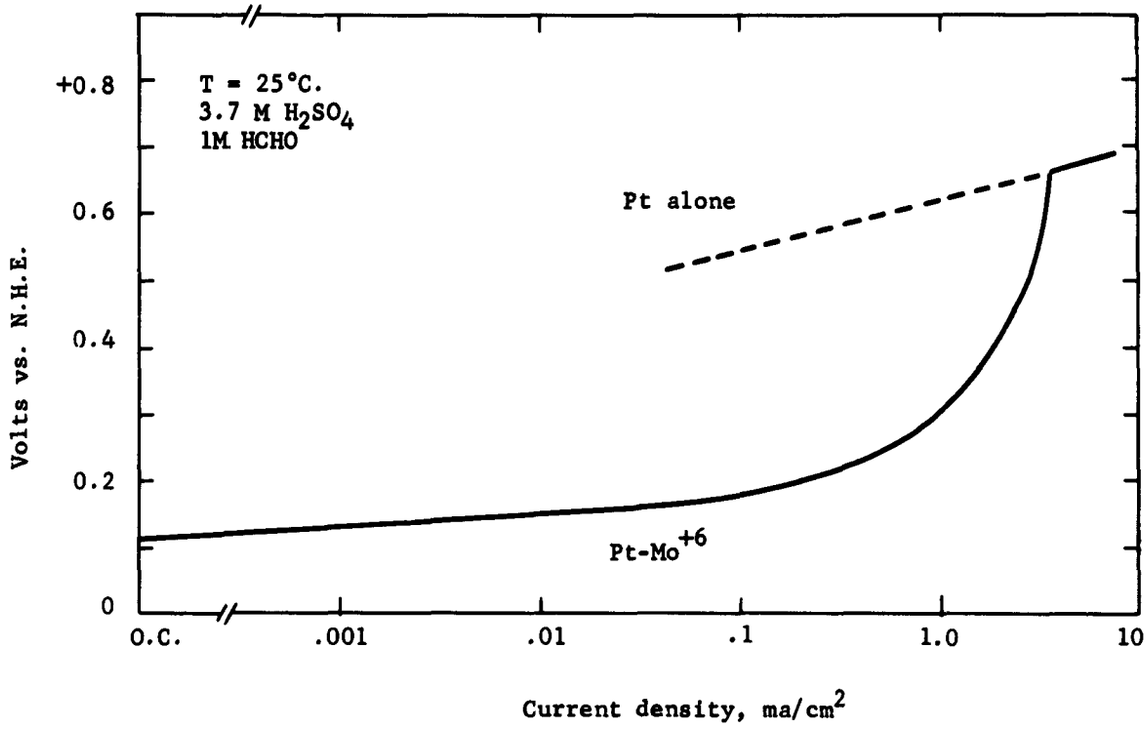

APPENDIX A-10

EFFECT OF FIFTY SUCCESSIVE OXIDATION - REDUCTIONS ON ADSORBED MOLYBDATE LAYER

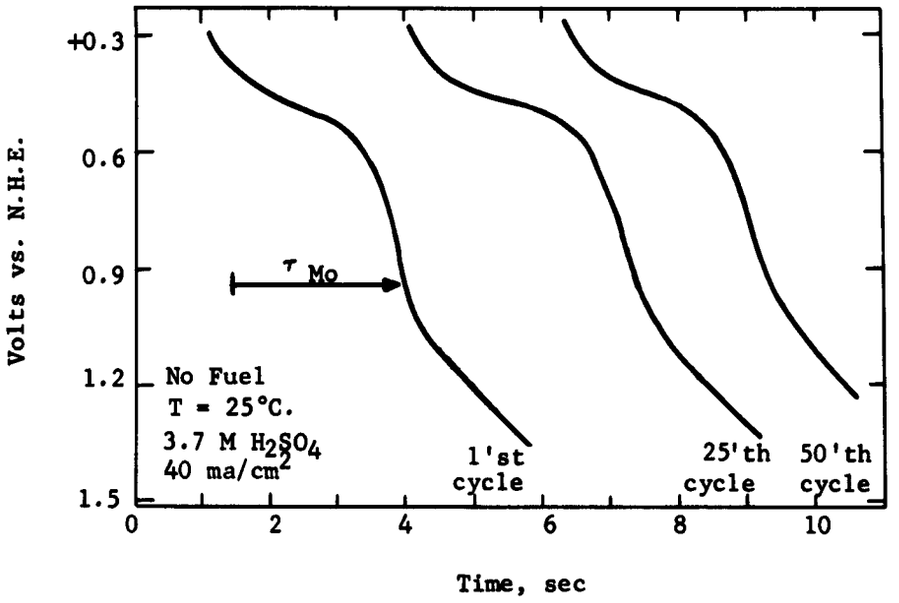

In absence of fuel, fifty sucessive oxidation cycles decrease Mo on electrode only slightly.

APPENDIX A-11

EFFECT ON MOLYBDATE LAYER OF OXIDATION IN PRESENCE OF FUEL LAYER

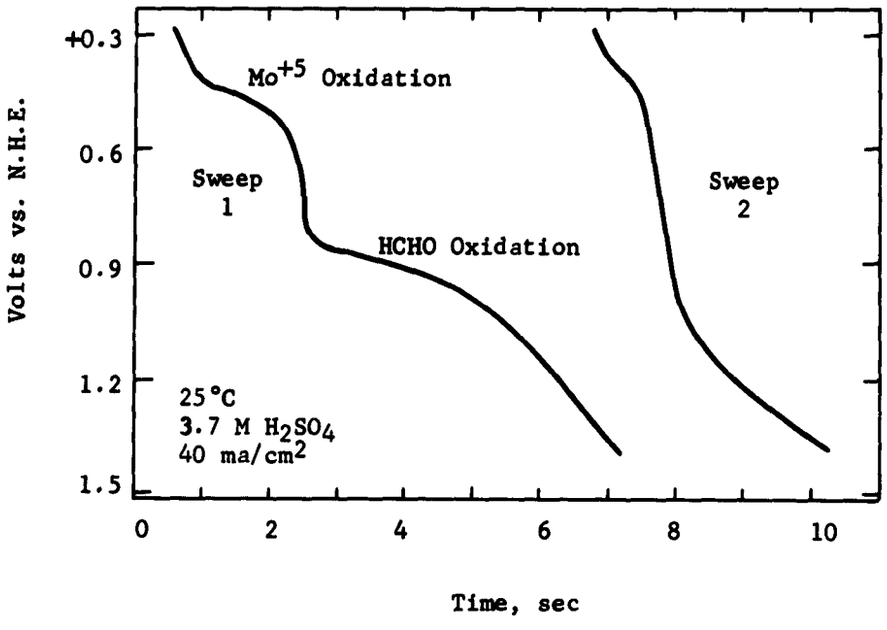

One oxidation in presence of fuel removes all Mo.

APPENDIX A-12

EFFECT OF RINSING ON ADSORBED LAYERS OF Mo^{+5} AND Mo^{+6}

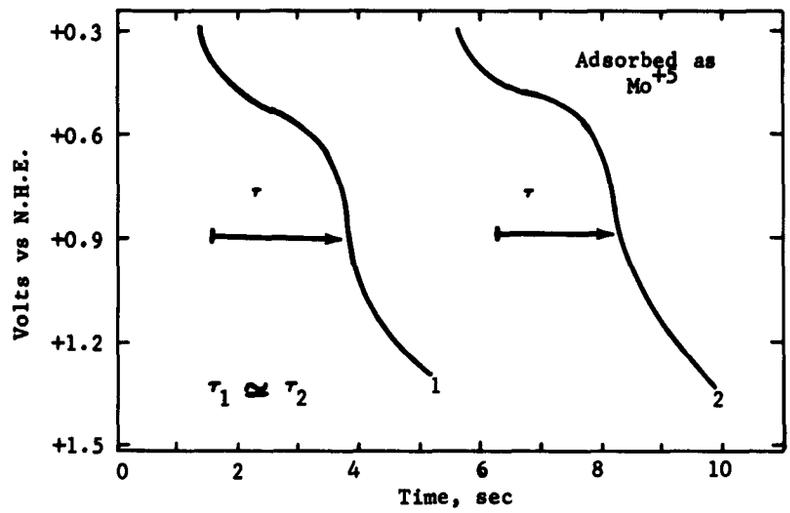

1 = 2 sec rinse; 2 = 5 minute rinse

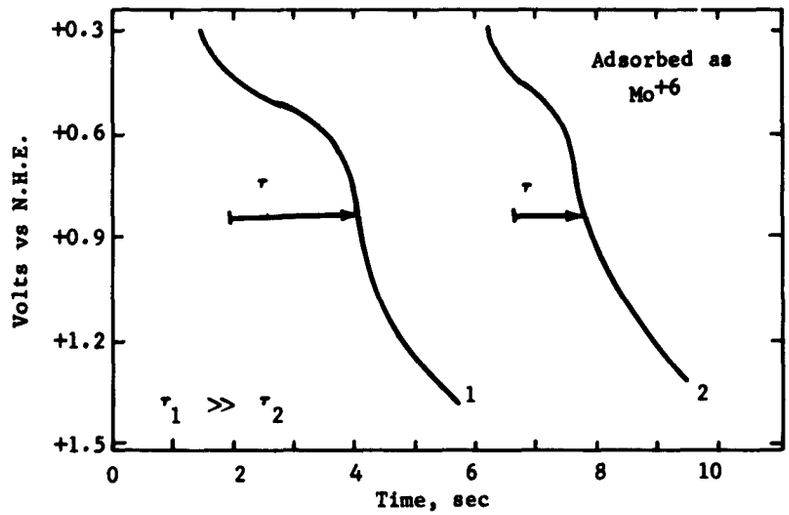

APPENDIX A-13

EFFECT OF FUEL PREADSORPTION ON SUBSEQUENT MOLYBDATE ADSORPTION

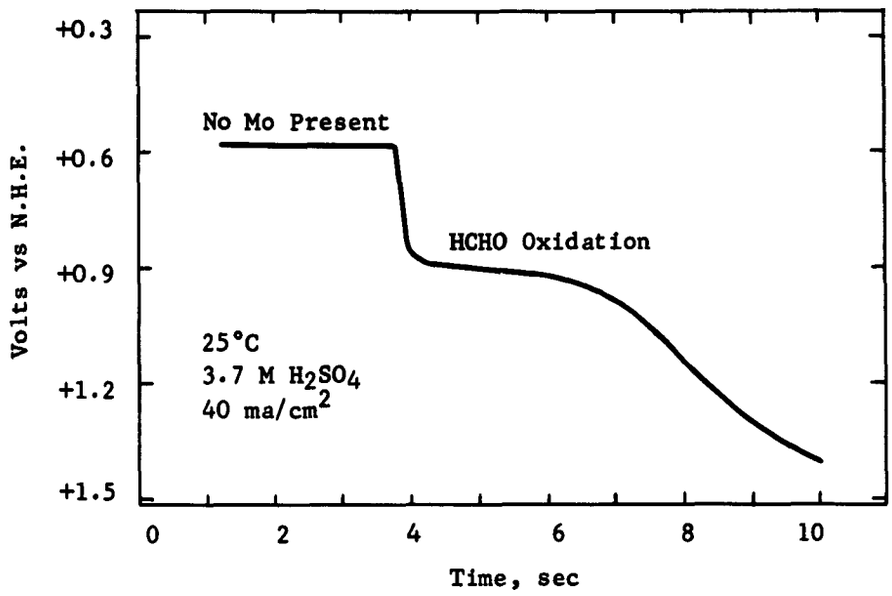

2 min HCHO adsorption first;
2 min Mo^{+6} adsorption directly following.

APPENDIX A-14

PERFORMANCE OF HCHO ON BOROHYDRIDE - REDUCED Pt - 1 wt % Na_2MoO_4

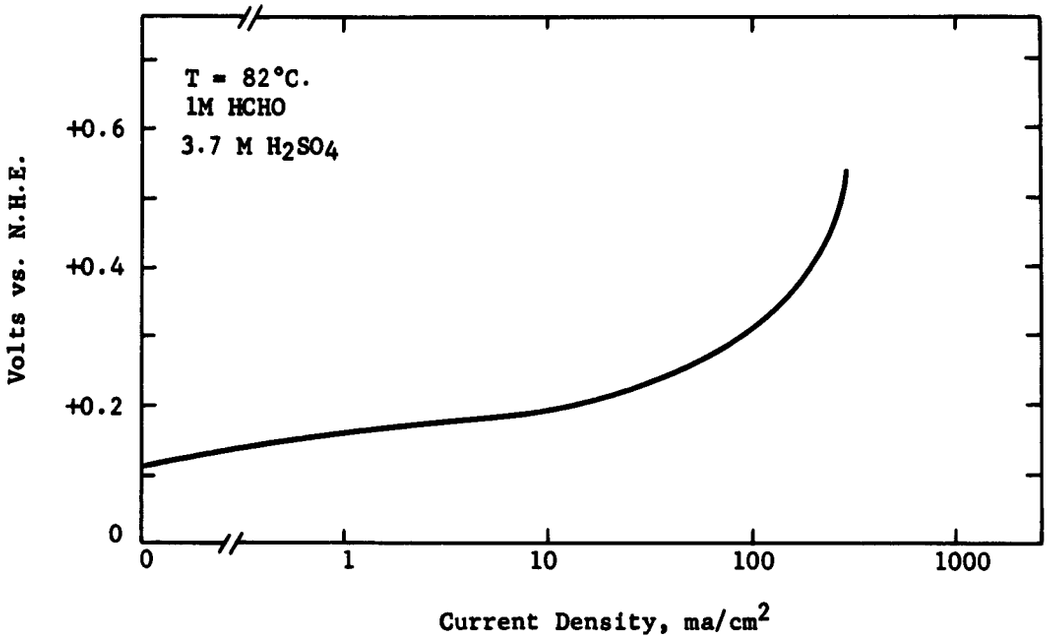

APPENDIX A-15

ACTIVATION ENERGY PLOT - Mo^{+5}
ELECTRO-OXIDATION ON Pt+Au ELECTRODE

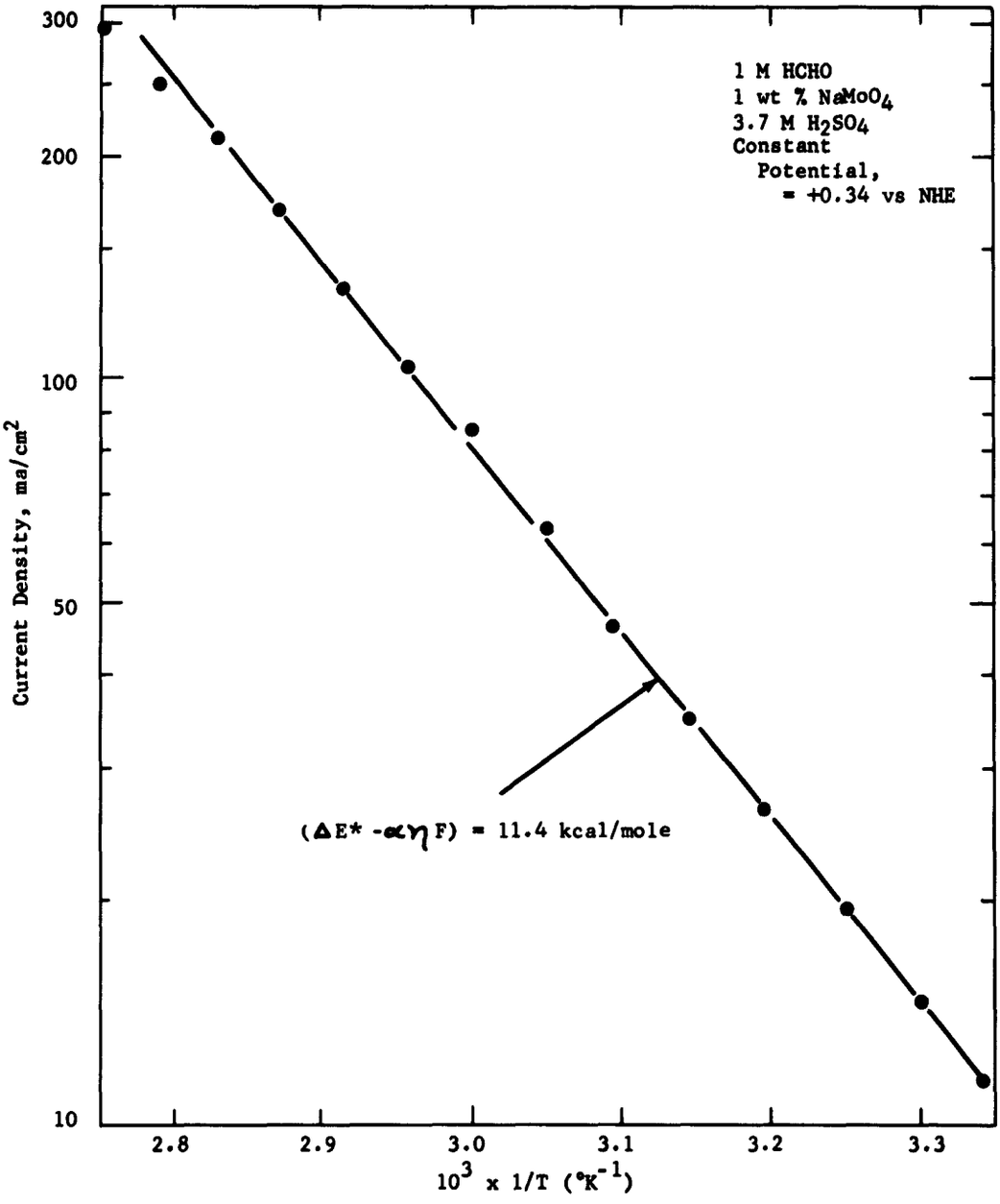

APPENDIX A-16

TYPICAL PERFORMANCE RUNS ON Pt IN MOLYBDATE-3.7 M H_2SO_4 SOLUTION

Run	Fuel	Catalyst	wt % Na_2MoO_4	T°C	Polarization, Volts From N.H.E. At Indicated ma/cm^2				
					0	1	10	50	100
3509-86	1 M HCHO	Pt+Au ($NaBH_4$)	1	82	0.21	0.22	0.24	0.30	0.36
3509-75	1 M HCHO	Pt ($NaBH_4$)	1	82	0.21	0.22	0.25	0.33	0.46
3509-70	1 M HCHO	Pt ($NaBH_4$)	1	82	0.16	0.18	0.22	0.33	0.41
3509-68	1 M HCHO	Pt ($NaBH_4$)	1	82	0.13	0.16	0.18	0.26	0.32
3509-55	1 M HCHO	Pt+Au ($NaBH_4$)	1	25	0.22	0.27	0.39	0.56	0.71
3509-48	1 M HCHO	Pt+Au ($NaBH_4$)	1	82	0.18	0.19	0.23	0.33	0.43
3509-39	1 M CH_3OH	Pt black	1	82	0.21	0.34	0.60	-	-
3509-51	1 M CH_3OH	Pt+Au ($NaBH_4$)	1	82	0.41	0.44	0.49	0.60	0.70
3509-61	1 M CH_3OH	Pt+Au ($NaBH_4$)	1	82	0.21	0.42	0.52	0.64	0.72
3509-63	1 M CH_3OH	Pt+Au ($NaBH_4$)	1	82	0.18	0.34	0.52	0.61	0.68
3509-65	1 M CH_3OH	Pt+Au ($NaBH_4$)	1	82	0.16	0.22	0.50	0.58	0.63

APPENDIX A-17

DIAGRAM OF EQUIPMENT USED TO OBTAIN VOLTAGE SCANS ON CH_3OH

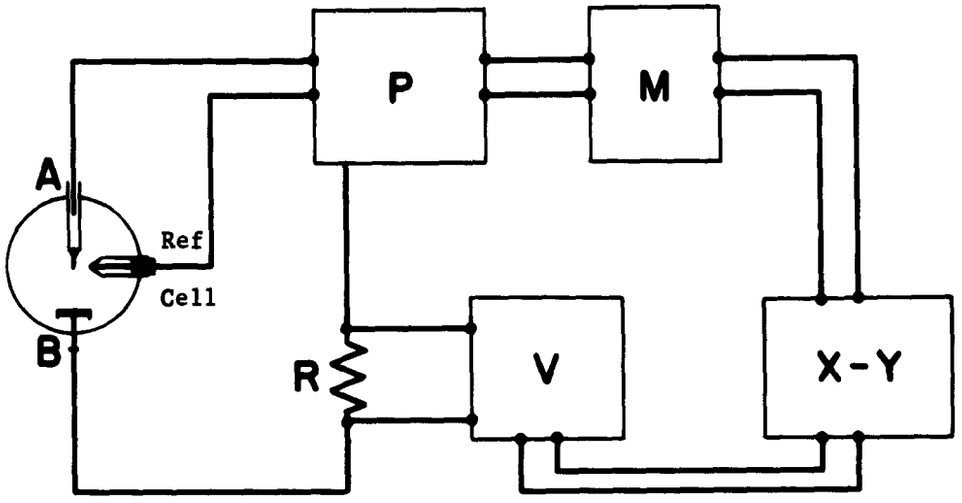

A = Measuring electrode, platinized Pt
B = Counter electrode, Pt
Ref = Saturated Calomel electrode
P = Potentiostat and power supply, Duffers Associates Models 600 and 620.
M = Motor driven linear potentiometer
V = Keithley Electrometer 610A with recorder output
R = Precision resistor
X-Y = Moseley "Autograf", X-Y plotter

APPENDIX A-18

TEMPERATURE DEPENDENCE OF FORWARD AND REVERSE PEAKS FOR CH_3OH OXIDATION

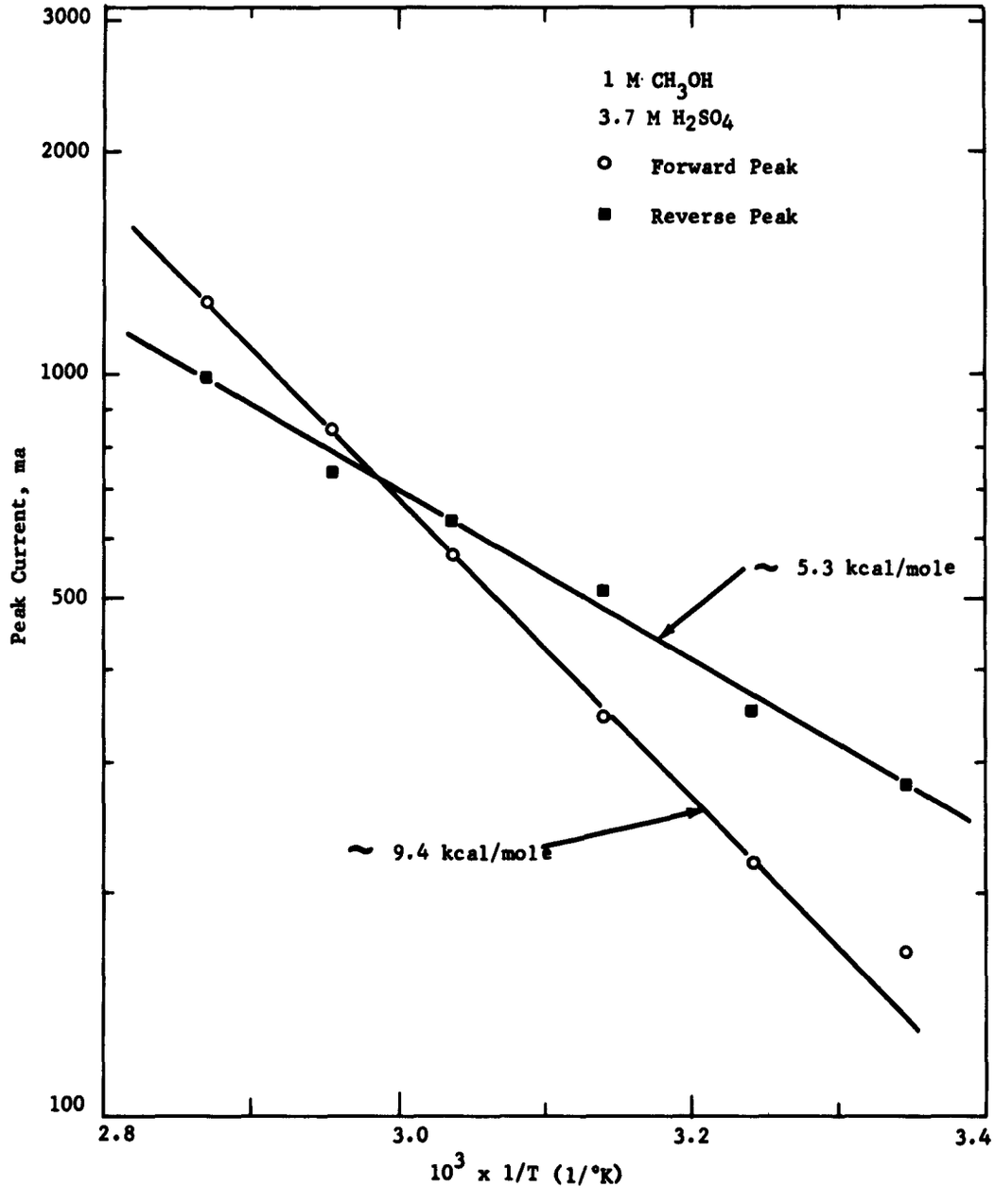

APPENDIX B-1

HNO_3 REGENERATION WITH SURFACTANTS

3.7 M H_2SO_4, 0.2 M HNO_3 82°C. 3 Electron Reaction
Electrodes: Cathode: platinized platinum basket with 6 mg/cm^2 platinum black
Anode: bright platinum basket, concentric to cathode
Gas Injection: glass frit, pore size 10 to 50 microns, placed directly above cathode, injecting downwards
For further experimental details see (1)

Surfactant, wt %	Gas Flow Rate, cc/min.	Average Current Density, ma/cm^2	Coulombs Measured x 10^{-3}	Regeneration Efficiency, Coulombs/Coulomb Equiv. to HNO_3 Consumed
I. Experiments With Oxygen				
None (for comparison)	30	32	9.7	4.2
Benax 2A1* 0.2 wt %	15	31	18.4	8.0
Benax 2A1* 1 wt %	15	31	63.4	28.0
Benax 2A1* 0.5 wt %	15	31	44.5	19.4
C_{12}-Benax 2A1**, 1 wt %	15	29	32.0	13.3
C_{12}-Benax 2A1** 1 wt % + ET 374# 1 wt %	40	28	18.8	7.5
C_9-Benax 2A1*** 1 wt %	15	31	80.4	35.2
C_9-Benax 2A1*** 1 + 1 wt %	15	31	335.0	40.4
C_9-Benax 2A1*** 1 wt %	25	93	13.4	10.0
C_9-Benax 2A1*** 0.2 wt %	20	72	468.0	225.0
II. Experiments With Air				
None (for comparison)	30	30	4.8	2.1
Benax 2A1* 1 wt %	12	31	32.0	14.0
Benax 2A1* 1 wt %	15	31	26.4	10.5
C_{12}-Benax 2A1** 1 wt %	15	31	24.0	5.7
C_9-Bonax 2A1*** 1 wt %	10	31	25.5	11.0
C_9-Benax 2A1*** 0.1 wt %	20	31	25.5	11.0
C_9-Benax 2A1*** / 0.2 wt %	15	31	13.3	5.8
C_9-Benax 2A1*** / 0.2 wt %	12	32	40.2	14.6
C_9-Benax 2A1*** 0.05 wt %	20	31	30.6	12.0
Use of Fine SiO_2 Powder (Cab-o-sil)				
No surfactant, Cab-o-sil## 1.0 wt %	15	30	8.8	3.5
No surfactant, Cab-o-sil## 5.0 wt %	30	31	4.3	2.5
C_9-Benax 2A1*** 0.2 wt % + Cab-o-sil## 0.5 wt %	15	31	21.2	9.3
C_9-Benax 2A1*** 0.2 wt % + Cab-o-sil## 1.0 wt %	20	31	64.8	25.2
C_9-Benax 2A1*** 1.0 wt % + Cab-o-sil## 3.0 wt %	15	30	5.0	2.7

Composition of Surfactants:

* Sodium dodecylated oxydibenzene disulfonate (Dow Chemical Co.)

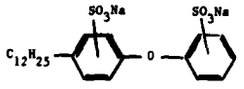

** Same as * but of higher purity

*** Sodium nonylated oxydibenzene disulfonate (Dow Chemical Co.)

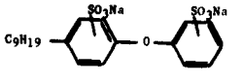

\# Oxydibenzene of higher molecular weight (Dow Chemical Co.)

Description of Fine Powder

Fine silica powder, 0.07-0.15 micron particle size (Cabot Corp.). The powder was soaked for 24 hours in electrolyte prior to its use.

/ 0.2 M $NaNO_3$ used instead of HNO_3.

APPENDIX B-2

TEFLON RESEARCH FUEL CELL

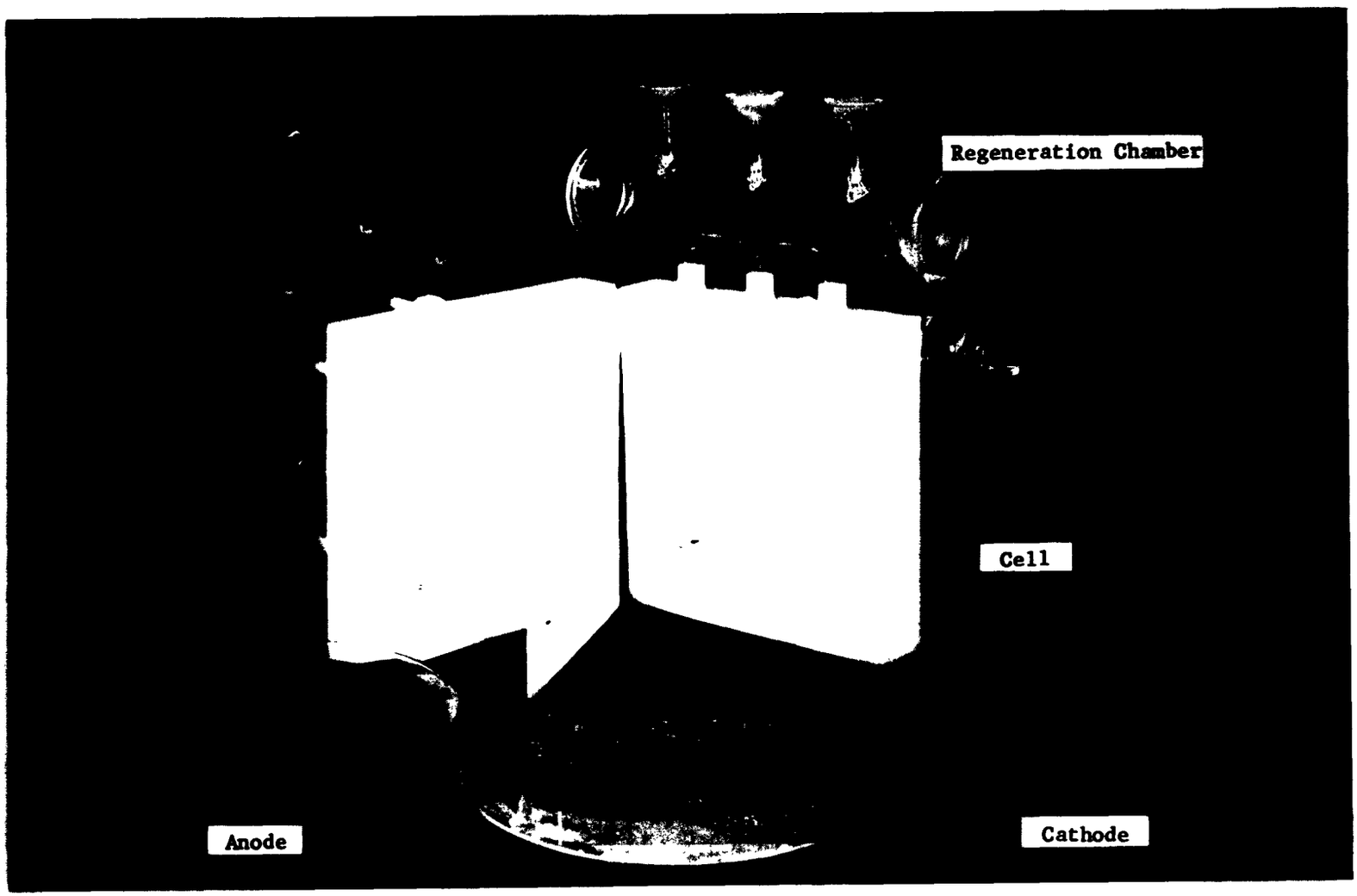

APPENDIX B-3

EQUIPMENT USED IN ENGINEERING STUDIES OF HNO_3 REGENERATION

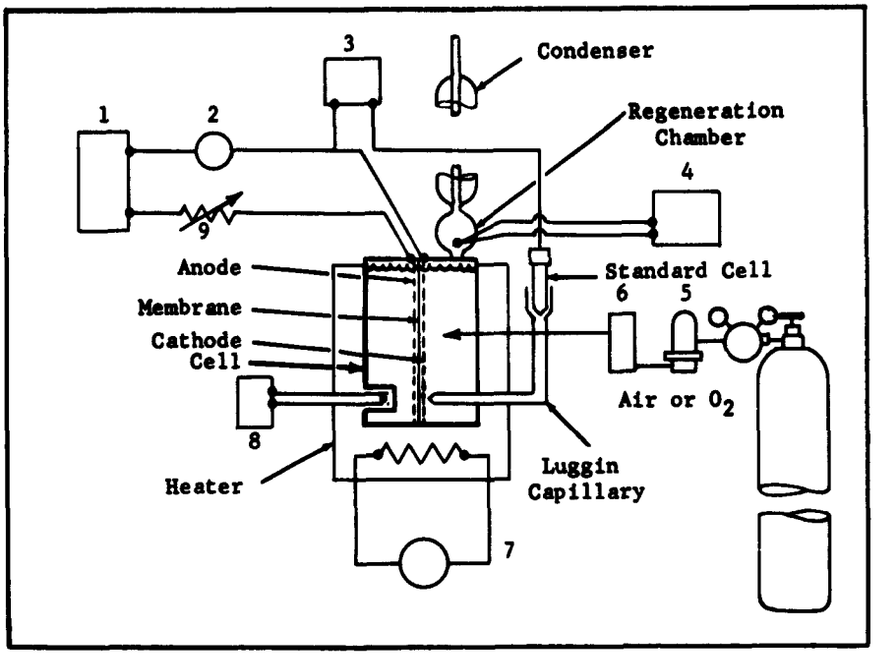

1 - ATR Rectifier Power Supply, Model 620 C-ELIT
2 - Esterline-Angus Graphic Ammeter, Model AW
3 - Keithley Electrometer, Model 610A
4 - Leeds and Northrup Potentiometer, Model 291897
with Pt-Pt 10% Rh Thermocouple
5 - Fischer Regulator, 67FR108
6 - Fischer and Porter Rotameter
FP 1/8-16-5/70 or 02F - 1/8-16-5/70
7 - Heating and Control Circuit
Glas-Col Heater
West Gardsman, Model JP
Iron, Constantan Thermocouple
Variac Autotransformer, Type WIOMT-3
HB Mercury Relay
8 - Thermo-Electric Potentiometric Pyrometer, Model
7020H with Iron, Constantan Thermocouple and
Thermowell
9 - Variac Autotransformer, Type WIOMT-3

APPENDIX B-4

THE EFFECT OF NITRIC ACID CONCENTRATION ON LIMITING CURRENT

T = 82°C. P = 1 atm
Electrolyte: 3.7 M H_2SO_4
Electrodes: Pt Screens with 8 mg/cm^2 Pt Black

Electrode Mesh	HNO_3 Concentration, wt %	Limiting Current Density, ma/cm^2
52	0	0
52	0.4	10
52	0.6	45
52	0.8	105
52	1.0	165
80	0	0
80	0.7	90
80	1.0	160
150	0	0
150	0.54	30
150	0.91	150
150	1.0	155

Figure B-1

Limiting Current for Nitric Acid Solutions

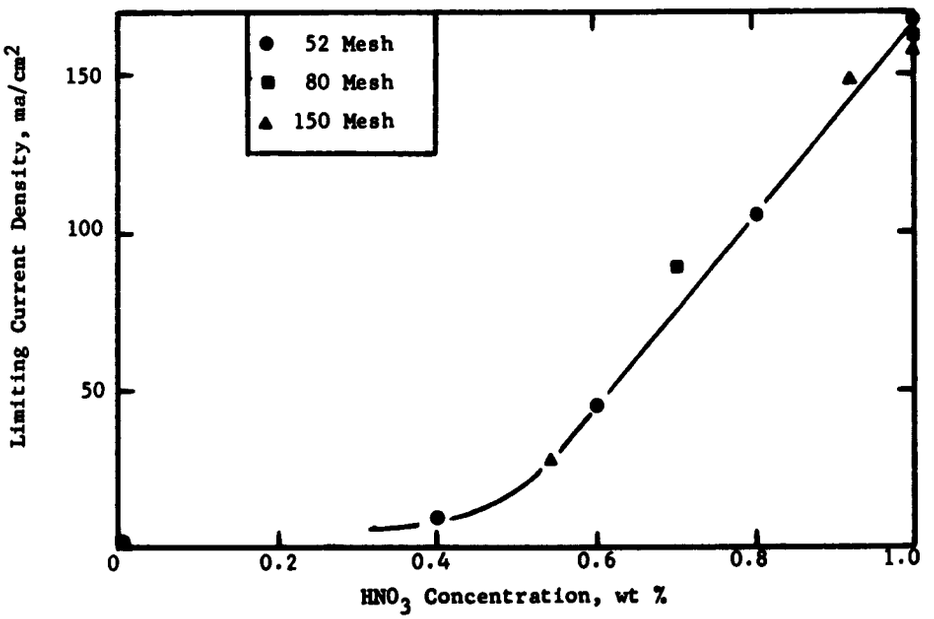

APPENDIX B-5

SUMMARY OF DATA FROM ENGINEERING STUDIES OF NITRIC ACID REGENERATION

Ref. Notebook (Pg.)	Anolyte 30 wt % H_2SO_4 Vol, cc's	Anolyte 30 wt % H_2SO_4 HNO_3 Conc, wt %	Catholyte 30 wt % H_2SO_4 Initial Vol, cc's	Catholyte 30 wt % H_2SO_4 Initial HNO_3 Conc, wt %	Catholyte 30 wt % H_2SO_4 Initial Coulombs	Catholyte 30 wt % H_2SO_4 Final Vol, cc's	Catholyte 30 wt % H_2SO_4 Final I_f, amps	Catholyte 30 wt % H_2SO_4 Final HNO_3 Conc, wt %	Catholyte 30 wt % H_2SO_4 Final Coulombs	Coulombs Consumed	I, amps	Time of Run, sec	Coulombs Delivered	Regeneration Efficiency Coul/Coul Equiv. to HNO_3 Consumed	Gas Flow Metered at 1 atm and 21°C. Gas	Gas Flow Metered at 1 atm and 21°C. Rate	Gas Flow Metered at 1 atm and 21°C. Flow Rate Relative to Stoichiometric Requirement	Special Conditions Surfactant, wt %	Special Conditions Packing	Special Conditions Details
3621 (108)	50	0	140	1	7830	140	9.0	0.76	5951	1879	3	5400	16200	8.6	Air	5.0	73	1.4	Benax 2A1 C_9 1.0	None	Regeneration Chamber* Temperature: Cell 82°C Reg. Chamber ~75°C Flow Pattern: Gas Exit-Center Port Recycle-Side Ports Comments: NO_2 observed in chamber
3621 (112)	71	0	145	1	8110	145	3.0	0.56	4542	3568	3	2220	6660	1.9	Air	4.0	196	3.7	Benax 2A1 C_9 1.0	None	Regeneration Chamber* Temperature: Cell 82°C Reg. Chamber ~75°C Flow Pattern: Gas Exit-Center Port -Side Ports Recycle-None Comments: NO_2 observed in chamber
3621 (115)	70	0	150	1	8389	150	5.5	0.64	5369	3020	3	3480	10440	3.5	Air	5.0	100	1.9	Benax 2A1 C_9 1.0	None	Regeneration Chamber* Temperature: Cell 82°C Reg. Chamber ~75°C Flow Pattern: Gas Exit-Center Port -Side Ports Recycle: None Comments: NO_2 observed in chamber
3621 (115)	70	0	150	1	8389	150	4.3	0.60	5033	3356	3	4800	14400	4.3	Air	5.0	58	1.1	Benax 2A1 C_9 2.7	None	Regeneration Chamber* Temperature: Cell 82°C Reg. Chamber ~75°C Flow Pattern: Gas Exit-Center Port -Side Ports Recycle-None Comments: NO_2 observed in chamber
3621 (116)	75	0	160	1	8948	160	4.0	0.59	5279	3669	3	3480	10440	2.8	Air	4.0	123	2.3	Benax 2A1 C_9 4.0	None	Regeneration Chamber * Temperature: Cell 82°C Reg. Chamber ~75°C Flow Pattern: Gas Exit-Center Port - Side Ports Recycle -None Comments: NO_2 observed in chamber
3621 (118)	75	0	165	1	9228	165	3.0	0.56	5168	4060	3	3060	9180	2.3	Air	5.5	32	0.6	Benax 2A1 C_9 4.0	None	Regeneration Chamber* Temperature: Cell 82°C Reg. Chamber ~75°C Flow Pattern: Gas Exit-Center Port -Side Ports Recycle -None Comments: NO_2 observed in chamber
3621oo (116)	75	0	230	1	12863	230	3.0	0.56	7203	5660	3	4800	14400	2.5	Air	9.0	105	2.0	Benax 2A1 C_9 4.3	None	Regeneration Chamber * Temperature: Cell 82°C Reg. Chamber ~75°C Flow Pattern: Gas Exit-Center Port -Side Ports Recycle -None Comments: NO_2 observed in chamber 1cc of Benax 2A1 C_9 added through sparger
3621 (118)	55	0	130	1	7271	130	3.0	0.56	4072	3199	3	2760	8280	2.6	Air	2.0	73	1.4	Benax 2A1 C_9 1.0	None	Regeneration Chamber*** Temperature: Cell 82°C Reg. Chamber ~75°C Flow Pattern: Gas Exit-Center Port -Side Ports Recycle -None Comments: NO_2 observed in chamber

* 2 inch diameter

oo A run was also attempted at ~ 350 cc/min of air but was not completed because of mechanical difficulties. However, it appeared that the regeneration efficiency would have been approximately 1-2 coulombs/coulomb equiv. to HNO_3 consumed.

*** 1 inch diameter

APPENDIX B-5 (CONT'D.)

Ref. Note-book (No.)	Analyte 30 wt % H_2SO_4 Vol, cc's	Analyte 30 wt % H_2SO_4 HNO_3 Conc, wt %	Catholyte 30 wt % H_2SO_4 Initial Vol, cc's	Initial HNO_3 Conc, wt %	Initial Coulombs	Final Vol, cc's	Final I_{ss}, amps	Final HNO_3 Conc, wt %	Final Coulombs	Coulombs Consumed	I, amps	Time of Run, sec	Coulombs Delivered	Regeneration Efficiency Coul/Coul Equiv. to HNO_3 Consumed	Gas Flow Metered at 1 atm and 21°C. Gas	Gas rate, cc's/min	Flow Rate Relative to Stoichiometric Requirement	Special Conditions Surfactant, wt %	Special Conditions Packing	Special Conditions Details
3621 (118)	60	0	140	1	7830	140	3.0	0.56	4385	3445	3	1320	3960	1.2	Air	2.0	1.4	Benax 2Al C_9 1.0	Coarse Glass Wool Dry	Regeneration Chamber[000] Temperature: Cell 82°C Reg. Chamber ~75°C Flow Pattern: Gas Exit-Center Port -Side Ports Recycle -None Comments: NO_2 observed in chamber
3621 (119)	60	0	140	1	7830	140	3.0	0.56	4385	3445	3	2520	7560	2.2	O_2	2.0	7.0	Benax 2Al C_9 1.0	None	Regeneration Chamber[000] Temperature: Cell 82°C Reg. Chamber ~75°C Flow Pattern: Gas Exit-Center Port -Side Ports Recycle -None Comments: NO_2 observed in chamber
3621 (119)	60	0	140	1	7830	140	3.0	0.56	4385	3445	3	1740	5220	1.5	O_2	2.0	7.0	None	Coarse Glass Wool Dry	Regeneration Chamber[000] Temperature: Cell 82°C Reg. Chamber ~58°C Flow Pattern: Gas Exit-Center Port -Side Ports Recycle -None Comments: NO_2 observed in chamber
3621 (120)	60	0	145	1	8110	145	7.0	0.69	5596	2514	3	13500	40500	15.0	O_2	2.0	7.0	Benax 2Al C_9 1.0	Coarse Glass Wool Satu-rated with 1 wt % HNO_3	Regeneration Chamber[000] Temperature: Cell 82°C Reg. Chamber ~75°C Flow Pattern: Gas Exit-Center Port Recycle -Side Ports Comments: No NO_2 observed in chamber
3621 (123)	60	0	150	1	8309	150	5.0	0.62	5201	3188	3	4680	14040	4.4	Air	1.0	1.5	Benax 2Al C_9 1.0	None	Regeneration Chamber[000] Temperature: Cell 82°C Reg. Chamber ~75°C Flow Pattern: Gas Exit-Center Port Recycle -Side Ports Comments: NO_2 observed in chamber
3621 (123)	60	0	155	1	8669	155	5.0	0.62	5375	3294	3	4920	14760	4.5	O_2	1.0	7.5	Benax 2Al C_9 1.0	None	Regeneration Chamber[000] Temperature: Cell 82°C Reg. Chamber ~75°C Flow Pattern: Gas Exit-Center Port Recycle -Side Ports Comments: NO_2 observed in chamber
3621 (126)	60	0	150	1	8309	150	5.0	0.62	5201	3188	3	6600	19800	6.2	Air	1.0	1.5	Benax 2Al C_9 1.0	Coarse Glass Wool Satu-rated with 1 wt % HNO_3	Regeneration Chamber[000] Temperature: Cell 82°C Reg. Chamber ~75°C Flow Pattern: Gas Exit-Center Port Recycle -Side Ports Comments: NO_2 observed in chamber
3621 (127)	60	1	148	1	8277	148	4.3	0.60	4966	3311	3	2400	7200	2.2	Air	2.0	1.8	None	Coarse Glass Wool Satu-rated with H_2O	Regeneration Chamber[000] Temperature: Cell 82°C Reg. Chamber ~66°C Flow Pattern: Gas Exit-Side Ports Recycle -Center Port Comments: NO_2 observed in chamber
3621 (127)	60	1	148 4 0.7	0.60 1.0 70.0	4966 224 3182	152	4.3	0.60	5101	3271	3	2280	6840	2.1	Air	2.0	1.8	None	Coarse Glass Wool Satu-rated with H_2O	Regeneration Chamber[000] Temperature: Cell 82°C Reg. Chamber ~66°C Flow Pattern: Gas Exit-Side Ports Recycle -Center Port Comments: NO_2 observed in chamber

APPENDIX B-5 (CONT'D.)

Ref. Note-book (Pg.)	Anolyte 30 wt % H_2SO_4 Vol, cc's	HNO_3 Conc, wt %	Catholyte 30 wt % H_2SO_4 Initial Vol, cc's	Initial HNO_3 Conc, wt %	Initial Coulombs	Final Vol, cc's	Final I_f, amps	Final HNO_3 Conc, wt %	Final Coulombs	Coulombs Consumed	I, amps	Time of Run, sec	Coulombs Delivered	Regeneration Efficiency Coul/Coul Equiv. to HNO_3 Consumed	Gas	Gas Flow Metered at 1 atm and 21°C: cc/s	cc's HNO_3	Flow Rate Relative to Stoichiometric Requirement	Surfactant, wt %	Special Conditions: Packing	Details
3621 (128)	50	1	150	1.0	8389	150	5.8	0.65	5453	2936	3.0	5400	16200	5.5	Air	2.0	97	1.8	None	Coarse Glass Wool Saturated with 1 wt % HNO_3 30 wt % H_2SO_4	Regeneration Chamber*** Temperature: Cell 82°C Reg. Chamber ~66°C Flow Pattern: Gas Exit-Side Ports Recycle -Center Port Comments: NO_2 observed in chamber
3621 (129)	50	1	150 0.7	0.65 70.0	5453 3182	150	4.3	0.60	3034	3601	3.0	2580	7740	2.1	Air	1.0	97	1.8	None	Coarse Glass Wool Saturated with 1 wt % HNO_3 30 wt % H_2SO_4	Regeneration Chamber*** Temperature: Cell 82°C Reg. Chamber ~66°C Flow Pattern: Gas Exit-Side Ports Recycle -Center Port Comments: NO_2 observed in chamber
3621 (129)	50	1	150 1.0 5.0	0.60 70.0 1.0	5034 4545 280	156	5.8	0.65	5671	4188	3.0	7860	23580	5.6	O_2	1.0	97	9.0	None	Coarse Glass Wool Saturated with 1 wt % HNO_3 30 wt % H_2SO_4	Regeneration Chamber*** Temperature: Cell 82°C Reg. Chamber ~66°C Flow Pattern: Gas Exit-Side Ports Recycle -Center Port Comments: NO_2 observed in chamber
3621 (130)	50	1	156 1.5	0.65 70	5671 6817	157.5	4.3	0.60	5285	7203	3.0	5220	15660	2.2	Air	2.0	97	1.8	None	Coarse Glass Wool Saturated with 1 wt % HNO_3 30 wt % H_2SO_4	Regeneration Chamber*** Temperature: Cell 82°C Reg. Chamber ~66°C Flow Pattern: Gas Exit-Side Ports Recycle -Center Port Comments: NO_2 observed in chamber
3621 (131)	50	1	158 1.5	0.60 70	5285 6817	159.5	4.3	0.60	5352	6750	3.0	3960	11880	1.8	Air	2.0	97	1.8	None	Coarse Glass Wool Saturated with 1 wt % HNO_3 30 wt% H_2SO_4	Regeneration Chamber*** Temperature: Cell 82°C Reg. Chamber ~ 44°C Flow Pattern: Gas Exit-Side Ports Recycle -Center Port Comments: NO_2 observed in chamber
3621 (133)	60	1	148	1.0	8277	148	4.3	0.60	4966	3311	3.0	4320	12960	3.9	Air	1.0	97	1.8	None	Coarse Glass Wool 1 wt % HNO_3 30 wt % H_2SO_4	Regeneration Chamber*** Temperature: Cell 82°C Reg. Chamber ~66°C Flow Pattern: Gas Exit-Side Ports Recycle -Center Port Comments: NO_2 observed in chamber
3621 (134)	70	1	148 0.7 10.0	0.60 70 1	4966 3182 560	158	4.3	0.60	5302	3406	3.0	2760	8280	2.4	Air	1.0	160	3.1	None	Coarse Glass Wool 1 wt % HNO_3 30 wt% H_2SO_4	Regeneration Chamber*** Temperature: Cell 82°C Reg. Chamber ~66°C Flow Pattern: Gas Exit-Side Ports Recycle -Center Port Comments: NO_2 observed in chamber
3621 (134)	70	1	158 0.74 1.0 0.76	0.60 70 1 70	5302 3363 56 3434	160	4.3	0.60	5369	6806	3.0	2880	8640	1.3	Air	1.0	192	1.8	None	Coarse Glass Wool 1 wt % HNO_3 30 wt% H_2SO_4	Regeneration Chamber*** Temperature: Cell 82°C Reg. Chamber ~66°C Flow Pattern: Gas Exit-Side Ports Recycle -Center Port Comments: NO_2 observed in chamber
3621 (134)	70	1	160 0.74	0.60 70	5369 3363	161	4.3	0.60	5403	3329	3.0	3120	9360	2.8	Air	1.0	123	2.3	None	Coarse Glass Wool 1 wt % HNO_3 30 wt% H_2S_4	Regeneration Chamber*** Temperature: Cell 82°C Reg. Chamber ~66°C Flow Pattern: Gas Exit-Side Ports Recycle -Center Port Comments: NO_2 observed in chamber

APPENDIX B-5 (CONT'D.)

Ref. Notebook (Pg.)	Analyte 30 wt % H_2SO_4 Vol, as's	Analyte 30 wt % H_2SO_4 HNO_3 Conc, wt %	Catholyte 30 wt % H_2SO_4 Initial Vol, as's	Catholyte 30 wt % H_2SO_4 Initial HNO_3 Conc, wt %	Catholyte 30 wt % H_2SO_4 Initial Coulombs	Catholyte 30 wt % H_2SO_4 Final Vol, as's	Catholyte 30 wt % H_2SO_4 Final I_f, amps	Catholyte 30 wt % H_2SO_4 Final HNO_3 Conc, wt %	Catholyte 30 wt % H_2SO_4 Final Coulombs	Coulombs Consumed	I, amps	Time of Run sec	Coulombs Delivered	Regeneration Efficiency Coul/Coul Equiv. to HNO_3 Consumed	Gas Flow Metered at 1 atm and 21°C. Gas	Gas rate	Gas rate as's/min	Flow Rate Relative to Stoichiometric Requirement	Special Conditions Surfactant, wt %	Special Conditions Packing	Special Conditions Details
3621 (134)	70	1	161 0.74 1.0	0.60 70 1	5403 3343 56	162	4.3	0.60	5436	3386	3.0	3460	7380	2.2	Air	1.0	66	1.3	None	Coarse Glass Wool Saturated with 1 wt % HNO_3 30 wt% H_2SO_4	Regeneration Chamber[000] Temperature: Cell 82°C Reg. Chamber ~66°C Flow Pattern: Gas Exit-Side Ports Recycle -Center Port Comments: NO_2 observed in chamber
3621 (134)	70	1	162 0.74 1.0	0.60 70 1	5436 3343 56	164	4.3	0.60	5503	3352	3.0	1920	5760	1.7	Air	1.0	90	1.7	None	Coarse Glass Wool Saturated with 1 wt % HNO_3 30 wt% H_2SO_4	Regeneration Chamber[000] Temperature: Cell 82°C Reg. Chamber ~66°C Flow Pattern: Gas Exit-Side Ports Recycle -Center Port Comments: NO_2 observed in chamber
3621 (135)	70	1	164 1.0	0.6 70	5503 4545	165	4.3	0.60	5537	4511	3.0	3300	9900	2.2	Air	1.0	97	1.8	None	Coarse Glass Wool Saturated with 1 wt % HNO_3 30 wt% H_2SO_4	Regeneration Chamber[000] Temperature: Cell 82°C Reg. Chamber ~66°C Flow Pattern: Gas Exit-Side Ports Recycle -Center Port Comments: NO_2 observed in chamber
3621 (135)	70	1	165 1.0	0.60 70	5537 4545	166	4.3	0.60	5570	4512	3.0	2160	6480	1.4	Air	1.0	97	1.8	None	Coarse Glass Wool Saturated with 1 wt % HNO_3 30 wt% H_2SO_4	Regeneration Chamber[000] Temperature: Cell 82°C Reg. Chamber ~66°C Flow Pattern: Gas Exit-Side Ports Recycle -Center Port Comments: NO_2 observed in chamber
3621 (135)	70	1	166 1.0	0.60 70	5570 4545	167	4.3	0.60	5604	4511	3.0	2460	7380	1.6	Air	1.0	97	1.8	None	Coarse Glass Wool Saturated with 1 wt % HNO_3 30 wt% H_2SO_4	Regeneration Chamber[000] Temperature: Cell 82°C Reg. Chamber ~66°C Flow Pattern: Gas Exit-Side Ports Recycle -Center Port Comments: NO_2 observed in chamber
3621 (136)	70	1	167 1.0	0.60 70	5604 4545	168	4.3	0.60	5638	4511	3.0	2640	7920	1.8	--	--	--	--	None	Coarse Glass Wool Saturated with 1 wt % HNO_3 30 wt% H_2SO_4	Regeneration Chamber[000] Temperature: Cell 82°C Reg. Chamber ~75°C Flow Pattern: Gas Exit-None Recycle -C.Side Pts Comments: NO_2 observed in chamber
3621 (136)	70	1	168 0.7	0.60 70	5638 3182	169	4.3	0.60	5671	3149	3.0	1320	3960	1.3	Air	1.0	97	1.8	None	Coarse Glass Wool Saturated with 1 wt % HNO_3 30 wt% H_2SO_4	Regeneration Chamber[000] Temperature: Cell 82°C Reg. Chamber ~66°C Flow Pattern: Gas Exit-Side Ports Recycle -Center Port Comments: NO_2 observed in chamber
3621 (136)	70	1	169 0.7	0.60 70	5671 3182	170	4.3	0.60	5705	3148	3.0	1680	5040	1.6	Air	1.0	97	1.8	Rexon 2A1 C_9 I	Coarse Glass Wool Saturated with 1 wt % HNO_3 30 wt% H_2SO_4	Regeneration Chamber[000] Temperature: Cell 82°C Reg. Chamber ~75°C Flow Pattern: Gas Exit-Side Ports Recycle -Center Port Comments: NO_2 observed in chamber. Packing discolored
3621 (136)	70	1	170 0.7 5	0.60 70 1	5705 3182 280	175	4.3	0.60	5872	3295	3.0	2160	6480	2.0	Air	1.0	97	1.8	Rexon 2A1 C_9 I	Coarse Glass Wool Saturated with 1 wt % HNO_3 30 wt% H_2SO_4	Regeneration Chamber[000] Temperature: Cell 82°C Reg. Chamber ~75°C Flow Pattern: Gas Exit-Side Ports Recycle -Center Port Comments: NO_2 observed in chamber. Packing discolored

APPENDIX B-5 (CONT'D.)

Ref. Note-book (Pg.)	Analyte 30 wt % H_2SO_4 Vol, cc's	Analyte 30 wt % H_2SO_4 HNO_3 Conc, wt %	Catholyte 30 wt % H_2SO_4 Initial Vol, cc's	Initial HNO_3 Conc, wt %	Initial Coulombs	Final Vol, cc's	Final I_f, amps	Final HNO_3 Conc, wt %	Final Coulombs	Coulombs Consumed	I, amps	Time of Run, sec	Coulombs Delivered	Regeneration Efficiency Coul/Coul Equiv. to HNO_3 Consumed	Gas Flow Metered at 1 atm and 21°C Gas	psig	cc's RVR	Flow Rate Relative to Stoichiometric Requirement	Surfactant, wt %	Pechini	Special Conditions Details
3621# (147)	64.5	1	114	1	6376	114	7.0	0.69	4396	1980	3.0	3180	9540	4.8	Air	1	105	2.0	Benax 2A1 C_9 0.33	None	Regeneration Chamber*** Temperature: Cell 86°C Reg. Chamber ~85°C Flow Pattern: Gas Exit-Center Port Recycle -Side Ports Comments: NO_2 observed in chamber
3621 (148)	65.0	1	115	1	6432	115	11.5	0.84	5402	1030	3.0	4455	13365	13.0	Air	1	105	2.0	Benax 2A1 C_9 0.46	None	Regeneration Chamber*** Temperature: Cell 82°C Reg. Chamber ~58°C Flow Pattern: Gas Exit-Center Port Recycle -Side Ports Comments: No NO_2 observed in chamber
3621 (149)	65.0	1	115	1	6432	115	7.0	0.69	4442	1990	3.0	3570	10710	5.4	Air	1	105	2.0	Benax 2A1 C_9 0.46	None	Regeneration Chamber*** Temperature: Cell 82°C Reg. Chamber ~77°C Flow Pattern: Gas Exit-Center Port Recycle -Side Ports Comments: NO_2 observed in chamber
3621 (150)	65.0	1	115	1	6432	115	7.5	0.71	4562	1870	3.0	5352	16056	8.6	O_2	1	105	10.0	Benax 2A1 C_9 0.46	None	Regeneration Chamber*** Temperature: Cell 82°C Reg. Chamber ~77°C Flow Pattern: Gas Exit-Center Port Recycle -Side Ports Comments: NO_2 observed in chamber
3621 (151)	65.0	1	115	1	6432	115	14.5	0.94	6046	386	3.0	5430	16290	42.3	O_2	1	105	10.0	Benax 2A1 C_9 0.46	None	Regeneration Chamber*** Temperature: Cell 82°C Reg. Chamber ~50°C Flow Pattern: Gas Exit-Center Port Recycle -Side Ports Comments: No NO_2 observed in chamber
3621 (152)	65.0	1	115	1	6432	115	11.0	0.82	5272	1160	3.0	5640	16920	14.6	Air	1	97	1.8	Benax 2A1 C_9 0.46	None	Regeneration Chamber*** Temperature: Cell 82°C Reg. Chamber ~52°C Flow Pattern: Gas Exit-Center Port Recycle -Side Ports Comments: No NO_2 observed in chamber.
3621 (153)	65.0	1	115	1	6432	115	10.0	0.79	5082	1350	3.0	3912	11736	8.7	Air	1	73	1.4	Benax 2A1 C_9 0.46	None	Regeneration Chamber*** Temperature: Cell 82°C Reg. Chamber ~43°C Flow Pattern: Gas Exit-Center Port Recycle -Side Ports Comments: No NO_2 observed in chamber
3621 (154)	65.0	1	115	1	6432	115	11.0	0.82	5272	1160	3.0	3120	9360	8.1	Air	1	123	2.3	Benax 2A1 C_9 0.46	None	Regeneration Chamber*** Temperature: Cell 82°C Reg. Chamber ~55°C Flow Pattern: Gas Exit-Center Port Recycle -Side Ports Comments: NO_2 observed in chamber
3621 (155)	65.0	1	115	1	6432	115	10.2	0.80	5142	1290	3.0	9884	29652	23.1	Air	1	58	1.1	Benax 2A1 C_9 0.46	None	Regeneration Chamber*** Temperature: Cell 82°C Reg. Chamber ~43°C Flow Pattern: Gas Exit-Center Port Recycle -Side Ports Comments: No NO_2 observed in chamber. Extended run ##

All runs after 147 used an improved air injector to give denser foam.
Extended runs are explained on page 31

APPENDIX B-3 (CONT'D.)

Ref. Notebook (Pg.)	Anolyte 30 wt % H_2SO_4 Vol, cc's	Anolyte 30 wt % H_2SO_4 MnO_2 Conc, wt %	Catholyte 30 wt % H_2SO_4 Initial Vol, cc's	Initial MnO_2 Conc, wt %	Initial Coulombs	Final Vol, cc's	Final I_f, amps	Final MnO_2 Conc, wt %	Final Coulombs	Coulombs Consumed	I, amps	Time of Run sec	Coulombs Delivered	Regeneration Efficiency Coulo/Coul Equiv. to MnO_2 Consumed	Metered at 1 atm and 21°C Gas	psig	cc's min	Flow Rate Relative to Stoichiometric Requirement	Special Conditions Surfactant, wt %	Special Conditions Peaking	Special Conditions Details
3621 (157)	65.0	1	120	1	6711	120	7.4	0.70	4697	2014	3.0	5984	17952	8.9	Air	1	32	0.6	Benax 2A1 C_9 0.46	None	Regeneration Chamber*** Temperature: Cell 81°C Reg. Chamber ~42°C Flow Pattern: Gas Exit-Center Port Recycle -Side Ports Comments: MnO_2 observed in chamber. Extended run
3621 (158)	65.0	1	115	1	6432	115	11.6	0.84	5403	1029	3.0	6032	18096	17.5	Air	1	73	1.4	Benax 2A1 C_9 0.46	None	Regeneration Chamber*** Temperature: Cell 82°C Reg. Chamber ~47°C Flow Pattern: Gas Exit-Center Port Recycle -Side Ports Comments: No MnO_2 observed in chamber. Extended run
3621 (159)	65.0	1	115	1	6432	115	10	0.79	5081	1351	3.0	10959	32877	24.4	Air	1	73	1.4	Benax 2A1 C_9 0.46	None	Regeneration Chamber*** Temperature: Cell 82°C Reg. Chamber ~45°C Flow Pattern: Gas Exit-Center Port Recycle -Side Ports Comments: No MnO_2 observed in chamber. Extended run
945 (3)	65.0	1	115	1	6432	115	4.6	0.61	3924	2508	3.0	6451	19353	7.7	Air	1	14	0.3	Benax 2A1 C_9 0.46	None	Regeneration Chamber*** Temperature: Cell 82°C Reg. Chamber ~ 36°C Flow Pattern: Gas Exit-Center Port Recycle -Side Ports Comments: MnO_2 observed in chamber. Extended run
945 (4)	65.0	1	115	1	6432	115	6.2	0.66	4245	2187	3.0	9392	28176	12.9	Air	1	32	0.6	Benax 2A1 C_9 0.44	None	Regeneration Chamber*** Temperature: Cell 82°C Reg. Chamber ~ 32°C Flow Pattern: Gas Exit-Center Port Recycle -Side Ports Comments: MnO_2 observed in chamber. Extended run
945 (5)	65.0	1	115	1	6432	115	11.8	0.85	5467	965	3.0	10373	31119	32.2	Air	1	105	2.0	Benax 2A1 C_9 0.46	None	Regeneration Chamber*** Temperature: Cell 82°C Reg. Chamber ~28°C Flow Pattern: Gas Exit-Center Port Recycle -Side Ports Comments: No MnO_2 observed in chamber Extended run
945 (5)	65.0	1	115	1	6432	115	3.2	0.36	3602	2830	3.0	2349	7047	2.5	--	--	--	--	Benax 2A1 C_9 0.46	None	Regeneration Chamber*** Temperature: Cell 82°C Reg. Chamber ~75°C Flow Pattern: Gas Exit-None Recycle -Center Port -Side Ports Comments: MnO_2 observed in chamber

APPENDIX C-1

METHANOL ELECTRODE LIFE STUDIES

Conditions, Performance and Compositions

Run Number	3618-7						
Run Hours	0	22	48	72	96	120	144***
Cell Temperature, °C	95	82	82	82	80	82	82
Current Collector	0.001" thick x 3/16" wide Pt sheet on edges						
Cathode, 8 mils thick*	Pt black on 52 mesh Pt screen						
Anode, 8 mils thick*	Pt black on 52 mesh Pt screen						
Membrane, 5.6 mils thick	AMFion C313						
Electrolyte Between Electrodes	77 mils						
Current Density, ma/cm^2	55	15	45	64	30	50	32
Volts Polarization At Constant Current	0.63	0.57	0.74	-	-	-	-
Volts Polarization With Open Circuiting	-	-	0.67	0.70	0.73	0.70	-
Feed Solution During Period:							
Methanol, ml	-	20.4	40.8	23.8	74.2	55.7	-
Water, ml	-	9.6	19.2	11.2	34.8	26.3	-
Total, ml	-	30.0	60.0	35.0	109.0	82.0	-
Feed Solution For Run:							
Methanol, ml	-	20.4	61.2	95.0	159.2	215.9	-
Water, ml	-	9.6	28.8	40.0	74.8	101.1	-
Total, ml	-	30.0	90.0	125.0	234.0	316.0	-
Methanol, ml/hr	-	0.93	1.28	1.18	1.66	1.80	
Condensate From Exit Gas Streams	Returned to cell through gas exits						
Anolyte Electrolyte Recycle:							
H_2SO_4, wt%	30.0	-	-	30.0	26.3	-	-
Methanol, vol%	1.0 nominal						
Fuel Fed:							
Methanol, vol%	68**						
Water, vol%	32						

* Electrodes square shape, 90 cm^2 area in use.
** Matheson Spectroquality grade methanol.
*** Shut down because of poor performance caused by membrane breakage, catalyst loss, and electrode warpage.

APPENDIX C-1 (CONT'D.)

METHANOL ELECTRODE LIFE STUDIES

Run Conditions, Electrical Performance, Feed and Product Rates

Run Number	3618-13																		
Run Hours	0	26	48	72	100	124	138	162	186	210	234	269	294	330	354	378	403	476	500#
Cell Temp °C	82	82	82	81	81	81	78	77	82	82	82	80	82	82	82	82	82	80	80
Current Collector	0.001" thick x 3/16" wide Pt sheet around periphery of electrodes																		
Cathode*	80 mesh Pt-Rh screen plus 8 mg Pt black/cm^2, 6 mils thick																		
Anode*	80 mesh Pt-Rh screen plus 8 mg Pt black/cm^2, 6 mils thick																		
Membrane	AMFion C313 cation membrane, 5.6 mils thick																		
Electrolyte between Electrodes	87 mils																		
Current Density, ma/cm^2	50	48	50	50	50	48	50	50	48	48	50	48	50	48	48	49	48	48	48
Volts Polarization at Constant Current	0.65	0.66	0.70	0.67	0.66	0.67	0.69	0.73	0.74	0.68	0.68	0.70	0.70	0.74	0.76	--	--	--	--
Volts Polarization with Open Circuiting	--	--	--	--	--	--	--	--	--	--	--	--	--	--	0.67	0.69	0.69	0.70	0.70
Feed Solution During Period:																			
Methanol, ml	--	56	31	97	73	69	69	14	37	48	45	77	99	82	69	80	75	139	107
Water, ml	--	26	14	43	33	31	31	6	82	22	20	113	81	68	57	50	62	113	88
Total, ml	--	82	45	140	106	100	100	20	119	70	65	190	180	150	126	130	137	252	195
Feed Solution For Run:																			
Methanol, ml	--	56	87	184	257	326	395	409	446	494	539	616	715	797	866	946	1021	1160	1267
Water, ml	--	26	40	83	116	147	178	184	266	288	308	421	502	570	627	677	739	852	940
Total, ml	--	82	127	267	373	473	573	593	712	782	847	1037	1217	1367	1493	1623	1760	2012	2207
Methanol, ml/hr	--	2.15	1.81	2.55	2.57	2.63	2.86	2.52	2.40	2.35	2.30	2.29	2.43	2.42	2.45	2.50	2.53	2.44	2.53
Condensate From CO_2 Anode at 26°C**																			
For Period, ml	--	5	9	7	9	10	14	11	6	4	5	20	13	20	15	24	10	30	7
Total for run, ml	--	5	14	21	30	40	54	65	71	75	80	100	113	132	148	172	182	212	219
Total methanol, ml calc	10.0						--	23.8	--	27.4	29.0	--	39.7	45.7	--	--	63.3	73.3	75.6
" " ml/hr	0.081						--	0.147	--	0.130	0.123	--	0.135	0.138	--	--	0.157	0.154	0.151
Condensate From H_2 Cathode at 26°C**																			
For Period, ml	--	14	20	23	33	36	42	48	40	37	39	76	60	78	57	77	61	140	34
Total for run, ml	--	14	34	57	90	126	168	216	256	293	332	408	468	536	593	670	731	871	905
Total methanol, ml calc	37.8						--	87.3	105.3	115.3	126.4	150.7	172.0	197.4	--	--	262.9	308.4	318.6
" " ml/hr	0.30						--	0.54	0.57	0.55	0.54	0.56	0.58	0.60	--	--	0.65	0.65	0.64
Additional Methanol in Dry Ice Trap, ml/hr	--	--	--	--	--	--	--	--	--	--	--	--	--	--	--	--	0.39***	--	--

* Electrodes square shape 90 cm^2 area in use.
** Condensed in exit system at room temperature.
*** Collected from H_2 plus CO_2 streams. Total liquid had 0.860 sp.gr. and 82 vol % methanol
\# Shut down voluntarily because of higher than predicted anode voltage polarization.

APPENDIX C-1 (CONT'D.)

METHANOL ELECTRODE LIFE STUDIES

Solution Analyses @ 26°C

Run Number	3618-13																		
Run Hours	0	26	48	72	100	124	138	162	186	210	234	269	294	330	354	378	403	476	500
Anolyte Electrolyte Recycle:*																			
Density, gm /ml	1.21	--	--	--	--	--	--	1.18	--	--	--	--	--	--	--	--	1.18	--	1.18**
H_2SO_4 Normality	7.5	--	7.7	7.6	8.0	7.5	7.0	7.3	7.2	7.3	7.4	--	6.8	6.9	6.9	--	6.9	7.5	7.2
H_2SO_4 wt %	30.5	--	30.8	30.6	31.7	30.5	28.3	29.9	29.8	29.9	30.0	--	28.0	28.3	28.3	--	28.3	30.5	29.1
Methanol vol %	2.1	3.3					8.5		--	--	--	--	--	--	9.7			--	9.1
" " Calc	--	3.6					10.0		5.4		4.6	4.9		4.5	5.4			5.0	5.0
Methanol in Catholyte, Calc vol %		5.0					10.4		8.3	4.5	4.8	5.5	6.4	5.6	4.8		7.2	5.6	5.0
Condensate from CO_2 Anode:																			
Density, gm /ml		0.960					0.913		0.944		0.951	0.949		0.953	0.944			0.948	0.948
H_2SO_4 Normality		0.19					0.23		0.08		--	0.10		0.08	0.12			0.17	0.20
H_2SO_4 wt %		0.8					1.0		0.3		--	0.4		0.3	0.5			0.8	0.9
Methanol vol % Calc #		25.0					55.0		36.0		31.0	32.5		30.0	36.0			33.2	33.2
Condensate from H_2 Cathode:																			
Density, gm /ml		0.953					0.912		0.930	0.957	0.955	0.950	0.945	0.949	0.955		0.941	0.949	0.953
H_2SO_4 Normality		0.10					0.13		0.09	0.06	0.06	0.07	0.06	0.06	0.37		0.10	0.13	0.27
H_2SO_4 wt %		0.4					0.5		0.4	0.3	0.3	0.3	0.3	0.3	1.7		0.4	0.5	1.3
Methanol vol %***	--	--	--	--	--	--	--	--	--	--	--	--	--	--	--		41.2	--	--
" " Calc#		33.3					55.0		47.5	30.4	32.2	35.2	39.0	36.2	32.2		41.2	36.2	33.3
Fuel Fed:																			
Methanol vol %		69										55					55		
Water vol %		31										45					45		
Methanol grade		Commercial Union Carbide															Spectroquality		
Anolyte Sample Removed, ml	0	0	0	8	10	12	14	26	28	29	40	40	42	44	46	46	57	60	74

* Operated at 520 ml/hour recycle through cell.
** Analysis at end of run showed 9.1 vol % CH_3OH, 0.054 wt % HCHO and 0.13 wt % HCOOH in recycled anolyte.
*** Methanol concentrations were determined by colorimetric chemical analysis.
# Calculated from solution densities at 26°C.

APPENDIX C-1 (CONT'D.)

METHANOL ELECTRODE LIFE STUDIES

Run Conditions, Electrical Performance, Feed and Product Rates

Run Number	3618-26											3618-29					
Run Hours	0	2	20	46	72	99	123	148	164	188	212***	0	22	46	70	94	119#
Cell Temp °C	69	77	78	82	82	82	80	80	80	80	79	80	80	82	82	82	101
Current Collector	0.001" thick x 3/16" wide Pt sheet around periphery of electrodes																
Cathode, 6 mils thick*	Pt-black on 80 mesh Pt-Rh Screen											Pt-black on 80 mesh Pt-Rh Screen					
Anode, 6 mils thick *	"											"					
Membranes, 5.6 mils thick	AMFion C313											AMFion C313					
Electrolyte between electrodes	87 mils											87 mils					
Current Density, ma/cm^2	50	48	49	48	48	47	46	46	46	45	45	50	45	48	48	48	15
Volts Polarization at Constant Current	0.64	--	--	0.63	--	0.68	0.80	0.85	--	0.93	--	--	--	--	--	--	--
Volts Polarization With Open Circuiting	--	0.61	0.65	0.63	0.69	0.68	0.70	0.70	0.73	0.73	0.73	0.65	0.61	0.70	0.70	0.73	--
Feed Solution During Period:																	
Methanol, ml	--	4.4	51.6	60.5	66.5	90.3	87.1	77.0	49.0	56.0	47.3	--	58.3	41.2	45.6	36.3	71.0
Water, ml	--	3.6	42.4	49.5	50.5	57.7	54.9	63.0	40.0	46.0	38.7	--	47.7	33.8	37.4	29.7	58.0
Total, ml	--	8.0	94.0	110.0	117.0	148.0	142.0	140.0	89.0	102.0	86.0	--	106.0	75.0	83.0	66.0	129.0
Feed Solution For Run:																	
Methanol, ml	--	4.4	56.0	116.5	183.0	273.3	360.4	437.4	486.4	542.4	589.7	--	58.3	99.5	145.1	181.4	252.4
Water, ml	--	3.6	46.0	95.5	146.0	203.7	258.6	321.6	361.6	407.6	446.3	--	47.7	81.5	118.9	148.6	206.6
Total, ml	--	8.0	102.0	212.0	329.0	477.0	619.0	759.0	848.0	950.0	1036.0	--	106.0	181.0	264.0	330.0	459.0
Methanol, ml/hr	--	2.20	2.80	2.53	2.54	2.76	2.93	2.96	2.96	2.88	2.78	--	2.65	2.16	2.07	1.93	2.12
Condensate From CO_2 Anode at 26°C**																	
For Period, ml	--	0.0	7.0	13.0	12.0	12.0	8.0	21.0	9.0	15.0	10.0	--	1.0	1.0		3.0	11.0
Total for run, ml	--	0.0	7.0	20.0	32.0	44.0	52.0	73.0	82.0	97.0	107.0	--	1.0	--	2.0	5.0	16.0
Total methanol, ml calc	--	18.2						--	32.5	--	42.1	--	--	--	--	--	--
" " ml/hr	--	0.148						--	0.198	--	0.198	--	--	--	--	--	--
Condensate From H_2 Cathode at 26°C**																	
For Period, ml	--	0.0	33.0	14.0	46.0	46.0	38.0	79.0	38.0	55.0	48.0	--	49.0	35.0	32.0	34.0	91.0
Total for run, ml	--	0.0	33.0	47.0	93.0	139.0	177.0	256.0	294.0	349.0	397.0	--	49.0	84.0	116.0	150.0	241.0
Total methanol, ml calc	--	--	4.9	--	--	--	10.4	--	16.0	--	19.9	--	2.9	--	18.0	30.6	--
" " ml/hr	--	--	0.245	--	--	--	0.084	--	0.098	--	0.094	--	0.131	--	0.257	0.325	--

* Electrodes square shape, 90 cm^2 in use.
** Condensed in exit system at room temperature.
*** Shutdown because of severe voltage oscillations on high polarization. Membrane had slipped sufficiently to cause gas bypassing.
\# Shutdown because of recycle pump failure, whichcaused fuel depletion in cell, severe polarization and H_2SO_4 reduction to sulfur and H_2S.

APPENDIX C-1 (CONT'D.)

METHANOL ELECTRODE LIFE STUDIES

Solution Analyses @ 26°C

Run Number	3618-26											3618-29					
Run Hours	0	2	20	46	72	99	123	148	164	188	212	0	22	46	70	94	119
Anolyte Electrolyte Recycle:*																	
Density, gm /ml	--	--	--	--	--	--	--	--	--	--	1.17	--	--	--	1.19	--	--
H_2SO_4 Normality	--	--	7.2	--	--	--	6.6	--	6.1	--	6.6	--	7.2	--	7.4	7.5	--
H_2SO_4 wt %	--	--	29.1	--	--	--	26.7	--	24.6	--	26.7	--	29.1	--	30.0	30.5	--
Methanol vol %	--	--	--	--	--	--	--	10.6		--	--	--	--	8.5		--	--
" " Calc	1.0	4.9						8.3		6.2		1.0	--	--	--	--	--
Condensate From CO_2 Anode:																	
Density, gm /ml	0.952							0.930		0.946		--	--	--	--	--	--
H_2SO_4 Normality	0.15							0.17		0.16		--	--	--	--	--	--
H_2SO_4 wt %	0.68							0.79		0.74		--	--	--	--	--	--
Methanol vol % Calc	35.0							47.8		38.5		--	--	--	--	--	--
Condensate From H_2 Cathode:																	
Density, gm /ml	0.977			0.946				0.932		0.946		1.094		0.971		0.947	--
H_2SO_4 Normality	0.075			0.060				0.070		0.090		3.6		0.13		0.05	--
H_2SO_4 wt %	0.35			0.28				0.33		0.42		15.6		0.60		0.23	--
Methanol vol % Calc	14.7			38.5				47.4		38.5		6.0		22.5		37.3	--
Fuel Fed:																	
Methanol vol %	55											55					
Water vol %	45											45					
Methanol Grade	Spectroquality									Commercial Union Carbide		Commercial Union Carbide					
Anolyte Sample Removed, total ml	--	--	2.2	--	--	--	4.1	--	14.7	--	16.7	--	2	--	13	15.6	--

*Operated at 520 ml/hour recycle through cell.

APPENDIX C-1 (CONT'D.)

METHANOL ELECTRODE LIFE STUDIES

Run Conditions, Electrical Performance, Feed and Product Rates

Run Number	3618-40									
Run Hours	0	20	44	68	98	123	140	164	188#	193
Cell Temperature, °C	75	82	80	81	79	77	82	84	82	82
Current Collector	0.001" thick x 3/16" wide Pt Sheet Around Periphery Of Electrodes									
Cathode*	80 Mesh Pt-Rh Screen Plus 8 mg Pt-Black/cm^2, 6 mils thick									
Anode*	80 Mesh Pt-Rh Screen Plus 8 mg Pt-Black/cm^2, 6 mils thick									
Membrane	AMFion C313, 5.6 mils thick, Not Tight Between Electrodes									
Electrolyte Space Between Electrodes***	92 mils									
Current Density, ma/cm^2	50	50	45-51	45-51	49	48	48	33	30	49
Volts Polarization at Constant Current	0.66	0.57	0.59	-	-	-	-	-	-	0.69
Volts Polarization With Open Circuiting	-	-	-	0.59	0.59	0.59	0.79	0.70	0.78	-
Feed Solution During Period:										
Methanol, ml	-	32.4	28.1	31.1	72.9	37.1	26.8	27.8	49.3	Once Thru Feed
Water, ml	-	26.6	47.9	52.9	197.1	120.9	77.2	47.2	66.7	With 1 wt% CH_3OH in
Total, ml	-	59.0	76.0	84.0	270.0	158.0	104.0	75.0	116.0	30 wt % H_2SO_4
Feed Solution For Run:										
Methanol, ml	-	32.4	60.5	91.6	164.5	201.6	228.4	256.2	305.5	
Water, ml	-	26.6	74.5	127.4	324.5	445.4	522.6	569.8	636.5	
Total, ml	-	59.0	135.0	219.0	489.0	647.0	751.0	826.0	942.0	
Methanol, ml/hr	-	1.62	1.37	1.35	1.68	1.64	1.63	1.56	1.62	
Makeup 96% H_2SO_4 Soln, ml total	-	-	-	-	-	-	30.0	-	-	-
Condensate From CO_2 Anode At 26°C:**										
For Period, ml	-	5	17	20	25	22	25	34	24	-
Total For Run, ml	-	5	22	42	67	89	114	148	172	-
Total Methanol, ml calc	-	2.3		5.1	10.4	14.8	18.3	-	28.1	-
Total Methanol, ml/hr	-	0.052		0.075	0.106	0.120	0.131	-	0.149	-
Condensate From H_2 Cathode At 26°C:**										
For Period, ml	-	32	165	72	143	69	16	23	11	-
Total For Run, ml	-	32	197	269	412	481	497	520	531	-
Total Methanol, ml calc	-	1.1	6.1	8.2	19.7	25.2	27.4	-	32.2	-
Total Methanol, ml/hr	-	0.055	0.138	0.120	0.201	0.204	0.196	-	0.171	-

* Electrodes square shape, 90 cm^2 in use.
** Condensed in chilled water cooled condenser at about 20°C.
*** Started with 670 ml electrolyte in total system.
# Shut down because of severe voltage oscillation and excessive polarization.

APPENDIX C-1 (CONT'D.)

METHANOL ELECTRODE LIFE STUDIES

Solution Analyses @ 260°C

Run Number	3618-40								
Run Hours	0	20	44	68	98	123	140	164	188
Anolyte Electrolyte Recycle:*									
Density, gm /ml	1.212	1.200	1.220	--	1.186	1.153	--	--	1.171
H_2SO_4 Normality	7.7	8.0	8.2	7.6	6.9	5.6	5.6	--	6.3
H_2SO_4 wt %	30.8	31.9	32.3	30.5	27.8	23.0	23.0	--	25.6
Methanol vol %	0.9	--	--	1.26	--	2.88	--	--	--
" " Calc	1.0	-----1.90------		1.85	2.97	2.86	1.90	--	2.40
Catholyte Electrolyte:									
Density, gm /ml	--	--	--	1.180	--	1.139	--	--	--
H_2SO_4 Normality	--	--	--	6.57	--	5.17	4.93	--	--
H_2SO_4 wt %	--	--	--	26.7	--	21.3	20.2	--	--
Methanol vol %	--	--	--	--	--	2.79	--	--	--
" " Calc	--	0.44	0.35	0.35	1.05	1.05	1.90	--	1.92
Condensate From CO_2 Anode:									
Density, gm /ml	----------0.978----------			0.980	0.969	0.970	0.979	--	0.974
H_2SO_4 Normality	----------0.06----------			0.02	0.03	0.03	0.02	--	0.11
H_2SO_4 wt %	----------0.28----------			0.09	0.14	0.14	0.09	--	0.51
Methanol vol %	--	--	--	10.9	--	21.3	--	--	--
" " Calc	----------13.9----------			13.8	21.0	20.2	13.9	--	17.0
Condensate From H_2 Cathode:									
Density, gm /ml	--	0.992	1.064	1.063	1.099	1.089	0.979	--	0.977
H_2SO_4 Normality	--	0.045	2.45	2.41	3.86	3.52	0.08	--	0.05
H_2SO_4 wt %	--	0.21	11.2	11.0	16.2	14.9	0.37	--	0.23
Methanol vol %	--	--	--	--	--	--	--	--	--
" " Calc	--	3.5	3.0	3.0	8.0	8.0	13.9	--	14.0
Fuel Fed:									
Methanol, vol %	55	55	37	37	22	22	22	37	37
Water, vol %	45	45	63	63	78	78	78	63	63
Methanol Grade	----------Commercial Union Carbide----------								
Electrolyte Sample:									
Anolyte, Total ml	--	6.0	12.8	22.2	29.2	37.2	39.1	39.1	40.7
Catholyte, Total ml	--	--	--	3.0	3.0	9.0	11.0	11.0	11.0

* Operated at 520 ml/hr recycle through cell.

APPENDIX C-1 (CONT'D.)

METHANOL ELECTRODE LIFE STUDIES

Run Conditions, Electrical Performance, Feed and Product Rates

Run Number	-3618-55-																						
Run Hours	0	21	45	69	98	141	189	213	237	290	333	357	381	405	477	501	525	573	604	645	669	693	744	813
Cell Temperature, °C	82	82	82	82	82	83	82	83	83	82	81	82	82	81	81	82	84	82	85	80	80	82	80	82
Current Collectors	-0.001" thick x 3/16" wide Pt Sheet Around Periphery Plus Center Electrode Contacts-																						
Cathode*	-52 mesh Pt Screen Plus 8 mg Pt Black/cm² (8 mils thick)-																						
Anode*	-80 mesh Pt Rh Screen Plus 8 mg Pt Black/cm² (6 mils thick)-																						
Membrane	-Ionics CR-61 Cationic (21.3 mils thick), Tight Between Electrodes-																						
Electrolyte Between Electrodes	-None-																						
Current Density, ma/cm²	49	50	50	50	50	50	50	50	49	49	48	49	49	49	48	49	50	49	50	48	49	50	50	50
Volts Polar. At Constant Current	0.58	0.58	0.59	0.60	0.61	0.61	0.61	0.61	0.62	0.61	0.62	0.63	0.62	0.63	0.63	0.63	0.63	0.63	0.65	0.63	0.62	0.64	0.65	0.67
Volts Polar. With Open Circuiting	-	-	-	-	0.59	-	-	0.59	0.60	-	0.59	0.59	-	0.61	0.61	0.61	0.58	0.62	0.62	0.59	0.61	0.62	0.63	0.62
Feed Solution During Period:																								
Methanol, ml	-	29.6	48.2	32.0	38.2	90.4	95.8	47.1	36.5	81.7	81.7	27.9	31.6	37.4	122.0	27.0	33.3	75.8	38.8	62.9	38.8	31.2	70.2	98.8
Water, ml	-	32.4	46.8	66.0	63.8	147.6	156.2	76.9	59.5	133.3	133.3	59.1	61.4	72.6	237.0	57.0	70.7	161.2	66.2	107.1	66.2	64.8	148.8	210.2
Total, ml	-	72.0	95.0	98.0	102.0	238.0	252.0	124.0	96.0	215.0	215.0	87.0	93.0	110.0	359.0	84.0	104.0	237.0	105.0	170.0	105.0	96.0	219.0	309.0
Feed Solution Per Run:																								
Methanol, ml	-	39.6	87.8	119.8	158.0	248.4	344.2	391.3	427.8	509.5	591.2	619.1	650.7	688.1	810.1	837.1	870.4	946.2	985.0	1047.9	1086.7	1117.9	1188.1	1286.9
Water, ml	-	32.4	79.2	145.2	209.0	356.6	512.8	589.7	649.2	782.5	915.8	974.9	1036.3	1108.9	1345.9	1402.9	1473.6	1634.8	1701.0	1808.1	1874.3	1939.1	2089.9	2298.1
Total, ml	-	72.0	167.0	265.0	367.0	605.0	857.0	981.0	1077.0	1292.0	1507.0	1594.0	1687.0	1797.0	2156.0	2240.0	2344.0	2581.0	2686.0	2856.0	2961.0	3057.0	3276.0	3585.0
Methanol, ml/hr	-	1.88	1.95	1.73	1.61	1.76	1.82	1.84	1.80	1.75	1.77	1.73	1.71	1.70	1.90	1.67	1.66	1.63	1.63	1.62	1.62	1.61	1.59	1.58
Makeup 30% H_2SO_4 Soln, ml	-	-	35(H_2O)	-	-	-	67	125	90	25	-	-	-	-	-	25	19	-	-	-	-	55	-	-
Condensate From CO_2 Anode At 26°C **																								
Per Period, ml	-	10	15	25	(22)	50	38	19	16	27	26	13	14	19	40	15	14	23	18	20	17	15	26	38
Total Per Run, ml	-	10	25	50	72	100	138	157	173	200	226	239	253	272	312	327	341	364	382	402	419	434	460	498
Total Methanol, ml calc	-	1.1	3.8	8.8	-	18.1	28.9	34.3	37.0	41.4	47.0	49.6	51.1	53.6	60.8	62.5	63.7	66.7	68.3	68.8	72.2	74.7	76.3	79.0
Total Methanol, ml/hr	-	0.050	0.085	0.127	-	0.128	0.153	0.161	0.156	0.143	0.141	0.139	0.134	0.132	0.128	0.124	0.121	0.116	0.113	0.107	0.108	0.108	0.102	0.097
Condensate From Hz Cathode At 26°F**																								
Per Period, ml	-	30	57	32	(49)	236	294	75	62	116	105	64	64	63	169	66	61	78	75	71	70	50	133	153
Total Per Run, ml	-	30	87	119	168	355	649	724	786	902	1007	1071	1135	1198	1367	1431	1492	1570	1645	1716	1786	1836	1969	2122
Total Methanol, ml calc	-	1.1	6.7	10.3	-	13.1	16.9	24.3	30.2	38.3	46.7	47.7	49.3	51.2	63.0	66.2	68.6	74.1	76.0	79.6	87.3	96.3	97.6	97.6
Total Methanol, ml/hr	-	0.052	0.149	0.148	-	0.093	0.079	0.114	0.127	0.132	0.125	0.133	0.129	0.126	0.132	0.132	0.130	0.129	0.126	0.123	0.130	0.139	0.131	0.120
Total CO_2, CF At 26°C	-	0.46	1.11	2.18	3.18	4.35	5.65	6.23	6.86	8.77	9.40	10.04	10.62	11.26	13.22	13.86	14.51	15.75	16.68	17.64	18.32	19.00	20.41	22.39
Total H_2, CF At 26°C	-	1.55	3.54	5.05	7.27	11.09	14.81	16.69	18.67	23.01	26.64	28.63	30.58	32.55	38.52	40.49	42.49	46.46	49.02	52.20	54.31	56.41	60.76	66.77

* Electrodes square shape, 82 cm^2 in area.
** Condensed in chilled water cooled condenser.

APPENDIX C-1 (CONT'D.)

METHANOL ELECTROLYSIS LIFE STUDIES

Solution Analyses @ 26°C

Run Number	-3618-55-																						
Run Hours	0	21	45	69	98	141	189	213	237	290	333	357	381	405	477	501	525	573	604	645	669	693	746	813
Anolyte Electrolyte Recycle: *																								
Density, gm/ml	1.21	-	-	-	-	-	-	-	-	-	-	-	-	1.21	-	1.19	1.19	1.16	1.16	1.16	1.18	1.19	1.20	1.20
H_2SO_4 Normality	7.5	-	7.9	7.5	-	7.2	6.8	6.8	7.0	7.1	6.7	6.9	7.4	7.2	6.3	6.6	6.5	6.2	6.5	6.4	7.1	7.2	7.2	7.0
H_2SO_4, wt %	30.2	-	31.5	30.2	-	29.1	27.3	27.3	28.2	28.5	27.0	27.8	30.0	29.1	25.6	26.7	26.3	26.0	26.3	26.0	28.5	29.1	29.3	28.2
Methanol, vol %	-	-	-	-	-	-	-	-	3.0	-	-	2.9	-	-	-	-	1.2	-	-	2.5	-	-	-	-
Methanol, vol % calc	1.0	1.5	2.5	2.9	-	2.6	4.2	4.2	2.4	2.3	3.1	2.9	1.4	1.7	2.6	1.5	1.1	1.7	1.1	1.6	2.9	2.4	0.82	0.90
Catholyte Electrolyte:																								
Density, gm/ml	1.21	-	-	-	-	-	-	-	-	-	-	1.16	-	-	-	-	1.15	-	-	-	-	-	-	-
H_2SO_4 Normality	7.5	-	-	6.42	-	6.28	-	-	-	-	-	5.75	-	-	-	-	5.25	-	-	-	-	-	-	-
H_2SO_4, wt %	30.2	-	-	26.3	-	25.5	-	-	-	-	-	23.8	-	-	-	-	25.3	-	-	-	-	-	-	-
Methanol, vol %	0.0	-	-	-	-	-	-	-	-	-	-	1.3	-	-	-	-	0.99	-	-	-	-	-	-	-
Methanol, vol % calc	-	0.45	1.1	1.5	-	1.4	0.75	1.7	1.1	0.9	1.0	0.9	0.30	0.35	0.90	0.62	0.90	0.90	0.3	0.6	1.5	2.5	0.25	0.00
Condensate From CO_2 Anode:																								
Density, gm/ml	-	1.014	0.973	0.970	-	0.972	0.960	0.960	0.974	0.975	0.968	0.970	0.982	0.979	0.975	0.981	0.985	0.979	0.985	0.980	0.970	0.974	0.980	0.987
H_2SO_4 Normality	-	1.07	0.03	0.03	-	0.03	0.04	0.03	0.17	0.08	0.05	0.05	0.05	0.03	0.06	0.04	0.05	0.06	0.05	0.05	0.05	0.05	0.03	0.02
H_2SO_4, wt %	-	5.0	0.14	0.14	-	0.14	0.19	0.14	0.79	0.37	0.23	0.23	0.23	0.14	0.27	0.19	0.23	0.27	0.23	0.23	0.23	0.23	0.14	0.09
Methanol, vol %	-	-	-	-	-	20.1	-	-	-	-	-	13.5	-	-	-	-	8.6	-	-	-	-	-	-	-
Methanol, vol % calc	-	11.0	18.0	20.1	-	18.6	28.3	28.3	17.0	16.2	21.8	20.2	10.6	13.0	18.0	11.5	8.6	13.0	8.6	12.1	20.2	17.0	6.3	7.0
Condensate From Hz Cathode:																								
Density, gm/ml	-	0.992	1.056	0.982	-	1.085	1.113	1.051	1.018	1.037	1.034	1.039	1.067	1.055	1.036	1.049	1.036	1.023	1.054	1.034	1.048	1.017	1.072	1.038
H_2SO_4 Normality	-	0.20	2.42	0.21	-	3.28	4.22	2.44	1.17	1.70	1.65	1.63	2.50	2.15	1.69	2.02	2.13	1.20	2.07	1.51	2.29	1.52	2.52	1.98
H_2SO_4, wt %	-	0.96	10.9	0.98	-	14.5	18.2	11.2	5.5	7.9	7.7	7.5	11.4	9.9	7.8	9.3	9.8	5.7	9.6	7.1	10.5	7.2	11.5	9.1
Methanol, vol %	-	-	-	-	-	11.5	-	-	-	-	-	6.3	-	-	-	-	3.1	-	-	-	-	-	-	-
Methanol, vol % calc	-	3.8	9.8	11.2	-	11.8	6.0	12.5	9.5	7.0	8.0	4.5	2.5	3.0	7.0	5.0	4.0	7.0	2.5	5.0	11.0	18.0	1.0	0.0
Fuel Fed:																								
Methanol, vol % **	55	55	50	30	38	38	38	38	38	38	38	34	34	34	34	32	32	32	37	37	37	32	32	32
Water, vol %	45	45	50	70	62	62	62	62	62	62	62	66	66	66	66	68	68	68	63	63	63	68	68	68
H_2SO_4 Normality	-	-	-	-	-	-	-	-	-	-	-	-	-	-	-	0.79	0.79	0.79	0.79	0.79	0.79	0.79	0.90	0.90
Electrolyte Sample From Cell																								
Anolyte, Total ml	-	0.0	1.8	3.1	3.1	9.7	11.5	13.5	22.3	24.3	26.4	33.1	34.6	36.5	38.5	41.3	47.8	50.2	52.6	59.7	61.0	62.4	64.1	66.1
Catholyte, Total ml	-	0.0	0.0	1.5	1.5	3.5	3.5	3.5	3.5	3.5	3.5	9.7	9.7	9.7	9.7	9.7	16.1	16.1	16.1	16.1	16.1	16.1	16.1	16.1

* Operated at 530 ml/ hr recycle through cell. Total liquid in system was 650 ml at start.
** Methanol grade, Commercial Union Carbide.

APPENDIX C-2

METHANOL ELECTRODE WASHING STUDIES

Run Number	3618-46 and 47														
Cell Temperature, °C	83	84	83	82	82	82	82	82	82	83	82	86	85	85	85
Cathode*	80 Mesh Pt-Rh Screen Plus 8 mg Pt black/cm^2, 6 mils thick														
Membrane*	Ionics CR-61 cationic, 21.3 mils thick, not tight between electrodes														
Electrolyte, wt % H_2SO_4	30.0, 88 mils soln between electrodes														
CH_3OH, vol % in H_2SO_4**	1.0														
Pt-Black on Anode, mg/cm^2	8														
CH_3OH Anode Mesh Pt-Rh	80														
Anode Tilt, Degrees From Vertical	None	None	18	None	9	18	None	None							
Current, amps	5.0	5.0	5.0	5.0	5.0	5.0	5.0	1.1	1.5	3.0	4.9	6.0	7.5	9.2	9.8
Current Density, ma/cm^2	50	50	50	50	50	50	50	11	15	30	49	60	75	92	98
Volume of Electrolyte Solution Through Cell, ml Total***	500	1000	2000	2500	2750	3000	3250	400				200			
Volts Polarization at Anode Measured With Reference Electrode at Center of CH_3OH Electrode	.608	.608	.528-.548	.533-.548	.528-.568	.508-.548	.518-.558	.528	.538	.573	.608	.623	.653	.678	.708
IR Loss Thru Membrane and Solution	--	--	--	--	--	--	--	.035	.050	.100	.155	.150	.175	.220	.245
Current Collector	0.001" thick x 3/16" wide Pt sheet around periphery of electrode														

* Electrodes square shape, 90 cm^2 in use.

** Commercial Union Carbide methanol.

*** 1 vol % CH_3OH in 30 wt % H_2SO_4 operated once through at 520 ml/hr.

APPENDIX C-3

METHANOL ELECTRODE CONFIGURATION STUDIES

Run Number	3618-47				3618-48				3618-49			3618-51	3618-55
Cell Temperature, °C	82	82	82	82	82	81	82	82	83	83	83	82	81
Cathode*	80 mesh Pt-Rh Screen Plus 8 mg Pt-black/cm^2, 6 mils thick												
Membrane	Ionics CR-61 Cationic, 21.3 mils thick, not tight between electrodes												#
Electrolyte, Wt % H_2SO_4	30.0 (88 mils soln between electrodes)												
Methanol, Vol % in H_2SO_4**	1.0												
Pt Black on Anode, mg/cm^2	8												
Methanol Anode Mesh	80	80	80	80	150	150	150	150	52	52	52	80	80
Anode Tilt, Degrees From Vertical*	None	9	18	26	None	18 Up	18 Down	None	None	None	None	None	None
Current, amps	5.0	5.0	5.0	5.0	5.0	5.0	5.0	5.0	5.0	5.0	3.3	5.0	5.0
Current Density, ma/cm^2	50				50				50	50	33	50	50
Volts Polarization At Anode Measured With Reference Electrode Located In Middle And From Cell Bottom By:													
0 inches	.653-.668	.658-.673	.643-.653	.658	.653	.646	.628-.631	.626-.631	.698-.708	.633-.643	.623-.628	.613-.623	.663
0.5 "	.628	.638-.646	.646-.651	.646	.628	.628	.621-.626	.628	.693-.703	.633-.640	.608-.616	-	-
1.0 "	.621	.588-.638	.568-.608	.633	.586-.638	.568-.613	.611	.588-.658	.693-.698	.628-.633	.598-.608	.593-.598	.613
1.5 "	.548-.608	.546-.608	.553-.568	.608-.628	.558-.618	.571	.586-.606	.558-.618	.691-.696	.633-.643	.613-.623	-	-
2.0 "	.533-.548	.528-.568	.508-.548	.573-.598	.548-.596	.543	.553-.563	.568-.573	.678-.688	.623-.633	.598-.603	.563-.573	.598
2.5 "	.518-.533	.503-.533	.503-.523	.553-.563	.533-.558	.528	.533-.543	.546-.548	.626-.638	.578-.618	.568-.588	.533-.538	-
3.0 "	.513-.523	.488-.508	.488-.508	.553-.558	.563-.513	.523	.521-.526	.526-.531	.628-.638	.548-.578	.538-.548	.533-.538	.618
3.5 "	.493-.503	.483-.503	.488-.498	.563-.568	.516-.521	.513	.516-.521	.518-.521	.608-.618	.538-.558	.533-.543	.533-.538	.618
3.75 "	.488-.508	.483-.498	.488-.503	.558-.566	.516-.521	.518	.513-.518	.516-.518	.593-.598	-	-	-	-
4.0 "	-	-	.488-.503	.558-.566	-	-	-	-	-	-	-	-	-
Current Collector	0.001" thick by 3/16" wide Pt Sheet Around Periphery Of Electrode											0.002" x 1-1/4" Au Sheet	##
Anode Prepared With Pt Black And Stored In Water For, Days	16				72				8			16	35
Anode Washed In Cell With Electrolyte Solution, ml Total***	2250	2500	2750	3000	725	1000	1155	1400	1160	1490		3000+	400

* Electrodes square shape, 90 cm^2 in use.
** Commercial Union Carbide methanol.
*** 1 vol % methanol in 30 wt % H_2SO_4 operated once through at 520 ml/hour
# CR-61 membrane packed tight between electrodes.
0.001" thick x 3/16" Pt sheet around periphery of electrode and contacting across electrodes in an "X" form.

APPENDIX C-4

METHANOL LOSS IN CO_2 EXHAUST

The CH_3OH contents of 3.7 M H_2SO_4 electrolyte, and condensate from the CO_2 exhaust plotted in Figure C-1 were determined by colorimetric chemical analysis. Chemical analysis involved distillation of CH_3OH from the sample to free it of H_2SO_4 and reacting with ceric ammonium nitrate solution. The CH_3OH hydroxyl group produces a red color. The intensity of the color, related to the CH_3OH concentration, is determined on a colorimetric electrophotometer (7). The CH_3OH contents of the solutions were also calculated (8) from the solution densities, determined by weighing a measured volume at 25°C. Correction was made for H_2SO_4 content. The calculated data are shown in Appendix C-1.

Figure C-1

Effect Of CH_3OH Concentration In Electrolyte On Its Concentration In CO_2 Exhaust Condensate

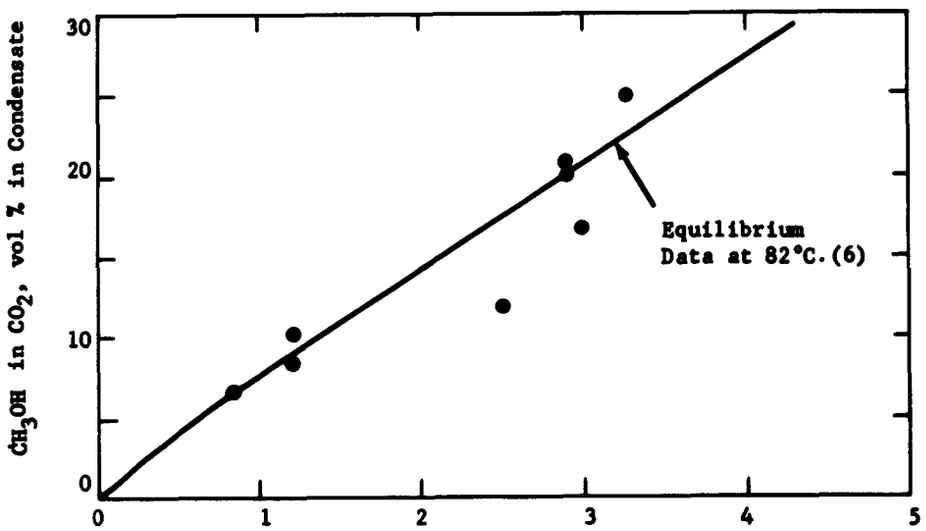

APPENDIX C-5

TOTAL CELL EQUIPMENT DETAILS

1. The Teflon cell consists of two halves machined from a 5-3/4" x 5-3/4" x 3/4" block fastened together with twelve #10-32 stainless steel bolts through 13/64" holes around the outside cell chamber. The cell chamber is 1/4" deep x 4" x 4" provided with a 0.025" depth by 3/16" ledge for support of electrodes and current collectors. Four 1/4" pipe thread holes are provided for liquid passage, and a top hole and slot for gas escape. Five 1/4" x 1/4" Teflon posts assure firm support of electrodes and membrane.

2. The cell is heated with a Glas-Col heater, 500 watt, 110 volt, using I.C. thermocouples of inside dimensions 6-1/2" x 2-1/2" x 6" depth with open top and two vertical side slots on each side of 1/2" width by 4-3/4" depth centered 3-1/4" apart, and a center slot on each side 1" deep. A Viton rubber cup in the heater bottom provides protection from acid leakage. The temperature is controlled by a Duenna controller Model J.

3. The acid electrolyte was recycled with a Model 2-6000 Buchler Micro-pump, 115 volt, 14 RPM, 60-950 ml/hour. The feed was pumped with a 5.7 rpm Buchler pump, 25-450 ml/hour. Lower rates were obtained by using an Eagle Signal Flexopulse timer.

4. Sealed fiber type Calomel electrodes, Beckman Model 11-505-80, were contacted with the back side of each electrode via a capillary tube.

5. Esterline Angus Recorders, Model AW, were used for recording voltages and currents. One ma recorders, operated from a Model 610A Keithley Electrometer, were used for voltages. Shunts in the ranges of 0.5, 1.5, 5, 10, 15 and 50 amperes were used with the 150 ma Model AW recorders for currents.

6. The coulometric timer (diagram shown in Appendix C-6) was operated across the 100 mv Esterline Shunts through a 20 ohm resistor. With the 5 amp shunt, 0.1% of current passed through the coulombic timer, and 0.33% passed with a 15 amp shunt. The resultant voltage drop in the timer is superimposed on a generated ramp voltage signal designed to trigger a timer for operating the feed pumps.

The superimposed voltage is dependent on the current from the cell. The level of the superimposed voltage determines the time on the ramp during which the pump timer operates. This combination of current dependent voltage and comparison ramp voltage results in a running pump time which is a function of cell output current. Since the ramp signal is not perfectly linear, calibration under cell conditions was necessary. Calibration was made with 5 and 15 amp shunts at currents from 0.45 to 10.5 amps. The deviation from linearity for timer on versus % of shunt used was found to average less than 1%. But if operation of the cell is confined to a given current density than essentially a perfect match between feed control and coulombic cell output can be made from the calibration. Of course, suitable allowances have to be made for chemical losses. The calibration below shows that the coulombic timer is on 51.2% of the time at 100% of the shunt reading and 1% of the time at zero shunt reading or no current. The 1% at zero shunt reading represents the trigger level point with no superimposed voltage drop on the ramp signal.

TABLE C-1

COULOMETRIC TIMER CALIBRATION

Amps to Shunt	Shunt Scale Reading	Basic Timer, % of Time On	% Time On, Deviation From Mean Linearity Line
5.0	100	51.2	-2.0
4.0	80	42.8	0.0
10.5	70	37.5	0.1
3.0	60	32.9	0.5
2.0	40	22.1	0.8
6.0	40	22.3	1.0
0.89	17.8	10.0	0.3
0.45	9.0	5.6	0.1
0.0(Est.)	0.0	1.0	0.0

7. A standard vacuum tube controlled relay shut off was provided for opening the circuit of the direct current source and shutting off the fresh feed pump in case of excessive polarization at the methanol electrode. The shut-off point may be selected. The controller was hooked in parallel across the 610A Keithley Electrometer measuring the methanol voltage.

8. Standard recycle timers were used in series connection with the current flow for opening the circuit at fixed intervals to decrease the polarization at the methanol electrode. The circuit was opened at 1 to 3 hour intervals for 10 to 15 seconds. The timers hooked in tandem are manufactured by the Industrial Timer Corporation, Models ET 3H and ET 60S.

APPENDIX C-6

COULOMETRIC TIMER CIRCUIT LAYOUT

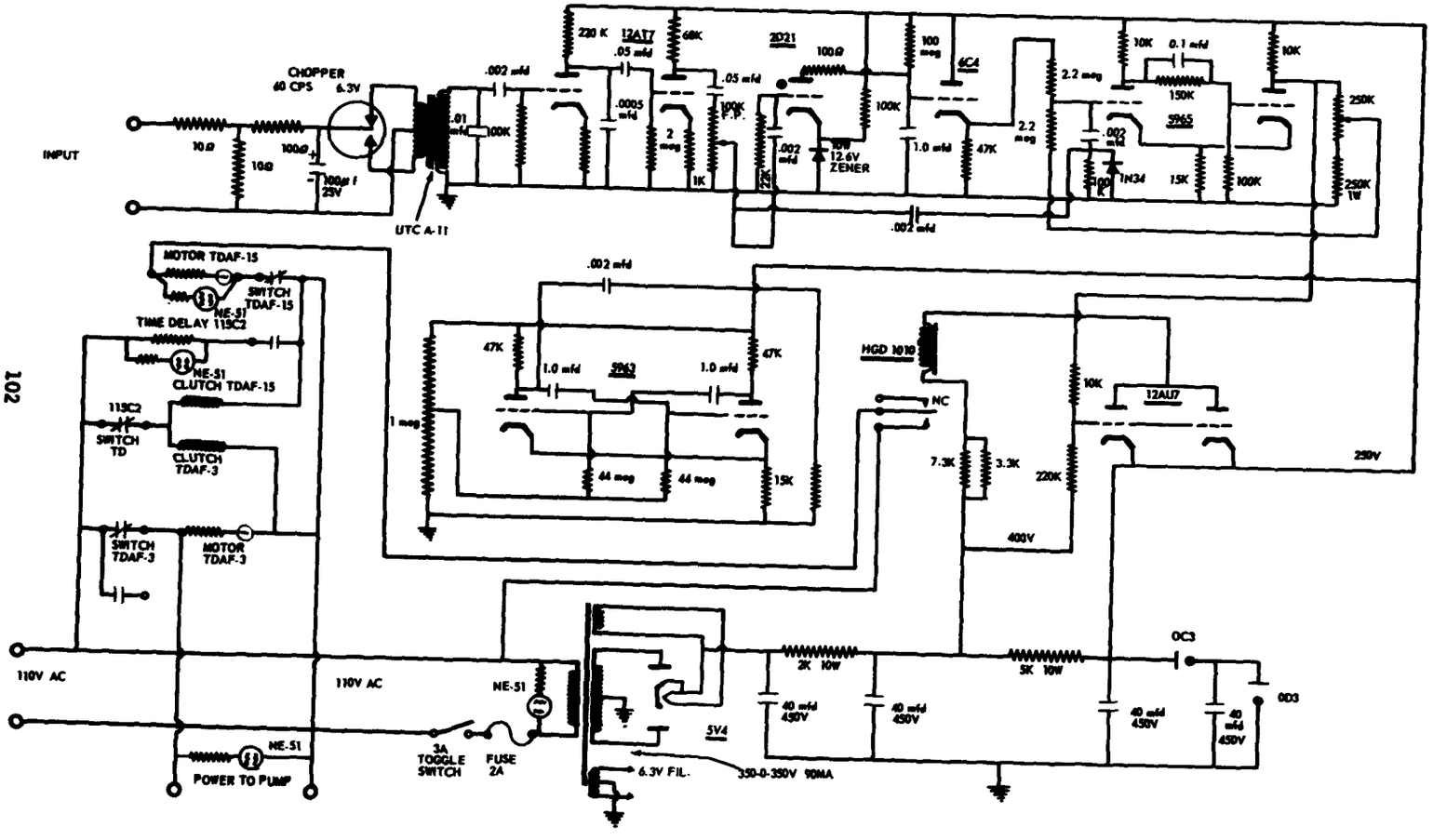

APPENDIX C-7

TOTAL CELL STUDIES WITH CH_3OH FUEL AND AIR-HNO_3 REDOX SYSTEM

Run Number	3618-2				3618-4						
Pressure, Atm Abs	1.0				1.0						
Temp, °C	70-72				70						
Cathode *	-- Au Plated 250 mesh 304 stainless steel*** -				80 Mesh Pt-Rh Screen Plus 8 mg/cm² Pt black						
Anode *	80 Mesh Pt-Rh Screen Plus 8 mg/cm² Pt black				80 Mesh Pt-Rh Screen Plus 8 mg/cm² Pt black						
Membrane	AMFion C313				AMFion C313						
Cell Spacing in Order of Assembly, Mils:											
Cathode	3.5				6.0						
Catholyte	64				30						
Membrane	5.6				5.6						
Anolyte	None				None						
Anode	6.0				6.0						
Between Electrodes	69.6				35.6						
Current Collector	0.001" thick by 3/16" wide Pt sheet around periphery of electrodes										
Catholyte	1 wt % HNO_3 in 30 wt % H_2SO_4				1 wt % HNO_3 in 30 wt % H_2SO_4						
Anolyte #	1 vol % CH_3OH in 30 wt % H_2SO_4				1 vol % CH_3OH in 30 wt % H_2SO_4						
Operation With Electrolytes	once-through				once-through						
Run Minutes	80-130	130-150	180-240	275-300	29	59	63	69	96	103	118
Current Density, ma/cm²											
Volts Polarization at:	19	32-33	27-28	29-31	38	9	21	42	59	54	4.5
CH_3OH Anode	0.58	0.62	0.71	0.64	0.658	0.553	0.613	0.703	0.779##	0.765##	0.497##
AIR-HNO_3 Cathode	**				0.264	0.219	0.239	0.265##	0.334	0.339	0.204
IR Drop	--	--	--	--	0.030	0.005	0.005	0.029##	0.039##	0.038##	0.031##
Observed Cell Volts	0.34	0.24	0.21	0.22	0.260	0.435	0.355	0.215	0.060	0.070	0.480
Efficiency, %	27	19	17	18	21	35	28	17	5	6	38
Power, watts/cm²											
Ex. IR	--	--	--	--	11.0	4.0	7.6	10.2##	5.8##	5.8##	2.3##
Observed	6.5	7.8	5.8	6.6	9.9	4.9	7.5	9.0	3.5	3.8	2.2
Cell Resistance, ohms	--	--	--	--	.008	0.006	0.002	0.007 assumed			

* Electrodes square shape, 90 cm² in use.
** Cathode reference electrode not operating.
*** Microscope examination showed uneven gold coating with agglomeration in corner of openings. Wire openings were 0.0024 inches.
# Methanol spectrequality, H_2SO_4, Baker "Analyzed" Reagent 96 wt %.
Calculated using assumed resistance

APPENDIX C-7 (CONT'D.)

TOTAL CELL STUDIES WITH CH_3OH FUEL AND AIR-HNO_3 REDOX SYSTEM

Run Number	3618-35																					
Pressure, Atm Abs		1.0								1.0										1.0		
Temp, °C	82	71								77										82		
Cathode *	80 Mesh Pt-Rh Screen Plus 8 mg/cm² Pt black																					
Anode *	80 Mesh Pt-Rh Screen Plus 8 mg/cm² Pt black																					
Membrane	AMFion C313																					
Cell Spacings In Order of Assembly, Mils:																						
Cathode	6.0																					
Catholyte	15.0																					
Membrane	5.6																					
Anolyte	None																					
Anode	6.0																					
Between Electrodes	20.6																					
Current Collector	0.001" thick x 3/16" wide Pt sheet around periphery of electrodes																					
Catholyte	1 wt % HNO_3 in 30 wt % H_2SO_4																					
Anolyte **	1 vol % CH_3OH in 30 wt % H_2SO_4																					
Operation With Electrolytes	Recycled plus makeup of HNO_3 and CH_3OH respectively																					
Run Minutes	25	450-480								480-490										500-520		
Current Density, ma/cm²	22	24	45	82	83	30	10	5.0	3.0	11	18	26	49	55	94	14	26	55	88	94	57	6.5	7.0
Volts Polarization at:																							
CH_3OH Anode	.603	.608	.658	.718	.718	.623	.573	.548	.533	.576	.598	.623	.668	.678	.753	578	.618	.678	.718	.723	.658	.563	.553
Air-HNO_3 Cathode	.259	.214	.259	.329	.319	.224	.164	.144	.124	.142	.169	.176	.229	.244	.284	.164	.189	.234	.289	.299	.244	.134	.144
IR Drop	.015	.020	.035	.050	.060	.020	.010	.000	.000	.014	.005	.018	.035	.030	.045	.005	.015	.035	.050	.055	.040	.010	.000
Observed Cell Volts	.335	.370	.260	.115	.115	.345	.465	.520	.555	.480	.440	.395	.280	.260	.130	.465	.390	.265	.155	.135	.270	.505	.515
Efficiency, %	27	30	21	9	9	27	37	41	45	38	35	31	22	21	10	37	31	21	12	11	21	40	41
Power, watts/cm²:																							
Ex. IR	7.7	9.3	13.3	13.5	14.5	11.0	4.8	.26	1.7	5.4	8.0	10.8	15.5	16.0	16.4	6.6	10.5	15.4	18.0	17.9	17.7	3.3	3.6
Observed	7.4	8.9	11.7	9.4	9.6	10.3	4.7	2.6	1.7	5.3	7.9	10.3	13.7	14.3	12.2	6.5	10.2	14.6	13.6	12.7	15.4	3.2	3.6
Cell Resistance, ohms	.007	.008	.008	.006	.007	.007	.10	.000	.000	.013	.003	.007	.007	.006	.005	.004	.006	.006	.006	.006	.007	.015	.000

* Electrodes square shape, 90 cm^2 in use.

** CH_3OH, commercial Union Carbide. H_2SO_4 Baker "Analyzed" Reagent 96 wt %

APPENDIX C-7 (CONT'D.)

TOTAL CELL STUDIES WITH CH_3OH FUEL AND AIR-HNO_3 REDOX SYSTEM

Run Number	3618-45									3618-64	
Pressure, Atm Abs	1.0										
Temp, °C	82	86	86	86	86	85	83	83	83	66	
Cathode #	80 Mesh Pt-Rh Screen Plus 8 mg/cm² Pt black										
Anode #	80 Mesh Pt-Rh Screen Plus 8 mg/cm² Pt black										
Membrane * & **	AMFlon C313									Halfilm D-30 gold plated on anode side	
Cell Spacings In Order of Assembly, Mils:											
Cathode	6.0									6.0	
Catholyte	None									None	
Membrane	5.6									4.0	
Anolyte	None									None	
Anode	6.0									6.0	
Between Electrodes	5.6									4.0	
Current Collector	0.001" thick by 3/16" wide Pt sheet around periphery of electrodes									0.018" thick gold ♯	
Catholyte	1 wt % HNO_3 in 30 wt % H_2SO_4									30 wt % H_2SO_4 ***	1 wt % HNO_3 in 30 wt% H_2SO_4
Analyte ##	1 vol % CH_3OH in 30 wt % H_2SO_4									1 vol % CH_3OH in 30 wt % H_2SO_4	
Operation With Electrolytes	once-through									once-through	
Run Minutes	43	46	50	57	58	60	62	75	78	-	60
Current Density, ma/cm²	24	16	51	5.0	2.5	31	66	54	69	50	11
Volts Polarization At:											
CH_3OH Anode	0.608	0.578	0.658	0.508	0.483	0.628	0.723	0.698	0.736	0.73	0.76
Air-HNO_3 Cathode	0.229	0.219	0.294	0.184	0.174	0.239	0.314	0.294	0.294	-	0.26
IR Drop	0.050	0.035	0.115	0.030	0.030	0.095	0.085	0.080	0.087	-	0.03
Efficiency, %	26	30	12	39	42	20	7	11	8	-	13
Power, mwatts/cm²											
Ex IR	9.0	6.7	13.2	2.6	1.4	10.7	11.5	11.9	12.6	-	2.1
Observed	7.8	6.1	7.4	2.4	1.3	7.8	5.9	7.5	6.5	-	1.8
Cell Resistance, ohms	0.021	0.022	0.023	0.060	0.120	0.031	0.013	0.015	0.013	-	0.028

* C313 membrane, treated in catholyte before installation was buckled but unbroken on removal.
** The goldplated Halfilm membrane showed no damage in cell use.
*** Cathode was DC driven to check methanol electrode activity.
♯ Electrodes square shape 82 cm² in use.
Methanol Commercial Union Carbide. H_2SO_4, Baker "Analyzed" Reagent 96 wt %.
♯ Gold current collector 0.018" thick x 3/16" width around periphery of electrodes and contacting across the electrodes in form of an "H".

APPENDIX C- 7(CONT'D.)

TOTAL CELL STUDIES WITH CH_3OH FUEL AND AIR-HNO_3 REDOX SYSTEM

Run Number	3618-65											
Pressure, atm abs	1.0											
Temperature, °C	87	87	87	87	87	87	82	82	81	81	80	80
Cathode *	80 mesh Pt-Rh screen plus 8 mg/cm² Pt-black											
Anode*	80 mesh Pt-Rh screen plus 8 mg/cm² Pt-black											
Membrane	Ionics CR-61, Cationic											
Cell Spacings In Order Of Assembly, mils:												
Cathode	6.0											
Catholyte	0.0											
Membrane	21.3											
Anolyte	0.0											
Anode	6.0											
Between Electrodes	21.3											
Current Collectors	0.018" thick x 3/16" wide around periphery of electrodes and contacting across electrodes in "X" form											
Catholyte	30 wt % H_2SO_4						1 wt% HNO_3 in 30 wt% H_2SO_4		2 wt % HNO_3 in 30 wt % H_2SO_4			
Anolyte**	1 vol % methanol in 30 wt % H_2SO_4											
Operation With Electrolytes	Once-through											
Run Minutes	7	8	9	10	11	12	50	57	92	100	115	118
Current Density, ma/cm²	44.2	66.4	88.4	110.5	55.2	11.1	24.5	17.7	28.2	59.7	86.2	76.2
Volts Polarization At:												
CH_3OH Anode	0.570	0.588	0.603	0.618	0.590	0.528	0.593	0.581	0.608	0.650	0.698	0.688
Air-HNO_3 Cathode	DC Driven Cathode						0.259	0.229	0.209	0.240	0.279	0.279
IR Drop	0.021	0.042	0.052	0.062	0.031	0.002	0.030	0.022	0.025	0.062	0.095	0.072
Observed Volts	-	-	-	-	-	-	0.330	0.380	0.370	0.260	0.140	0.173
Efficiency, %	-	-	-	-	-	-	26	30	29	21	11	14
Power, m watts/cm²:												
Ex IR	-	-	-	-	-	-	8.9	7.1	11.1	19.2	20.3	18.7
Observed	-	-	-	-	-	-	8.1	6.7	10.4	15.5	12.0	13.2
Cell Resistance, Ohms	0.005	0.007	0.007	0.006	0.006	0.002	0.013	0.014	0.010	0.011	0.012	0.010

* Electrodes square shape, 82 cm² in use.
** Methanol, commercial Union Carbide. H_2SO_4, Baker "Analyzed" Reagent, 96 wt %.

APPENDIX C-8

EFFECT OF H_2SO_4 CONCENTRATION ON TOTAL CELL PERFORMANCE

Platinized Pt Electrodes, 0.5M CH_3OH, 82°C., 1 wt% HNO_3

50 ma/cm^2

H_2SO_4 Conc, wt%	Polarization, Volts		Total Cell Voltage	
	O_2	CH_3OH	Excluding IR	With 0.5 Ohm * Cell Resistance
10	---	0.53	---	---
20	0.30	.55	0.36	0.33
30	.26	.56	.39	.36
40	.24	.58	.39	.36
50	.22	.61	.38	.35
60	.23	.63	.35	.30

100 ma/cm^2

10	---	.55	---	---
20	---	.56	---	---
30	.34	.58	.29	.24
40	.33	.60	.28	.23
50	.33	.62	.26	.19
60	.44	.65	.12	.02

* Experimentally determined in complete cell.

AD- Div.

Esso Research and Engineering Company,
Linden, New Jersey
SOLUBLE CARBONACEOUS FUEL-AIR FUEL CELL, by
Barry L. Tarmy and others. Final report,
1 Jan. 1962-31 December 1962. 107 pages
incl. illus. tables. (Rept. No. 2; PR&C No.
62-ELP/R-4306)
(Contract DA 36-039 SC-89156) Unclassified report

Studies were continued aimed toward the ultimate development of a fuel cell using a partially oxidized hydrocarbon as the fuel and air as the oxidant at moderate temperatures and pressures. Included are work carried out on the effects of fuel type, catalyst composition, and other major operating variables on the design and operation of the fuel electrode, experiments performed to improve the overall efficiency of the HNO_3 redox air electrode and tests designed to evaluate the

(over)

UNCLASSIFIED

1. Power supplies-Fuel cells
2. Electrolyte-Soluble carbonaceous fuel
3. Acid electrolyte
4. Electrodes

I. Tarmy, B. L.
II. U.S. Army Electronics Research and Development Laboratory
III. Contract DA 36-039 SC-89156

UNCLASSIFIED

AD- Div.

Esso Research and Engineering Company,
Linden, New Jersey
SOLUBLE CARBONACEOUS FUEL-AIR FUEL CELL, by
Barry L. Tarmy and others. Final report,
1 Jan. 1962-31 December 1962. 107 pages
incl. illus. tables. (Rept. No. 2; PR&C No.
62-ELP/R-4306)
(Contract DA 36-039 SC-89156) Unclassified report

Studies were continued aimed toward the ultimate development of a fuel cell using a partially oxidized hydrocarbon as the fuel and air as the oxidant at moderate temperatures and pressures. Included are work carried out on the effects of fuel type, catalyst composition, and other major operating variables on the design and operation of the fuel electrode, experiments performed to improve the overall efficiency of the HNO_3 redox air electrode and tests designed to evaluate the

(over)

UNCLASSIFIED

1. Power supplies-Fuel cells
2. Electrolyte-Soluble carbonaceous fuel
3. Acid electrolyte
4. Electrodes

I. Tarmy, B. L.
II. U.S. Army Electronics Research and Development Laboratory
III. Contract DA 36-039 SC-89156

UNCLASSIFIED

AD- Div.

Esso Research and Engineering Company,
Linden, New Jersey
SOLUBLE CARBONACEOUS FUEL-AIR FUEL CELL, by
Barry L. Tarmy and others. Final report,
1 Jan. 1962-31 December 1962. 107 pages
incl. illus. tables. (Rept. No. 2; PR&C No.
62-ELP/R-4306)
(Contract DA 36-039 SC-89156) Unclassified report

Studies were continued aimed toward the ultimate development of a fuel cell using a partially oxidized hydrocarbon as the fuel and air as the oxidant at moderate temperatures and pressures. Included are work carried out on the effects of fuel type, catalyst composition, and other major operating variables on the design and operation of the fuel electrode, experiments performed to improve the overall efficiency of the HNO_3 redox air electrode and tests designed to evaluate the

(over)

UNCLASSIFIED

1. Power supplies-Fuel Cells
2. Electrolyte-Soluble carbonaceous fuel
3. Acid electrolyte
4. Electrodes

I. Tarmy, B. L.
II. U.S. Army Electronics Research and Development Laboratory
III. Contract DA 36-039 SC-89156

UNCLASSIFIED

AD- Div.

Esso Research and Engineering Company,
Linden, New Jersey
SOLUBLE CARBONACEOUS FUEL-AIR FUEL CELL, by
Barry L. Tarmy and others. Final report,
1 Jan. 1962-31 December 1962. 107 pages
incl. illus. tables. (Rept. No. 2; PR&C No.
62-ELP/R-4306)
(Contract DA 36-039 SC-89156) Unclassified report

Studies were continued aimed toward the ultimate development of a fuel cell using a partially oxidized hydrocarbon as the fuel and air as the oxidant at moderate temperatures and pressures. Included are work carried out on the effects of fuel type, catalyst composition, and other major operating variables on the design and operation of the fuel electrode, experiments performed to improve the overall efficiency of the HNO_3 redox air electrode and tests designed to evaluate the

(over)

UNCLASSIFIED

1. Power supplies-Fuel cells
2. Electrolyte-Soluble carbonaceous fuel
3. Acid electrolyte
4. Electrodes

I. Tarmy, B. L.
II. U.S. Army Electronics Research and Development Laboratory
III. Contract DA 36-039 SC-89156

UNCLASSIFIED

AD- operability of the fuel cell components in a complete cell. These tests demonstrate the feasibility of combining the cell components in a compact cell without severe losses in efficiency due to their interaction.	UNCLASSIFIED UNCLASSIFIED	AD- operability of the fuel cell components in a complete cell. These tests demonstrate the feasibility of combining the cell components in a compact cell without severe losses in efficiency due to their interaction.	UNCLASSIFIED UNCLASSIFIED
AD- operability of the fuel cell components in a complete cell. These tests demonstrate the feasibility of combining the cell components in a compact cell without severe losses in efficiency due to their interaction.	UNCLASSIFIED UNCLASSIFIED	AD- operability of the fuel cell components in a complete cell. These tests demonstrate the feasibility of combining the cell components in a compact cell without severe losses in efficiency due to their interaction.	UNCLASSIFIED UNCLASSIFIED

AD- Div.

Esso Research and Engineering Company, Linden, New Jersey
SOLUBLE CARBONACEOUS FUEL-AIR FUEL CELL, by Barry L. Tarmy and others. Final report, 1 Jan. 1962-31 December 1962. 107 pages incl. illus. tables. (Rept. No. 2; PR&C No. 62-ELP/R-4306)
(Contract DA 36-039 SC-89156) Unclassified report

Studies were continued aimed toward the ultimate development of a fuel cell using a partially oxidized hydrocarbon as the fuel and air as the oxidant at moderate temperatures and pressures. Included are work carried out on the effects of fuel type, catalyst composition, and other major operating variables on the design and operation of the fuel electrode, experiments performed to improve the overall efficiency of the HNO_3 redox air electrode and tests designed to evaluate the (over)

UNCLASSIFIED

1. Power supplies-Fuel cells
2. Electrolyte-Soluble carbonaceous fuel
3. Acid electrolyte
4. Electrodes

I. Tarmy, B. L.
II. U.S. Army Electronics Research and Development Laboratory
III. Contract DA 36-039 SC-89156

UNCLASSIFIED

AD- Div.

Esso Research and Engineering Company, Linden, New Jersey
SOLUBLE CARBONACEOUS FUEL-AIR FUEL CELL, by Barry L. Tarmy and others. Final report, 1 Jan. 1962-31 December 1962. 107 pages incl. illus. tables. (Rept. No. 2; PR&C No. 62-ELP/R-4306)
(Contract DA 36-039 SC-89156) Unclassified report

Studies were continued aimed toward the ultimate development of a fuel cell using a partially oxidized hydrocarbon as the fuel and air as the oxidant at moderate temperatures and pressures. Included are work carried out on the effects of fuel type, catalyst composition, and other major operating variables on the design and operation of the fuel electrode, experiments performed to improve the overall efficiency of the HNO_3 redox air electrode and tests designed to evaluate the (over)

UNCLASSIFIED

1. Power supplies-Fuel cells
2. Electrolyte-Soluble carbonaceous fuel
3. Acid electrolyte
4. Electrodes

I. Tarmy, B. L.
II. U.S. Army Electronics Research and Development Laboratory
III. Contract DA 36-039 SC-89156

UNCLASSIFIED

AD- Div.

Esso Research and Engineering Company, Linden, New Jersey
SOLUBLE CARBONACEOUS FUEL-AIR FUEL CELL, by Barry L. Tarmy and others. Final report, 1 Jan. 1962-31 December 1962. 107 pages incl. illus. tables. (Rept. No. 2; PR&C No. 62-ELP/R-4306)
(Contract DA 36-039 SC-89156) Unclassified report

Studies were continued aimed toward the ultimate development of a fuel cell using a partially oxidized hydrocarbon as the fuel and air as the oxidant at moderate temperatures and pressures. Included are work carried out on the effects of fuel type, catalyst composition, and other major operating variables on the design and operation of the fuel electrode, experiments performed to improve the overall efficiency of the HNO_3 redox air electrode and tests designed to evaluate the (over)

UNCLASSIFIED

1. Power supplies-Fuel Cells
2. Electrolyte-Soluble carbonaceous fuel
3. Acid electrolyte
4. Electrodes

I. Tarmy, B. L.
II. U.S. Army Electronics Research and Development Laboratory
III. Contract DA 36-039 SC-89156

UNCLASSIFIED

AD- Div.

Esso Research and Engineering Company, Linden, New Jersey
SOLUBLE CARBONACEOUS FUEL-AIR FUEL CELL, by Barry L. Tarmy and others. Final report, 1 Jan. 1962-31 December 1962. 107 pages incl. illus. tables. (Rept. No. 2; PR&C No. 62-ELP/R-4306)
(Contract DA 36-039 SC-89156) Unclassified report

Studies were continued aimed toward the ultimate development of a fuel cell using a partially oxidized hydrocarbon as the fuel and air as the oxidant at moderate temperatures and pressures. Included are work carried out on the effects of fuel type, catalyst composition, and other major operating variables on the design and operation of the fuel electrode, experiments performed to improve the overall efficiency of the HNO_3 redox air electrode and tests designed to evaluate the (over)

UNCLASSIFIED

1. Power supplies-Fuel cells
2. Electrolyte-Soluble carbonaceous fuel
3. Acid electrolyte
4. Electrodes

I. Tarmy, B. L.
II. U.S. Army Electronics Research and Development Laboratory
III. Contract DA 36-039 SC-89156

UNCLASSIFIED

AD- operability of the fuel cell components in a complete cell. These tests demonstrate the feasibility of combining the cell components in a compact cell without severe losses in efficiency due to their interaction.	UNCLASSIFIED UNCLASSIFIED	AD- operability of the fuel cell components in a complete cell. These tests demonstrate the feasibility of combining the cell components in a compact cell without severe losses in efficiency due to their interaction.	UNCLASSIFIED UNCLASSIFIED
AD- operability of the fuel cell components in a complete cell. These tests demonstrate the feasibility of combining the cell components in a compact cell without severe losses in efficiency due to their interaction.	UNCLASSIFIED UNCLASSIFIED	AD- operability of the fuel cell components in a complete cell. These tests demonstrate the feasibility of combining the cell components in a compact cell without severe losses in efficiency due to their interaction.	UNCLASSIFIED UNCLASSIFIED

DISTRIBUTION LIST
FINAL REPORT
CONTRACT NO. DA 36-039 SC-89156

Commanding Officer
U.S.A. Electronics Research and
Development Laboratory
Fort Monmouth, N.J.
ATTN: Logistic Division
(MARKED FOR PROJECT
ENGINEER)
ATTN: SELRA/P (2)
ATTN: Dir of Research/Engineering (1)
ATTN: File Unit #1 (1)
ATTN: Technical Document Center (1)
ATTN: Technical Information Div.
(UNCLASSIFIED REPORTS ONLY
FOR RETRANSMITTAL TO
ACCREDITED BRITISH AND
CANADIAN GOVERNMENT
REPRESENTATIVES) (3)

OASD (R&D), Rm. 3E1065
ATTN: Technical Library
The Pentagon
Washington 25, D.C. (1)

Chief of Research and Development
OCS, Department of the Army
Washington 25, D.C. (1)

Commanding General
U.S.A. Electronics Command
ATTN: AMSEL-AD
Fort Monmouth, N.J. (3)

Director
U.S. Naval Research Laboratory
ATTN: Code 2027
Washington 25, D.C. (1)

Commanding Officer and Director
U.S. Naval Electronics Laboratory
San Diego 52, California (1)

Air Force Cambridge Research
Laboratories
ATTN: CRZC
L. G. Hanscom Field
Bedford, Massachusetts (1)

Rome Air Development Center
ATTN: RAALD
Griffiss Air Force Base, N.Y. (1)

Commanding General
U.S.A. Electronics Research and
Development Activity
ATTN: Technical Library
Fort Huachuca, Arizona (1)

Commanding Officer
Harry Diamond Laboratories
ATTN: Library, Rm 211, Bldg 92
Connecticut Ave & Van Ness St.,
North West
Washington 25, D.C. (1)

Commanding Officer
U.S.A. Electronics Material
Support Agency
ATTN: SELMS-ADJ
Fort Monmouth, N.J. (1)

Deputy President
U.S.A. Security Agency Board
Arlington Hall Station
Arlington 12, Virginia (1)

Commander
Armed Services Technical
Information Agency
ATTN: TISIA
Arlington Hall Station
Arlington 12, Virginia (10)

Chief
U.S.A. Security Agency
Arlington Hall Station
Arlington 12, Virginia (2)

Commander
Aeronautical Systems Division
ATTN: ASAPRL
Wright-Patterson Air Force Base
Ohio (1)

Air Force Cambridge Research Laboratories
ATTN: CRXL-R
L. G. Hanscom Field
Bedford, Massachusetts (1)

Headquarters
U.S. Army Materiel Command
Research and Development Directorate
ATTN: AMCRD-DE-MO
Washington 25, D.C. (1)

Commanding General
U.S.A. Electronics Command
ATTN: AMSEL-RE-A
Fort Monmouth, N.J. (1)

Commanding General
U.S.A. Combat Developments Command
ATTN: CDCMA-E
Fort Belvoir, Virginia (1)

Commanding Officer
U.S.A. Communications and Electronics Combat Development Agency
Fort Huachuca, Arizona (1)

Director
Fort Monmouth Office
U.S.A. Communications and Electronics Combat Development Agency
Fort Monmouth, N.J. (1)

Air Force Systems Command
Scientific/Technical Liaison Office
U.S. Naval Air Development Center
Johnsville, Pennsylvania (1)

Corps of Engineers Liaison Office
U.S.A. Electronics Research and Development Laboratory
Fort Monmouth, N.J. (1)

Marine Corps Liaison Office
U.S.A. Electronics Research and Development Laboratory
Fort Monmouth, N. J. (1)

AFSC Scientific/Technical Liaison Office
U.S.A. Electronics Research and Development Laboratory
Fort Monmouth, N.J. (1)

Power Information Center
Moore School Building
200 South Thirty-Third St.
Philadelphia 4, Pennsylvania (1)

Director
Advanced Research Projects Agency
Washington 25, D.C. (6)

Chief Signal Officer
Department of the Army
Washington 25, D.C. (8)

Dr. Sidney J. Magram
Physical Sciences Division
Army Research Office
3045 Columbia Pike
Arlington, Va. (1)

Dr. Ralph Roberts
Head, Power Branch
Office of Naval Research (CODE 429)
Department of the Navy
Washington 25, D.C. (1)

Mr. Bernard B. Rosenbaum
Bureau of Ships (CODE 340)
Department of the Navy
Washington 25, D.C. (1)

Mr. George W. Sherman
Aeronautical Systems Division
ATTN: ASRMFP
Wright-Patterson Air Force Base
Ohio (1)

Dr. John H. Huth
Advanced Research Projects Agency
The Pentagon, Rm 3E157
Washington 25, D.C. (1)

Lt. Col. George H. Ogburn, Jr.
Auxiliary Power Branch (SNAP)
Division of Reactor Development
U.S. Atomic Energy Commision
Washington 25, D.C. (1)

Mr. Walter C. Scott
National Aeronautics & Space Administration
1520 H Street, N.W.
Washington 25, D.C. (1)

Institute for Defense Analysis
1666 Connecticut Avenue, N.W.
Washington 25, D.C.
ATTN: Dr. George Szego (1)
ATTN: Mr. Robert Hamilton (1)

Mr. R. A. Osteryoung
Atomics International
Canuga Park, California (1)

Dr. David M. Mason
Stanford University
Stanford, California (1)

Dr. Howard L. Recht
Astropower, Inc.
2968 Randolph Avenue
Costa Mesa, California (1)

Mr. L. R. Griffith
California Research Corp.
576 Standard Avenue
Richmond, California (1)

Dr. Ralph G. Gentile
Monsanto Research Corp.
Boston Laboratories
Everett 49, Massachusetts (1)

Mr. Ray M. Hurd
Texas Research Associates
1701 Guadalupe Street
Austin 1, Texas (1)

Dr. Richard H. Leet
American Oil Company
Whiting Laboratories
P.O. Box 431
Whiting, Indiana (1)

Dr. Douglas W. McKee
General Electric Company
Research Laboratories
Schenectady, New York (1)

Dr. E. A. Oster
General Electric Co., DECO
Lynn, Massachusetts (1)

Dr. Arthur J. Rosenberg
TICO, Incorporated
Materials Research Laboratory
Bear Hill
Waltham 54, Massachusetts (1)

Prof. Herman P. Meissner
Massachusetts Institute of Technology
Cambridge 39, Massachusetts (1)

Mr. Donald P. Snowden
General Atomics
P.O. Box 608
San Diego 12, California (1)

Dr. C. Tobias
Chemistry Department
University of California
Berkeley, California (1)

Mr. Y. L. Sandler
Westinghouse Research Laboratories
Pittsburgh, Pa. (1)

U.S. Army R&D Liaison Group
(9851 DV)
APO 757
New York, N.Y.
ATTN: Dr. B. R. Stein (1)

Director
U.S.A. Engineer Research and
Development Laboratory
Fort Belvoir, Virginia
ATTN: Mr. D. Looft (1)

Chief of Ordnance
Department of the Army
Washington 25, D.C.
ATTN: Mr. J. Creelin (ORDTB) (1)

Engelhard Industries, Inc.
Military Service Department
113 Astor Street
Newark 2, New Jersey
ATTN: Mr. V. A. Forlenza (1)

General Electric Company
Research Laboratory
Schenectady, New York
ATTN: Dr. H. Liebhoafsky (1)

University of Pennsylvania
John Harrison Laboratory of Chemistry
Philadelphia 4, Pennsylvania
ATTN: Dr. J. Bockris (1)